Università degli Studi della Basilicata

Department of Agricultural, Forestry, Food and Environmental Sciences

PhD in Agricultural, Forestry and Food Sciences

XXXVIII cycle

Scientific Disciplinary Sector:

AGRI-04/B – Agricultural Mechanics

(ex AGR/09 – Agricultural Mechanics)

PhD Thesis

Use of low-cost sensors for precision monitoring of agrifood systems

Supervisor

Prof. Genovese Francesco

PhD student

Tornese Iolanda

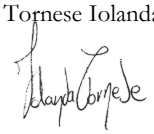

Co-supervisor

Prof. Di Renzo Giovanni Carlo

Coordinator

Prof.ssa Teresa Zotta

Academic Year 2024/2025

SUMMARY

Acronyms and Abbreviations

ADC: Analog-to-Digital converter

AI: Artificial Intelligent

ANN: Artificial Neural Network

API: Application Programming Interface

ASGI: Asynchronous Server Gateway Interface

BCD: Binary-Coded Decimal

BLE: Bluetooth Low Energy

CRNS: Cosmic Ray Neutron Sensor

CSA: Climate Smart Agriculture

DPHP: Double-Probe Heat Pulse

DSS: Decisional Support System

EC: Electrical Conductivity

ECa: Apparent Electrical Conductivity

ET: Evapotranspiration

FAO: Food and Agricultural Organization of the United Nations

FDR: Frequency-Domain Reflectometry

GIS: Global Information System

GPS: Global Positional System

GWC (θg): Gravimetric Water Content

HTTP: Hypertext Transfer Protocol

I^2C: Inter Integrated Circuit

ICT: information and communication technologies

IDE: Integrated Development Environment

IoT: Internet of Things

IoS: Internet of Service

LoRa: Long Range

ML: Machine Learning

NoSQL: Not only Structured Query Language

REST: Representational State Transfer

RH: Relative Humidity

RTC: Real Time Clock

SIWM: Smart Irrigation Water Management

SoC: System-on-a-Chip

SPHP: Single-Probe Heat Pulse sensor

SPI: Serial Peripheral Interface

SWC: Soil Water Content

TAA: Total Agricultural Area

TDR: Time-Domain Reflectometry

UAA: Utilised Agricultural Area

VWC (θv): Volumetric Water Content

WSN: Wireless sensor network

WU: Work Units

Summary Figures

Summary tables

Abstract

This thesis focuses on the design, calibration, and validation of a low-cost system for monitoring soil moisture and temperature, with potential applications in the field of smart farming. The research was developed following a progressive and structured approach, starting from an analysis of the main challenges of modern agriculture, characterized by the increasing demand for food and the scarcity of natural resources, with particular attention to sustainable water management. In this context, the use of smart sensors and automated systems emerges as a key factor in improving production efficiency and reducing environmental impact.

After outlining the regional agricultural framework and the main cropping systems, an analysis of the most relevant soil monitoring technologies was conducted, with a focus on systems for measuring soil moisture and nutrient content. Based on the strengths and limitations of the various solutions, the components most suitable for the implementation of the experimental system were selected.

The developed system integrates environmental sensors (DHT22, SHT10) and soil sensors (SEN0308, DS18B20) to continuously acquire data on relative humidity, soil temperature, and raw ADC values, which are then converted into volumetric water content (VWC). Through an extensive statistical analysis, the system was characterized and calibrated, confirming the reliability of the devices and enabling the development of a soil-specific calibration equation, which improved the performance of soil moisture monitoring ($R^2 = 0.99$).

Finally, the integration of data through FastAPI prepares the system for future remote data management and visualization, making it potentially suitable for field applications. However, in the current prototype version, remote data management has not yet been implemented.

Therefore, the study confirms that low-cost sensors, when properly calibrated through gravimetric methods, can serve as reliable tools for real-time monitoring of soil water dynamics under operational conditions.

1 INTRODUCTION

This chapter illustrates the main challenges that characterize modern agriculture, marked by a growing demand for food and the progressive scarcity of natural resources, with particular attention to water management. It provides an overview of water use as a strategic element for the sustainable development of the agriculture sector, with particular focus on the Italian context and, more specifically, on the Basilicata region, where water availability is strongly influenced by climatic conditions and the morphological characteristics of the territory. After outlining the regional agricultural framework and the main crop systems, the chapter offers a critical analysis of the level of digitalization in the agricultural sector, highlighting the factors that influence its diffusion at both national and local scales. In this context, the efficient use of water and the rational management of natural resources play a central role in ensuring agricultural productivity and the resilience of cropping systems. Finally, the evolution of agricultural systems, from traditional models to Agriculture 5.0, emphasizing how the integration of digital technologies, smart sensors, and automated systems can contribute to improving both production efficiency and environmental sustainability.

1.1. CONTEXT AND MOTIVATION OF THE STUDY

In recent decades, the global population has continued to grow steadily: according to estimates by the Food and Agricultural Organization of the United Nations (FAO), it will reach approximately 10 billion people by 2050 [1]. This demographic growth will, inevitably, drive an increase in global food demand, which must be met in a context where fundamental natural resources for agricultural production, such as water, fertile soil and nutrients, are becoming increasingly scarce. The agricultural sector is responsible for 70% of global water consumption (including irrigation, livestock and aquaculture), industrial 19% and municipal 11% (including domestic use) [2], as shown in *Figure 1.1.* The use of water, essential resource for sustainable development, is under growing pressure not only for agriculture, but also from urban and industrial sectors.

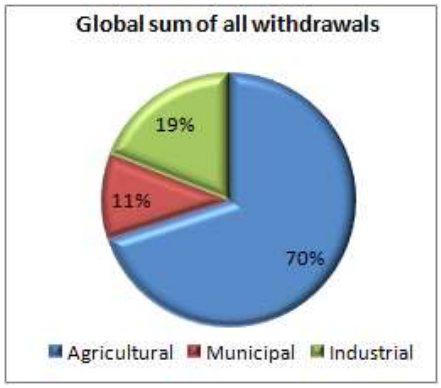

Figure 1.1 Global water withdrawals distribution among the main sectors: agricultural, industrial and municipal [2].

With the expansion of agricultural land, water withdrawals for irrigation have risen from 500 to 2500 cubic kilometres [3]. However, the efficiency of irrigation systems is often limited, as a significant portion of the distributed water is not actually absorbed by crops [4]. In this context, the effects of climate change further aggravate the situation, accentuating meteorological variability, reducing water availability, and increasing the frequency of extreme events. These consequences directly affect both agricultural productivity and the overall stability of agri-food systems. The result is a complex scenario in which the agricultural sector faces increasingly difficult challenges in ensuring higher food production without compromising the sustainability of natural resources. To address these issues, farms should adopt increasingly innovative and advanced technologies, aiming to make production processes more efficient and sustainable, allowing the sector to enter a new era of data-driven management and automation [3]. However, water management remains a critical factor at the global level, as there are significant disparities between countries in terms of both water availability and management. In this context, sustainable water management in agriculture must be considered a global strategic priority, regardless of the different water withdrawal ratios among continents. As shown in *Figure 1.2*, irrigation water withdrawals vary significantly across world regions: they exceed 80% of total consumption in Africa and Asia, while in Europe they amount to around 21%, where the largest share of withdrawals is instead associated with the industrial sector (57%) [2]. This disparity is closely related to climatic conditions, the role of agriculture within local economies and the level of industrialization of the different regions.

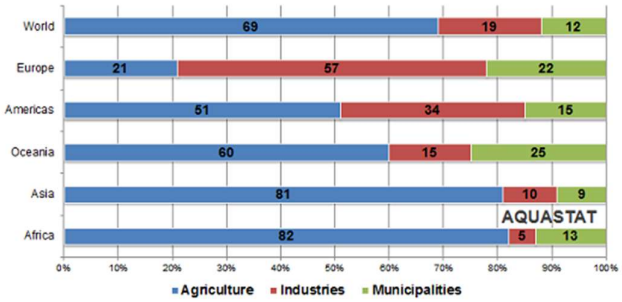

Figure 1.2 Sectoral distribution of water withdrawals (agriculture, industry and municipal use) across continents [2].

Being a highly developed and industrialized area, Europe has the responsibility to promote innovative management systems, serving as a model for other regions of the world. In this context, European policies have also played a strategic role in supporting the digitalization of the primary sector: the European Union has launched numerous programs aimed at promoting the digital transition in the agri-food sector. A crucial milestone was reached in 2019, when the Member States, together with the United Kingdom, signed the declaration for “A smart and sustainable digital future for European agriculture and rural areas”. The initiative promoted the use of technologies such as artificial intelligence, robotic, the Internet of Things (IoT), and

high-speed broadband connections to increase the efficiency of farms, improve food production, and promote both economic and environmental sustainability [5]. The vision also, seeks to modernize rural areas, strengthen food traceability, develop new business models, and attract younger generation to farming, thereby contributing to the improvement of quality of life in rural areas and enhancing European competitiveness. The commitment was further reinforced by the new Common Agricultural Policy (CAP 2023-2027), which identifies as one of the its strategic objectives the modernization of agricultural through knowledge sharing, innovation, and adoption of digital technologies, aimed at bridging the gap between urban and rural areas and enabling farmers and local communities to effectively integrate digital innovations into production processes [6]. Smart farming and advanced monitoring systems represent promising tools for reducing waste, improving crop resilience, and optimising water use.

1.2 WATER USE IN AGRICULTURE

Water is an essential resource for the life and economic development: it provides goods (potable water, availability for irrigation) and services (hydroelectric generation, recreation, etc.) that affect agriculture, industry and domestic use. Among the various sectors, agriculture is the main user of water resource on a global scale: it represents 70% of annual freshwater withdrawals [2], thus exerting significant pressure on available resources. According to the FAO report *"The State of the World's Land and Water Resources for Food and Agriculture: Systems at Breaking Point"* (SOLAW 2021), pressures on soil and water resources are reaching critical levels. Over the last decade, approximately 34% of agricultural land (1,660 million ha) has been degraded due to human activities, with direct impacts on productivity and the sustainability of food systems [7]. Since more than 95% of global food production depends on agricultural soils, which cannot be further expanded, and between 2000 and 2017 per capita land use decreased by 20%, improving the efficiency of existing resources becomes crucial, especially in light of the expected impacts of climate change on water availability [7]. Crops obtain water primarily from two sources: precipitation and irrigation. Irrigation water can be drawn from groundwater, rivers, and artificial reservoirs, and then distributed to field through various systems (flooding, channels, sprinkler systems, drip irrigation). At the soil level, the available water depends on soil water-holding capacity and root depth: the amount actually absorbed by crops is therefore the result of the interaction between water availability, soil properties, and crop water demand. Sustainable irrigation management is essential to reduce waste and increase productivity. In many cases, the efficiency of irrigation systems is limited, as a significant portion of the distributed water is not actually absorbed by crops [4]. At the same time, more efficient irrigation practices can reduce the volume of water applied by 30–70% and increase yields by 20–90% [8]. Therefore, to improve water sustainability, it is appropriate to adopt a set of complementary strategies: rainwater harvesting, soil moisture conservation practices (mulching, residue retention, conservation agriculture), crop management aimed at exploiting water stored in the soil, irrigation scheduling, and integrated agricultural systems that enhance the multiple uses of water (crop production,

livestock, aquaculture) [9]. When combined, these measures increase the resilience of agricultural systems and contribute to a more efficient use of water resources. Moreover, smart farming plays a particularly important role. In recent years, the increasing spread of advanced digital technologies, including artificial intelligence, IoT, and decision support systems (DSS), has opened new prospects for more efficient and sustainable water management in agriculture. In this context, the adoption of technological tools such as sensors for soil and crop monitoring, as well as agronomic models, represents a key step. These tools enable a more accurate estimate of the actual water requirements of crops throughout their entire growth cycle, integrating environmental data (precipitation, temperature, soil moisture) with the physiological parameters of the crops and soil characteristics . This makes it possible to plan irrigation in a targeted manner, reducing waste while ensuring water availability during the most critical stages of the crop cycle. The use of these technologies not only promotes a rational use of water resources but also aligns perfectly with the objectives of precision agriculture, improving productivity and enhancing crop resilience. However, it is important to also consider the limitations related to implementation costs, the need for specific technical skills, and adaptation to local conditions. In the following charapter, these technologies — sensors, IoT systems, and simulation models — will be discussed in detail, analyzing their potential and critical aspects for truly sustainable irrigation management.

1.2.1 The Italian context: agriculture, water resources and digitalisation

To outline the Italian context in terms of agriculture, water resources, and digitalisation, database from the National Institute of Statistics (IstatData) were consulted. This database collects and disseminates the results of the 7th General Agricultural Census. The census, referring to the 2019–2020 agricultural year, provides an updated and detailed overview of the national agricultural and livestock sector. According to Istat data, as of October 2020, the number of active farms in Italy amounted to 1.133.023 units, with a Total Agricultural Area (TAA) of 16.085.987 ha and a Utilised Agricultural Area (UAA) of 12.431.808 ha [10]. Historical data analysis, reported in the report *"Fewer farms (but larger) and new forms of land management"*, published on 28 June 2022, highlights a significant transformation of the sector over the last 40 years. As shown in *Table 1.1*, the number of farms has progressively decreased, while the average farm size has increased: the UAA increased from 5.1 to 11.1 ha per farm and the TAA from 7.1 to 14.5 ha [11, pp. 1–8]. This process reflects growing concentration and rationalisation of farms, which, although decreasing in number, are on average larger and potentially more efficient and productive.

Table 1.1 Evolution of agricultural holdings and cultivated areas in Italy (1982-2020): number of farms, UAA and TAA, and absolute values and average sizes [11].

	Absolute data (thousands of ha)			Averages per company (in ha)	
Years	**Number of companies**	**UAA**	**TAA**	**UAA**	**TAA**
2020	1.133.023	12.535	16.474	11.1	14.5
2010	1.620.884	12.856	17.081	7.9	10.5
2000	2.396.274	13.182	18.767	5.5	7.8
1990	2.484.136	15.026	21.628	5.3	7.6
1982	3.133.118	15.833	22.398	5.1	7.1

Arable crops represent the predominant crop type in Italy, with over 720.000 farms covering more than 7 million ha. Among these, cereals occupy the largest area, exceeding 3 million ha and involving 325.305 farms [10]. Cereals for grain production account for 44% of the cultivated area [11]; specifically, durum wheat is grown on over 135.000 farms, covering more than 1 million ha, confirming its essential role in the Italian cereal sector. The territorial distribution is mainly concentrated in Emilia-Romagna, Lombardia, Sicilia and Puglia, which together account for 44% of the area devoted to this crop type [11]. Woody crops represent a significant component of the agricultural system. They account for the highest number of farms, exceeding 800.000, for a total area of over 2 million ha. The olive tree is the most important species in the Italian agriculture sector, with over 619.000 farms and more than 985.000 ha cultivated nationwide [10]. Although olive growing is widespread throughout the country, production is predominantly concentrated in the southern regions. In Puglia, olive groves account for 71% of the region's utilised agricultural area and involves 94% of local farms. Sicilia follows with approximately 328.000 ha of olive orchards, while in Calabria olive cultivation represents 76% of the region's agricultural area [11]. The grapevine is the second most extensive and economically relevant woody crop, with 255.514 farms covering approximately 630.000 ha [10]. Veneto is the leading area with 27.000 farms and 100.000 ha under vineyards [11], confirming the strong viticultural tradition of north-eastern Italy. Fruit crops are represented by approximately 154.000 farms, covering more than 386.000 ha [10]. Apple is the most common fresh fruit species, with an area of about 55.000 ha and 38.000 farms; while hazelnut is the most widespread nut crop, mainly concentrated in Piemonte (over 8.000 farms) and Lazio (over 27.000 ha) [11]. Citrus crops occupy the smallest area among woody crops (112.000 ha), of which 55% is concentrated in Sicilia [11]. Values related to UAA and the number of farms for the main crop types are reported in *Table 1.2*.

Table 1.2 Main agricultural crops in Italy: Number of farms and cultivated areas (UAA and TAA) for the main crop types in Italy, referring to the year 2020. Data source: 7th ISTAT Agricultural Census [10].

TYPE OF CULTIVATION	UTILISED AGRICULTURAL AREA – ha	FARMS WITH UTILISED AGRICULTURAL AREA
Arable crops	7.185.011	721.605
• Cereals for grain production	3.134.768	325.305
• Dried pulses	264.646	52.613
• Vegetables crops	250.747	81.323
• Potato	27.920	23.356
Horticultural woody crops	2.164.034	800.586
• Olive tree For the production of table olives and oil	985.481	619.375
• Vineyard	629.517	255.514
• Orchards	386.631	154.101
• Citrus	112.033	49.087
Kitchen garden	13.956	161.277
Permanent grassland and pasture	3.068.532	284.774
Arboriculture for timber	83.733	20.073
Woods	2.864.890	268.532
Unused agricultural land	315.911	191.625
Other area	670.009	433.192
Used agricultural area (UAA)	12.431.808	1.120.524
Total area (TAA)	16.477.159	1.333.023

According to the ISTAT report *"Water Statistics"*, published on 21 March 2025 [12], during the 2019–2020 agricultural year, irrigated areas reached approximately 2.36 million ha, corresponding to 19% of the national UAA. *Figure 1.3* illustrates the distribution of irrigated areas in Italy by crop type for the year 2020.

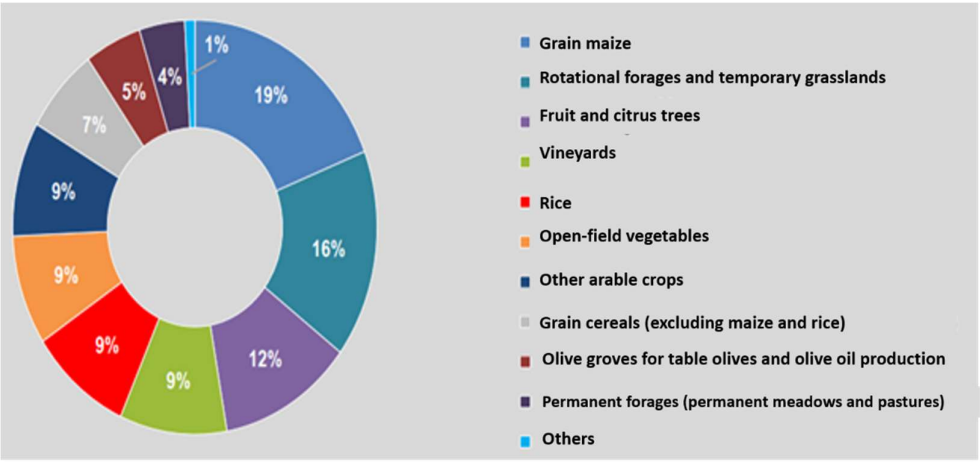

Figure 1.3 Distribution of irrigated areas in Italy by crop type for the year 2020 [12].

The largest share concerns arable crops, which account for 68.5% of irrigated areas, followed by woody crops (27.5%) and, to a lesser extent, permanent grassland and pastures (4%). Among arable crops, maize represents the most significant irrigated crop, covering about 448.000 ha [10]. Of this area, 19% is used for grain production and 7.4% for green maize. Rice follows, covering approximately 9% of irrigated areas. Among woody crops, vineyards account for the largest share (9.5%), followed by fruit crops (7.9% excluding citrus, 11.8% including citrus). Regarding irrigation techniques, sprinkler irrigation is the most widely used, covering 38% of irrigated areas, followed by surface flooding (28.4%), micro-irrigation (21.5%), submersion (7%), and other systems (5.1%) [12]. Concerning water supply, water from aqueducts, irrigation and reclamation consortia, or other irrigation authorities is used to irrigate more than half of the irrigated areas (59.7%). Groundwater, sourced within or near the farm, is used for 23.9% of irrigated areas, while surface water, either within the farm (natural and artificial basins) or outside the farm (lakes, rivers, or watercourses), accounts for 13.2%. Finally, other sources not included in the previous categories are used to irrigate 3.2% of the areas [12]. Furthermore, the 7th Agricultural Census highlights a significant growth in the digitalisation of the sector over the last decade. In 2020, 15.8% of farms used computers or digital tools for farm management, a share more than four times higher than in 2010 (3.8%) [11, pp. 16–21]. This strong digital adoption has affected the entire national territory, with an acceleration in the South and the Islands, where the number of digitalised farms has quadrupled. However, significant territorial gaps remain: only 6.7% of digitalised farms are located in the South and 10.3% in the Islands, compared to much higher values in the North (North-East 33.5%; North-West 32.9%) [11]. Digitalisation is particularly widespread among multifunctional farms: 61.7% of those engaged in connected activities (such as agritourism, social farming, or educational farms) use digital tools. Furthermore, the use of information technologies is more frequent in farms combining crop and livestock activities (26.1%), compared to those specialised exclusively in livestock (18.4%) or crop production (13.1%) [11]. Significant differences are also observed depending on the farm manager's profile: farms managed by young people under 45 are four times more digitalised than those run by individuals over 64 (32.2% vs. 7.6%). Education level and farm size also play a role: among large farms, 78.2% are digitalised compared to only 8.8% of small farms *(Figure 1.4)*, considering farm size in terms of Work Units (WU).

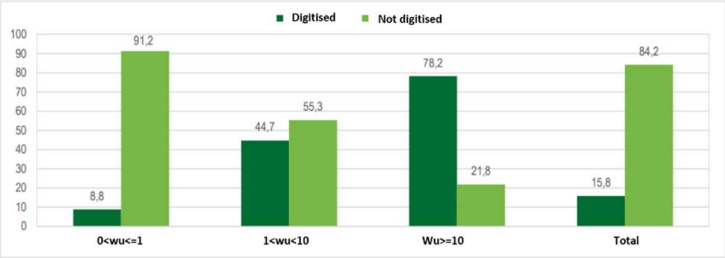

Figure 1.4 Percentage composition of digitised and non-digitised companies considering the size of companies in terms of WU[11].

Alongside digitalization, the survey also analyzed the propensity for innovation. Between 2018 and 2020, approximately 11% of farms made at least one innovative investment, with a strong prevalence in the North (over 20% of farms), while in the South and the Islands the shares did not exceed 5.4% and 7.1%, respectively. Investments mainly concerned mechanization (55.6%), followed by planting and sowing (23.2%), soil preparation (17.4%), and irrigation (16.5%) showed in *Figure 1.5*. Organizational and managerial innovations, on the other hand, remained marginal, adopted by less than 10% of farms. In conclusion, Italian agriculture is undergoing a major digital and technological transition, characterised by significant progress but still uneven across regions. This process is hampered by a lack of digital skills, insufficient infrastructure, high investment costs and a certain resistance to change, particularly in small farms. However, it also opens up numerous opportunities: the adoption of digital solutions can help improve production efficiency, support more sustainable management of natural resources and strengthen the long-term competitiveness of agricultural businesses.

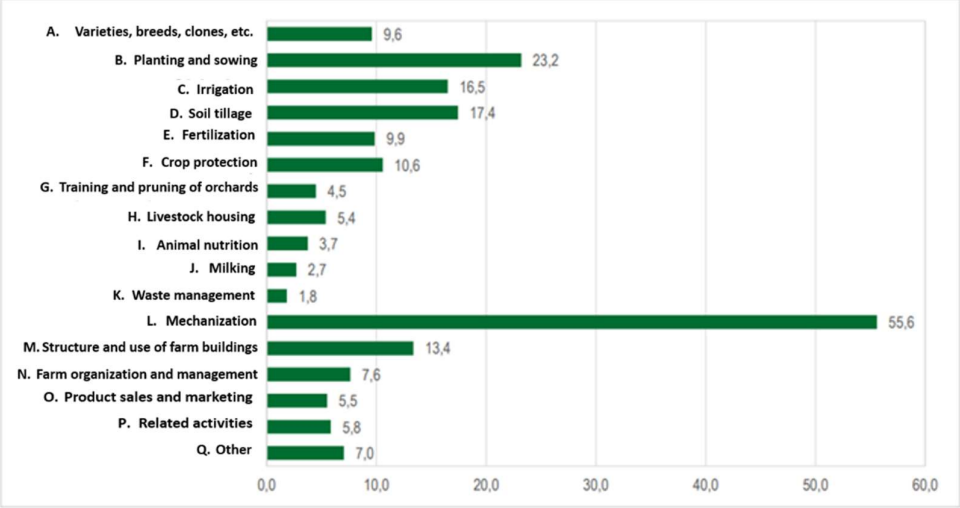

Figure 1.5. Percentage of companies that have made at least one innovative investment in the three-year period 2018-2020, by stage or area of application [11].

1.2.2 The context in Basilicata

Agriculture in Basilicata represents one of the fundamental columns of the regional economy, not only for its contribution to production and employment but also for the crucial role it plays in safeguarding the territory and maintaining social cohesion in rural areas. Thanks to the land reform, reclamation, and irrigation improvement projects initiated in the post-war period, it has been possible to reclaim vast agricultural areas, redefining production structures and the geographical distribution of crops. Today, the agricultural sector of Basilicata is characterized by strong productive diversification. The most significant sectors include livestock farming (meat, milk, and dairy production), cereal cultivation —

with a marked specialization in durum wheat — horticultural and fruit production, which is largely concentrated in the Metapontino area, and permanent crops, particularly viticulture and olive growing. Cereal cultivation covers an area of approximately 159.000 ha. According to available ISTAT data, in 2025 the area dedicated to durum wheat exceeded 115.000 ha, with a total production of over 300.000 t [13]. The remaining area is mainly devoted to the cultivation of barley (17.185 ha), oats (16.950 ha), and soft wheat (6.952 ha); other cereals (maize, rye, sorghum, etc.) occupy approximately 3.000 ha [14]. In the horticultural sector, open-field processing tomatoes covered just over 2.000 ha in 2025, yielding approximately 117.000 t, while fresh-market tomatoes recorded about 27.200 t produced on more than 667 ha. Greenhouse strawberry cultivation supplied around 12.100 t in 2024, while vineyards cover about 2.000 ha and olive groves reach 26.000 ha, with total production exceeding 30.000 t [13]. From a structural perspective, agriculture in Basilicata is characterized by the predominance of small, mostly family-run farms, with an average size of about 4 ha. According to the 7th General Agricultural Census, there has been a significant reduction in the number of farms, which declined from over 51.000 to just under 34.000 units [10]**.** The profile of human capital reveals a relatively low average level of education: most farm managers hold only primary or lower secondary school qualifications (around 23.330), followed by high school graduates (around 10.000), and a smaller number of university graduates (approximately 2.821) [13]. This demographic and educational composition directly affects the sector's propensity for innovation and the adoption of digital technologies. Over the past decade, the digitalization of Italian agricultural enterprises has grown significantly, with particularly notable progress in Southern Italy. However, Basilicata remains among the least digitalized regions: only about 7.4% of farms report using digital or intelligent tools, showing an increase still below the national average [13] [15]. The main factors limiting this diffusion are closely interconnected and include farm fragmentation, the predominance of small-scale family businesses, a lack of digital skills, and the high initial costs of investment. Added to these are infrastructural challenges, which are strongly influenced by the region's morphology: the predominantly mountainous and hilly landscape (47% mountains, 45% hills, and only 8% plains) makes the deployment of broadband and ultra-broadband networks more costly and technically complex, thereby exacerbating the existing difficulties in adopting digital technologies in the most remote rural areas. Despite these challenges, recent years have shown positive signs. Rural development policies (RDP 2007–2013 and 2014–2020) have encouraged the implementation of innovation projects and local partnerships, promoting collaboration among farmers, research centres, and advisory services. In particular, under the 2014–2020 RDP (Sub-measure 16.1 – Support for Operational Groups under the PEI), eleven Operational Groups were established. These groups have primarily focused on environmental sustainability and smart farming techniques, including precision agriculture and conservation practices, fostering the creation of public–private partnerships and specialized training programs [16]. Despite the progress made in innovation and in fostering collaboration between research institutions and agricultural enterprises, Basilicata

continues to face structural challenges related not only to digitalisation but also to the management of natural resources, particularly water. The region benefits from a significant hydrographic network, fed by major rivers, Agri, Basento, Bradano, Ofanto, and Sinni, along with numerous tributaries and springs, which together constitute a strategic resource for domestic, industrial, and agricultural uses. However, water availability is highly variable in both time and space and is often affected by episodes of water stress. The severe drought crises of recent years, such as the one in 2024, have seriously threatened agricultural production and local irrigation practices, highlighting the vulnerability of the regional production system to climate change and the lack of efficient management infrastructure. In this context, the adoption of digital technologies for resource monitoring and management, such as low-cost sensor systems, represents a crucial step toward improving irrigation efficiency, optimising water use, and mitigating the risks associated with the sustainability of agricultural production. In conclusion, agriculture in Basilicata is undergoing a transitional phase in which tradition and innovation coexist. To strengthen its competitiveness and sustainability, it is essential to act in an integrated manner on infrastructure, training, and organizational aspects, promoting cooperation and the adoption of digital technologies. In particular, the diffusion of low-cost monitoring systems could represent a strategic lever to enhance the resilience of the agricultural sector and foster sustainable long-term development.

1.3. EVOLUTION OF AGRICULTURAL SYSTEMS: FROM TRADITIONAL AGRICULTURE TO AGRICULTURE 5.0

Agriculture, since its origins, has represented one of the fundamental activities for the survival and development of human societies. Over the centuries, agricultural systems have undergone profound evolution, shifting from traditional models based on experience and direct observation, manual labour and animal traction, to increasingly technological and interconnected systems focused on productive efficiency and environmental sustainability. Today, sustainable agriculture plays a crucial role in the protection of natural resources, the conservation of biodiversity, and the reduction of greenhouse gas emissions [17]. It aims to meet current food needs without compromising the availability of resources for future generations, promoting a balance between productivity, environmental protection, and socio-economic well-being. Within this context, the evolution towards smart agriculture emerges, leveraging information and communication technologies (ICT) integrated into machinery, tools, and sensors to support data-driven decision-making processes. The main objective is to ensure a more efficient and sustainable management of resources, preserving soil quality, reducing environmental degradation, optimizing resource use, and enhancing biodiversity in agricultural systems. This approach is based on differentiated field management, which takes into account both spatial variability- such as differences in soil type, water availability, nutrient presence, pest

resistance- and temporal variability related to crop cycles and rotations [18]. The knowledge and analysis of these variabilities allow operations to follow the principle defined by Pierce and Novak (1999): "do the right thing, at the right place, at the right time," meaning to apply the most appropriate agronomic technique, in the right location, and when necessary. This approach enables the optimization of production, improved efficiency in resource use, and the reduction of environmental impacts resulting from non-rational agricultural practices [19].

Over the past century, the concept of agriculture has undergone numerous transformations. Building on the foundations of smart and sustainable agricultural practices, which aim to optimize productivity while preserving natural resources and reducing environmental impacts, technological and scientific advancements have gradually reshaped the sector. As a result, agriculture has evolved from traditional models to what is now referred to as Agriculture 5.0. This development can be summarized in five main stages (*Figure 1.6*), each reflecting significant innovations in machinery, management practices, digital technologies, and sustainability approaches.

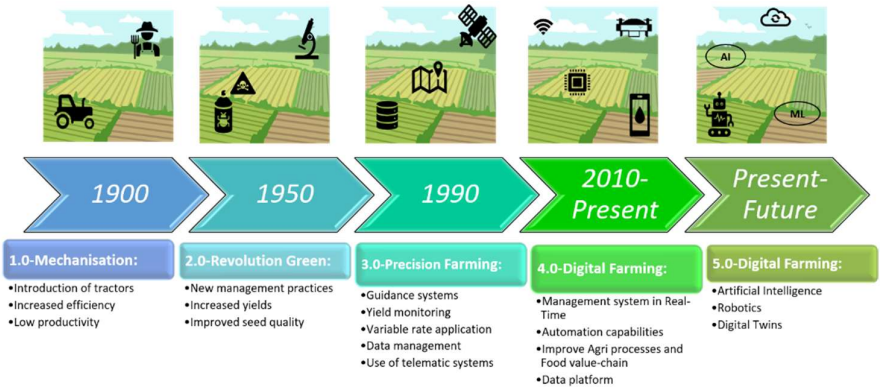

Figure 1.6 Evolution of agricultural systems: from traditional manual farming to modern Agriculture 5.0, characterized by digitalization, automation, and intelligent integration of sensors and advanced technologies.

i. ***Agriculture 1.0:*** starting from the beginning in the 20th century, the introduction of steam engines and new agricultural machinery marked a decisive shift in traditional agriculture, initiating the mechanization of production processes and significantly increasing operational efficiency. However, during this phase, agriculture remained highly intensive, relying heavily on manual labour and with overall productivity still limited compared to the standards achieved in later periods.

ii. ***Agriculture 2.0****:* In the 1950s, soil and crop management underwent a profound transformation thanks to advances in agricultural genetics and the widespread use of synthetic fertilizers, which allowed for increased yields and reduced losses. This phase, known as the Green Revolution, represented not only an evolution of farming techniques but a comprehensive modernization affecting multiple areas: from irrigation practices and mechanization to the genetic improvement of crop varieties. The large-scale adoption of these innovations led to a significant increase in cereal production and played a decisive role in meeting the growing

global food demand [20]. However, this progress also had significant side effects: the intensification of agricultural practices led to increased chemical pollution of soils and waters, ecosystem degradation, overexploitation of natural resources, and a substantial rise in energy consumption [21]. While Agriculture 2.0 marked a period of major productive expansion and technological innovation, it also highlighted the environmental and social limitations of intensive farming systems, paving the way for critical reflection on the need for more balanced and sustainable production models.

iii. ***Agriculture 3.0:*** In the 1990s and 2000s, a new production paradigm emerged: precision agriculture, as defined by Pierce and Nowak. This approach involves farm management strategies based on the use of information technologies to collect, analyze, and utilize data to support targeted agronomic decisions aimed at optimizing production and resource efficiency. This phase coincides with the introduction of Global Positional System (GPS) and the gradual integration of advanced digital technologies, initially derived from military applications, such as satellites, remote sensing, and Geographic Information Systems (GIS) [19]. The primary goal became the optimization of input use, intervening only where and when necessary. Innovative practices such as yield mapping, variable-rate applications, and assisted or automated guidance systems for agricultural machinery became widespread, allowing interventions to be calibrated according to the real needs of crops. Agriculture 3.0 thus represents a key step toward the digitalization of the primary sector, promoting more efficient, sustainable, and data-driven management. However, its initial adoption was limited by the high costs of technology and the operational complexity of the systems, factors that slowed widespread uptake, especially in small-scale farming contexts.

iv. ***Agriculture 4.0***: The Agriculture 4.0 era began in the early 2000s and is based on the concepts of the IoT and the Internet of Services (IoS), laying the foundation for the development of smart farming. This new production paradigm allows machines, operators, and monitoring systems to be interconnected through intelligent networks, enabling a high degree of automation in agricultural monitoring, management, and production processes.

The introduction of new digital technologies has profoundly transformed agricultural activities, thanks to the development of low-cost sensor platforms and networks that optimize production efficiency while reducing water and energy consumption, with lower environmental impact [22]. Smart agriculture represents the natural evolution of precision agriculture: it integrates advanced technologies for remote crop monitoring, automated machinery control, and predictive resource management. Automation based on sensors, actuators, drones, agricultural robots, and data analytics systems allows real-time detection of soil conditions, crops status, and environmental factors, supporting timely and targeted agronomic decisions. These innovations have reduced labor needs, increased productivity and product quality, and contributed to a more efficient, traceable, and sustainable supply chain [23] [24]. In summary, Agriculture 4.0 marks a technological revolution in the primary sector, where traditional methods are replaced by automated and interconnected systems, radically transforming

food production and paving the way for increasingly intelligent, resilient, and sustainable agriculture. Modern agricultural challenges, including soil variability, climatic factors, and water management, are now addressed through smart farming technologies and advanced monitoring systems, improving spatial management practices, optimizing productivity, and reducing excessive use of fertilizers and pesticides [25]. Specifically, Artificial Neural Network (ANN) models are applied in Smart Irrigation Water Management (SIWM), supporting DSS for irrigation scheduling. These models allow real-time estimation of irrigation efficiency, water productivity index, and supply-demand balance, contributing to more sustainable water resource management. Another emerging approach is Climate Smart Agriculture (CSA), increasingly adopted especially in developing countries due to its potential to improve food security, enhance agricultural system resilience, and reduce greenhouse gas emissions [26]. Overall, IoT-based smart agriculture provides significant benefits across all stages of the production process, enabling real-time management of irrigation, crop protection, fertilization, product quality enhancement, and disease forecasting [27] . Agriculture 4.0 thus paves the way for the next evolution, Agriculture 5.0, which involves fully automated operations with autonomous decision-making systems, leveraging robotics and artificial intelligence [28].

v. ***Agriculture 5.0:*** represents the next evolution of the primary sector, based on the full and intelligent integration of agricultural processes through automation and the complete digitalization of farms. It relies on advanced technologies such as Artificial Intelligence (AI), robotics, IoT, Big Data, and 5G networks, which enable the connection of machinery, sensors, and information systems into a single integrated and interactive platform. A key role is played by Fog Computing [29], which allows data to be processed close to the source , for example, directly on devices and sensors installed in the field , thereby reducing massive information traffic and sending to remote clouds only the final results that are truly useful for farmers' decision-making. This approach ensures more efficient data management, shorter response times, and real-time control of agricultural activities. Thanks to 5G networks, intelligent agricultural vehicles will be interconnected and equipped with the latest technologies and predictive cloud services, capable of providing rapid remote diagnostics in real time. Simultaneously, the adoption of autonomous driving systems and AI algorithms will optimize field operations, improving efficiency, reducing costs, and minimizing environmental impact. Agriculture 5.0 thus emerges as a new frontier of agricultural innovation, aimed at combining productivity with environmental, economic, and social sustainability, offering concrete solutions to the major global challenges: climate change, scarcity of natural resources, and the increasing demand for food.

1.4. CONCLUSION

In conclusion, the challenges posed by the growing demand for food, the scarcity of water resources, and the effects of climate change make it essential to adopt an innovative and sustainable approach to agriculture. The evolution of agricultural systems, from traditional models to Agriculture 5.0, demonstrates how the integration of digital technologies, smart sensors, and automated systems can help improve the efficiency of farming practices, optimize the use of natural resources, and reduce environmental impact. However, the solutions currently available are often costly and complex, limiting their adoption, especially among small and medium-sized farms.

To address these needs, this study aims to develop and evaluate low-cost monitoring solutions for detecting key environmental and agronomic parameters, such as soil and air temperature and humidity. The objective is to promote a more conscious and efficient use of water resources through reliable and accessible tools. In this way, the research seeks to make a tangible contribution to the planning of agricultural practices and the conservation of natural resources, supporting a sustainable and adaptive management of cropping systems.

The analysis carried out shows that soil monitoring is a key element for the sustainable management of water resources, particularly in regions such as Basilicata, where farm size, recent water crises, and the complex morphology of the territory make the use of efficient, flexible, and low-cost technologies essential.

2 STATE OF ART

The chapter presents the review published in the journal AgriEngineering on November 4, 2024**,** entitled *"Use of Probes and Sensors in Agriculture—Current Trends and Future Prospects on Intelligent Monitoring of Soil Moisture and Nutrients"* (DOI: https://doi.org/10.3390/agriengineering6040234).
The paper provides an in-depth analysis of the main technologies used for soil monitoring**,** with particular attention to systems for measuring soil moisture and nutrient content. It illustrates the operating principles, strengths, and limitations of the different available solutions, with a specific focus on low-cost implementations and IoT-based architectures, which are progressively transforming the way data are collected, transmitted, and utilized in agriculture. The aim of the chapter is to provide an updated overview of the state of the art of low-cost monitoring systems and to highlight the opportunities offered by technological innovation to promote a more sustainable, efficient, and digitally integrated agriculture**.**

2.1 Use of Probes and Sensors in Agriculture—Current Trends and Future Prospects on Intelligent Monitoring of Soil Moisture and Nutrients- *Review*

Iolanda Tornese [1,*], Attilio Matera [1], Mahdi Rashvand [2] and Francesco Genovese [1]

[1]DAFE, Department of Agricultural, Forestry, Food and Environmental Sciences, University of Basilicata, 85100 Potenza, Italy; attilio.matera@unibas.it (A.M.); francesco.genovese@unibas.it (F.G.)

[2]National Centre of Excellence for Food Engineering, Sheffield Hallam University, Howard Street, Sheffield S1 1WB, UK; mahdi.rashvand@unibas.it

*Correspondence: iolanda.tornese@unibas.it

Abstract: Soil monitoring is essential for promoting sustainability in agriculture, as it helps prevent degradation and optimize the use of natural resources. The introduction of innovative technologies, such as low-cost sensors and intelligent systems, enables the acquisition of real-time data on soil health, increasing productivity and product quality while reducing waste and environmental impact. This study examines various agricultural monitoring technologies, focusing on soil moisture sensors and nutrient detection, along with examples of IoT-based systems. The main characteristics of these technologies are analyzed, providing an overview of their effectiveness and the key differences among various tools for optimizing agricultural management. The aim of the review is to support an informed choice of the most appropriate sensors and technologies, thus contributing to the promotion of sustainable agricultural practices.

Keywords: smart farming; proximal sensing; soil monitoring; low cost.

2.1.1 Introduction

Soil exploitation, pollution, and climate change have had severe consequences on the quality and productivity of agricultural land. These interacting factors contribute to soil degradation and sterility. Since its biophysical functions are responsible for nutrient cycling and water dynamics and support crop growth [1], soil quality control is of fundamental importance to prevent its degradation and ensure optimal productivity. The agricultural sector is responsible for 70% of global water consumption [2], thereby exacerbating the growing crisis of water scarcity worldwide [3]. Beyond the high usage of water resources, agriculture also has a substantial impact on GHG emissions, contributing between 19% and 29% of global annual emissions [4]. Additionally, with the global population projected to reach 10 billion by 2050 [5], there is an anticipated increase in the demand for higher-quality food. These pressures highlight the urgent need to adopt innovative and sustainable agricultural strategies aimed at promoting effective soil monitoring, ensuring food security, and reducing environmental impact. Soil quality is determined through the monitoring of its characteristics. Electrical conductivity and dielectric properties provide information about nutrient content and moisture levels, respectively. Since these parameters are related to fertility and are essential for optimizing crop yields [6], the monitoring focuses on measuring and controlling these indicators. Soil monitoring techniques range from conventional methods to more recent and technological approaches. Conventional methods consist of laboratory analyses. These are extremely accurate but involve the destruction of samples, high costs, and long timescale, making them limited for large-scale use. Innovative methods leverage the potential of remote sensing and proximal sensing. Remote sensing uses satellite and drone imagery to facilitate the monitoring of large areas in high resolution. Nowadays, remote sensing is an effective method for obtaining useful information on soil health and crop growth; however, it does not provide real-time information. Satellite images are studied to develop predictive models for estimating soil quality indicators such as salinity, nutrients, and moisture [7–9]. Integrated multi- or hyperspectral sensor UAV systems present encouraging and promising aspects for plant disease detection and pest monitoring [10,11]. Proximal sensing involves the use of various technologies and sensors, which are useful for monitoring agro-meteorological conditions and soil characteristics. Proximal sensors collect data from the soil when the detector is in direct contact with it or in close proximity, providing information based on physical measurements that are related to the soil's properties [12]. The accessibility of low-cost sensors and components, combined with advanced technologies, has encouraged the implementation of intelligent monitoring systems. These systems, which fall under the concept of smart farming, rely on data collection and analysis, providing a more accurate monitoring of soil conditions. This enables farmers to make informed decisions and optimize agricultural practices, thereby contributing to preserving natural resources and mitigating climate change. A smart irrigation management and monitoring system has been developed, allowing for autonomous and optimized water distribution.

The system utilizes low-cost automatic sensors that detect soil moisture and plant health in real time [13]. An IoT-based drip irrigation system has been implemented to continuously monitor environmental conditions, soil moisture, and temperature levels. The integrated sensors send data to microcontroller, which processes the information and initiates irrigation if necessary [14]. Such systems allow for precise and automated irrigation regulation based on the crops' actual water needs. This enables plants to grow and develop optimally, preventing the risk of water stress or over-irrigation and promoting healthier, more vigorous and productive crops. Traditional irrigation systems tend to cause over-irrigation, with negative effects on crops such as slowed growth, wilting and yellowing of leaves, and increased vulnerability to molds and pathogens [15,16]. This occurs because, lacking precise control, traditional systems often supply excessive amounts of water, thereby disrupting the soil's water balance. In contrast, modern systems allow for the maintenance of optimal soil moisture levels, enabling more targeted and efficient irrigation. This promotes the rapid development and uniform growth of crops, with greener leaves and more fruits that tend to ripen earlier compared to those produced with traditional systems [16]. From soil monitoring, it is possible to identify areas of similar quality, called Management Unit Zones (MUZs), which are important for the planning and adoption of appropriate and precise soil management programs according to specific characteristics [7,17]. By knowing and monitoring the concentration of soil nutrients, the efficient use of fertilizers is enabled, avoiding deficiencies or excesses that could reduce productivity. An autonomous fertirrigation system is proposed, based on a wireless sensor network and equipped with a photovoltaic panel. This system monitors real-time weather conditions, soil moisture, and plant health. It integrates the collected data with a crop-specific database [18]. Implementing these solutions allows for the efficient use of water and fertilizers, which helps with environmental sustainability and leads to significant cost and waste reduction. The use of automated systems can save approximately 50% of resources [19,20] resulting in an economic savings of EUR 450/ha [21]. These aspects highlight how precision agriculture represents a management strategy that offers multiple long-term benefits, including reduced yield variability, improved environmental performance, and significant economic returns [22]. Nevertheless, its implementation and components present some critical elements that must be considered and overcome. The response and reliability of sensors and monitoring systems can be affected by various soil properties, including texture, bulk density, and environmental factors. It has been shown that the performance of various types of sensors is significantly influenced by the composition and structure of the soil. Devices such as the TDR and the Hydraprobe, the latter of which measures electrical conductivity, tend to underestimate soil moisture levels [23]. Sensors measuring the dielectric constant have a fairly linear response to moisture but can also be influenced by the presence of silt, clay, and sand in the soil [24]. Therefore, to reduce measurement errors and improve accuracy, it is necessary to develop specific

calibration formulas for each type of sensor and the specific soil type on which they are used [23]. Monitoring systems face significant challenges, particularly regarding connectivity, power supply, and data transmission, due to the lack of infrastructure, services, and internet access, especially in rural areas. Numerous researchers have developed effective solutions to ensure the continuous and accurate operation of these systems, even in the absence of cellular networks. To address this lack, researchers [25–27] propose monitoring systems using LoRa technology, which enables real-time data transmission over long distances (5–15 km) with low energy consumption [25]. In addition, LoRa technology ensures continuous monitoring at a low cost [26]. The lack of access to electrical supply has promoted the development of energy-autonomous systems for continuous monitoring. The system proposed in the following study [28] involves the use of long-lasting lithium batteries and small photovoltaic panels on individual sensor nodes, intended for soil health monitoring. The system is characterized by good energy efficiency and is capable of operating completely autonomously for an extended period. The authors [27] have implemented a monitoring system based on LoRa technology, equipped with a solar panel for collection and conversion into electricity, successfully powering the entire system and recharging the battery, with residual energy available. An innovative water monitoring system is described in [29], powered by a battery and self-sustained through a hybrid solar-hydroelectric energy collection system. The system uses a photovoltaic panel and a hydroelectric microgenerator, which together ensure optimized energy consumption and allow the system to operate continuously for approximately 432 h. These factors represent significant limitations for these systems, highlighting the need for particular attention from the scientific community. To overcome these challenges, it is essential to ensure operation even in disadvantaged areas while simultaneously enhancing the effectiveness and precision of the suggested solutions. The main proximal sensor technologies will be examined for monitoring soil moisture and nutrients. The aim of this study is to identify improvements in the performance and implementation of these sensors, as well as to highlight the critical challenges that must be addressed to optimize the effectiveness of soil monitoring.

The text is organized as follows: the introduction provides an overview of the need to adopt innovative and sustainable systems, such as IoT systems. It presents some recently developed low-cost systems, focusing on the main challenges to be addressed, particularly in disadvantaged areas. Section 2 analyzes the main technologies used in soil moisture monitoring systems. Section 3 focuses on the technologies employed for monitoring soil nutrients. Section 4 explores the implementation of IoT systems and the various associated communication technologies. Finally, Section 5 presents the conclusions and outlines future directions to improve the reliability of monitoring systems.

2.1.2 Soil Moisture Monitoring Technologies

The control and monitoring of soil-water concentration are essential to help farmers manage irrigation efficiently. Moisture, in addition to influencing the physical characteristics of the soil, is essential for the transport and dissolution of nutrients, making it crucial for crop survival and soil fertility [30]. Soil water exists in two forms: bound and unbound. Bound water refers to the portion adsorbed by soil mineral particles, making it unavailable and unabsorbed by plant roots [31]. In contrast, unbound water refers to water molecules that move freely in the soil and it is available to plants, defined as soil water content (SWC) [31], and expressed either as gravimetric water content (GWC, denoted as θ_g, *Eq.1*) or volumetric water content (VWC, denoted as θ_w, *Eq.2*), according to the formulas [31]:

Equation 1

$$\theta g = \frac{m\omega}{md} => \theta g = \frac{ms - md}{md} * 100$$

Equation 2

$$\theta v = \frac{m\omega}{\rho\omega * (md/\rho d,s)} => \theta v = \theta g * \frac{\rho d,s}{\rho\omega}$$

where $m\omega$ represents the mass of soil sample collect; *ms* is the mass of wet soil; *md* is the mass of dried soil; $\rho d,s$ is bulk density of soil; $\rho\omega$ is the density of water, usually taken to be 1000 kg/m^3 [31]. Direct methods for determining moisture involve the destruction of the sample and prolonged processing times. Gravimetric determination, although very accurate, is now less common as it does not lend itself to the automation of irrigation processes while still playing a fundamental role in sensor calibration. Indirect methods measure soil moisture content by monitoring its physical or chemical properties. Among these are various techniques that enable the efficient management of automated irrigation, which will be discussed in more detail later. However, there are many factors that directly and indirectly influence the distribution of water, including land use, cover, pedology, and climatologic properties [32]. Solar radiation and ambient temperature have an indirect influence on moisture content, as they alter soil temperature and humidity. Evapotranspiration and precipitation, on the other hand, directly affect moisture levels, decreasing it through evapotranspiration or increasing it in the case of precipitation [33]. The structure, texture, and slope of the soil influence water infiltration and drainage: sloped soils allow water to move downward and drain more quickly compared to flat areas [34]. Just as texture affects water drainage in soil, sandy soils with finer textures, like clay, will have

lower drainage compared to coarser-textured soils with a high sand content [33]. Knowing the characteristics of the soil, the crops, and the technologies of monitoring systems is essential for implementing reliable monitoring systems that address the field's specific conditions and the farmers' particular needs.

This section describes the main moisture sensing technologies used in intelligent monitoring systems, illustrating the principle of the operation of the sensors and providing examples of recently implemented systems. Additionally, the main strengths and weak- nesses will be highlighted to better understand the potential, allowing for guidance toward selecting the most appropriate technology.

2.1.3 Tensiometers

The tensiometer measures the matric potential of the soil or the water tension present in the soil. They are made up of a tube with distiller water, a porous ceramic tip attached to the lower end a vacuum gauge, acting as a pressure meter, located at the upper back [35] (see Figure 1). The measurement principle is simple and works in 0–1 intervals [33]. First, the ceramic tip must be placed at the optimal depth and have good contact with the soil to ensure an accurate reading and avoid errors [36]. If the soil is in a saturated condition, an equilibrium will be established between the water in the soil and that in the tube, causing the gauge to indicate a pressure close to atmospheric pressure, tending to 0 [35]. When the soil moisture changes, water is either absorbed or released through the ceramic tip. If the soil moisture is low, water is released from the tube, creating a vacuum inside and generating negative pressure. Conversely, when moisture increases, the vacuum decreases, and the gauge will register positive pressure [36]. These tools are easy to use and cost-effective, with performance unaffected by ambient temperature or soil salinity.

However, they do require specific attention, such as the regular refilling of the tube with water and periodic maintenance to prevent cavitation issues [37]. The authors [37] propose a self-refilling system for the METER T-8 tensiometer, utilizing two solenoid valves connected to the sides of the circuit. The inlet is connected to a 3 L water reservoir. This system, with a relatively low cost (around USD 100), significantly reduces the need for manual refilling, making it especially useful in arid and dry areas where this process needs to be performed more frequently. An affordable IoT tensiometer (USD 76) for measuring soil-water potential has been proposed [35]. It uses an isolated BMP180 barometric sensor connected to an ESP32 microcontroller, which allows for vacuum tension measurements every 6 h. The tensiometer provides high precision in measuring soil-water potential (R^2 = 0.99) down to −80 kPa. Additionally, the prototype is powered by a lithium battery recharged via a solar panel, and, thanks to the deep sleep function, the system is energy autonomous. Data are uploaded to a ThingSpeak platform, where it can be viewed online as a soil-water potential curve. Manufacturer companies such as Ecosearch and Irrometer offer a wide range of commercial tensiometers, ranging from traditional systems to

electronic and IoT models, with relatively affordable costs starting from USD 60 to USD 80 and up [38,39]. Among these, the "Full Range" dry tensiometer produced by Ecosearch Srl (Montone, Italy) stands out. This tensiometer, unlike traditional water-filled models, is capable of measuring soil tension up to 5–15 bar [38], as well as soil temperature. Its operating principle is based on applying a known pressure within the measurement chamber, which is reduced by soil tension; thus, rather than indirectly measuring water tension, it provides a direct measurement of pressure. A summary of the characteristics of the tensiometers is provided in Table 1.

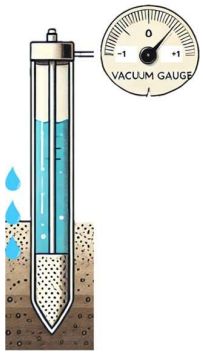

Figure 1. Schematic of a tensiometer's operation in the soil. This instrument, composed of a tube filled with distilled water and a porous ceramic tip, measures the matric potential of the soil. The pressure reading, taken with a vacuum gauge, varies with soil moisture: under saturated conditions, pressure approaches zero, while moisture changes result in negative or positive pressures based on water release or absorption (OpenAI, (2024)).

Table 1. The table presents tensiometers, highlighting their operating principle, strengths, and weaknesses.

Type Sensor	Operating Principle	Strengths	Weakness
Tensiometers	Measurement of soil matrix potential. Working temperature 10–45 °C.	- Affordable. - Simple. - Unaffected by temperature and salinity.	- Frequent maintenance. - Long stabilization times required once placed in the soil (from a few minutes to hours). - Not recommended for sandy soils.

2.1.4 Granular Matrix Sensor

Granular matrix sensors are electrical resistance sensors used to measure soil tension, as shown in Figure 2. The sensor consists of a pair of electrodes embedded in a gypsum block, either cylindrical or rectangular in shape, which is inserted directly into the soil [36]. The sensor transmits a current through the porous medium, with the system's electrical resistance varying proportionally to the amount of water absorbed [40]. When a small voltage is applied to the sensor, it produces a voltage proportional to the resistance of the block. When the soil is moist, water is absorbed by the gypsum, seeking to equilibrate with the soil's moisture. This results in a decrease in the resistance of the electrodes [36].

Figure 2. Granular matrix sensor, composed of a pair of electrodes embedded in a gypsum block.

The sensor can provide the matrix potential value using a specific calibration equation. One of the most common commercial granular matrix sensors is the WATERMARK, produced by Irrometer Company, Inc., Riverside, CA, USA. The Watermark sensor consists of a pair of corrosion-resistant electrodes immersed in a granular matrix that equilibrates with the surrounding soil moisture, providing a reliable measurement of soil-water tension in centibars or kPa [39]. This sensor is widely used in irrigation planning due to its ability to provide accurate data, and it can be read manually or be connected to a data logger for remote monitoring. The effective performance of the Watermark sensor was tested in the study [41]. The system worked well, but a response delay was observed under drought and high humidity conditions. Another significant finding from the study is that the sensor at shallow depths does not provide reliable readings, whereas installations at depths greater than 30 cm proved to be more effective. Additionally, specific calibration for each soil type is necessary to ensure reliable readings. These aspects are confirmed by [42]. Soil-specific calibration improved the accuracy of the sensor; however, the Watermark tends to underestimate moisture levels in coarse-textured soils and when installed at shallow depths. Granular matrix sensors are cost-effective, with prices ranging from USD 60 to USD 300 [39], depending on the size of the sensor and whether an additional data logger for remote monitoring is included. They do not require significant maintenance; however, the strength of gypsum is affected by temperature and tends to dissolve over time. Moreover, the systems requires specific calibration for different soil types because the accuracy is rather poor and can vary widely, between 10% and 25% of the actual measurement [40]. The main characteristics of the Watermark sensor are summarized in Table 2.

Table 2. The table presents the main characteristics of granular matrix sensors used for measuring soil moisture.

Sensor Type	Operating Principle	Strengths	Weakness
Granular matrix sensors	Measurement of soil tension, exploiting the change in resistance of the porous section in the soil. Measuring range: 0 to 200 kPa.	- Easy to use and inexpensive. - Low maintenance. - Good response to soil moisture variations.	- Low accuracy. - Slow response. - Gypsum dissolution. - Influence of T on gypsum strength. - Installation in the surface layers of the soil does not provide reliable results. - Underestimated value in coarse-textured soils.

2.1.5 Thermal Probe

Thermal probes, for determining soil moisture, utilize heat dissipation, measuring the temperature of a porous block or the soil, after the application of a thermal pulse [31]. The basic components of this type of sensor are a thermistor, which serves as a heat source, and a temperature sensor, both embedded in a porous block (made of gypsum or ceramic) and buried in the soil [31]. Heat dissipation sensors exploit the dependence of soil thermal conductivity on temperature and water content [43]. By applying a controlled heat pulse, the maximum temperature increase detected can be correlated to the volumetric water content of the soil [43]. Therefore, these systems relate the measured temperature to the conductivity of the material to obtain an accurate estimate of soil moisture. These can be of different implementations, the characteristics of which are summarized in Table 3.

Table 3. The table compares different thermal probe technologies (SPHP and DPHP) for estimating soil moisture, focusing on low-cost models.

Sensor Type	Characteristics	Strengths	Weakness
Thermal probe	They exploit the soil's thermal conductivity to estimate moisture based on heat dissipation.	- Low-cost sensor. - Temperature measurement. - Long life. - Maintenance-free. - Easy implementation.	- Thermal conductivity is influenced by proprieties of the soil, as well as by the content of organic matter.
Single-probe heat pulse (SPHP)	Uses a single component as a heat source and temperature sensor.	- Low cost. - High sensitivity.	- Few implementations.
Double-probe heat pulse sensor (DPHP)	Component separate.	- Low power. - Accurate sensor. - Cheap. - Easy implementation.	- Calibration for each soil type. - Affected by temperature and environment humidity.
Multi-probe heat pulse sensor (MPHP)	Separate components and multiple temperature sensors.	- Accurate sensor.	- Calibration for each soil type. - Affected by temperature and environment humidity.

A single-probe heat pulse sensor (SPHP) is implemented by [44], consisting of a single element: a bipolar transistor. This transistor acts as a heat source through the base- collector junction, while the base-emitter junction serves as the temperature sensing system. Subsequently, the system is incorporated into a porous capsule, which prevents direct contact with the soil, reducing potential interference and improving accuracy [45]. This encapsulation gives the system greater sensitivity in measurements, thus highlighting its potential as a soil

moisture sensor. A single-element SPHP system is implemented using nanocrystallized materials [46], both as a heat source and a temperature sensor. This technology offers superior sensitivity in measurements compared to previously described systems, making it particularly appealing for moisture monitoring. Additionally, the system is integrated with a microcontroller featuring a Bluetooth module, enabling easy and fast data transmission to mobile devices. Single-probe systems offer numerous advantages for soil moisture determination, including greater sensitivity, especially due to materials highly reactive to moisture changes, such as nanocrystals. Their simple design is based on a single element, making them more compact, less bulky, and low cost. However, there are still few studies in the literature on these technologies, and further research and development are needed, especially for implantation in the field. Double-probe heat pulse (DPHP) sensors feature a heat source and a temperature sensor on two separate probes. In the system proposed by [47] in 2015, the heating element consists of a bent copper wire, designed to increase resistance, enclosed in a steel tube. Meanwhile, a thermocouple is placed on the probe located 3 mm away to serve as the temperature sensor. This DPHP system is low power, powered by lithium batteries and equipped with solar cells for recharging. It is a low-cost solution that offers good measurement reliability. However, a dependency between the measured moisture value and soil density, as well as ambient temperature, has been observed. Therefore, specific calibration that accounts for these factors is essential [47]. These systems can also be configured in a multi-probe setup. A prototype was presented by [43] in 2019, which featured multiple temperature sensors arranged around the heating probe on a planar PCB platform. During the study, the sensor demonstrated reliability in measurements, successfully detecting VWC ranging from 5% to 41% with a sensitivity of 0.632 °C for each 1% change in VWC [43]. Among commercial sensors, Campbell Scientific offers a heat dissipation matric po- tential sensor that measures soil-water potential from −10 to −2500 kPa [48]. Comprising a heating element and a thermocouple embedded in resin within a porous ceramic matrix, the sensor applies a current of 50 mA and measures the temperature increase, which varies based on the water content in the ceramic matrix, influenced by the moisture in the surrounding soil [48]. Generally, these types of commercial sensors require specific soil calibration, are affected by environmental conditions (T and humidity), consume a lot of energy, and have a relatively low accuracy 5–10% [49].

2.1.6 Capacitive Sensor

Capacitive sensors are among the main tools used in low-cost systems for determining the VWC in soil and implementing smart irrigation systems. The probe is shown in Figure 3. They are characterized by their affordability and ease of implementation, and, after appropriate soil-specific calibrations, they provide high accuracy and reliability. They consist of electrodes that function as capacitors, with a hygroscopic material between them; in particular, the soil surrounding the electrodes is a dielectric medium that stores the charge [50].

Capacitive sensors exploit the difference between the dielectric constant of dry soil, ε_{soil} = 2–6, and that of water, which is significantly higher, ε_{water} = 80, at 20 °C [51]. Consequently, the dielectric properties of the soil depend on its moisture content, and its value varies according to the volumetric water content [52]. The capacitive sensor utilizes this property and emits a voltage, the inverse of which can be linearly adjusted to estimate the soil's volumetric water content through gravimetric methods [51].

Figure 3. The photo shows a low-cost capacitive probe designed for soil moisture measurement. The yellow line indicates the "warning line", which marks the part of the sensor that should not be inserted into the soil, while the area between the blue lines identifies the recommended depths for proper insertion into the soil.

This sensor type is known for its affordability and accuracy in readings. It allows for quick and continuous measurements, requiring minimal maintenance after installation. These advantages have sparked significant interest from scholars and researchers, making them one of the most widely used sensors in soil moisture monitoring systems. However, their performance and accuracy are significantly influenced by soil texture and composition, ambient temperature, and the frequency of the alternating current used for measurements, necessitating specific calibrations, the performance and accuracy of such systems are highly influenced by soil composition, ambient temperature, and the frequency of the alternating current used for measurement [51,53,54]. Considering the low cost and ease of implementation, several studies have focused on the development and validation of capacitive sensors for soil moisture monitoring. The solution proposed by Farm21 (Amsterdam, The Netherlands) is easy to install (30 s), factory-calibrated, and maintenance-free. It includes a soil moisture probe (FS21, manufactured by Farm21) and a weather station [55], providing precise data on air humidity and temperature, soil moisture, and soil temperature at varying depths, from 10 to 20 cm for temperature and 0 to 10 cm, 10 to 20 cm, and 20 to 30 cm depth for moisture [55].

The system has a rechargeable battery via USB-C that consumes little power, lasting up to a year on a single charge, and is also included in the Farm21 platform that also provides satellite imagery, scouting, and weather. The initial cost is EUR 295 per sensor, to which is added a cost of EUR 63/sensor/year for connectivity (2G/LTE-M/NB-IoT SIM card provided by Farm21), support, and data storage. It is a robust and reliable system for monitoring and optimizing irrigation and fertilization for applications in broccoli, potato, and apple crops [55]. Several experts have focused on implementing cost-effective and reliable solutions to provide farmers with accurate and reliable evaluations, overcoming some of the major shortcomings of commercial systems. As an example of the development

of generalized calibration equations relating the dielectric constant to soil properties and characteristics and possible solutions to sensor sensitivity to soil properties, several authors [56] highlight the higher accuracy of capacitive sensors compared to resistive sensors in determining moisture by means of the Spearman coefficient, which have r_s = 0.93 and 0.87, respectively. Furthermore, accuracy and performance are improved in relation to the manufacturer's specifications through specific calibration. The simplicity and reliability of SKU: SEN0193 (DFRobot, Shanghai, China), has been studied and tested [57] for its potential use in automatic humidity monitoring. The proposed system has proven reliable in predicting water content for organic-rich soils and distinguishing three different levels of soil moisture: dry to moderately moist, field capacity, and saturated. However, the study shows significant sensor-to-sensor variability, of 5% for the four sensors SKU: SEN0193 used [57]. The authors [58] propose a solder mask plus acrylic paint as an effective solution to salt water interference, which is one of the main problems with dielectric techniques. The intelligent monitoring system consists of an air temperature and humidity sensor (DHT11 sensor), soil temperature sensor (DS18B20), and capacitive soil moisture sensor, manufactured in a workshop for electronic industries in Egypt; the power supply unit comprises 120 W-22 V-6 A photovoltaic panels. In the study, both sensor-to-sensor variability and variability in measurements and replications of the sensor response are recognized; however, the coefficient of the variation of such sensors is less than 25%, providing high performance in estimating moisture content in clay soils. Several authors [59] proposed an individual calibration per sensor as the best option, especially if it was supplied with low voltage; the 3.3 V option produced the best correlation between SWC and sensor output (R^2 = 0.871) compared to the 5.5 V option (R^2 = 0.798) [59]. The existence of a temperature dependence on the sensor response has also been demonstrated, although with minimal effects. For a change of 20 °C, there was a variation in water content of 0.015 m^3/m^3 [59]. Various low-cost capacitive probes are available on the market, with prices ranging from USD 2 to USD 15 per probe.

This economic advantage has made it possible to develop remote monitoring systems, as these probes can be easily integrated with common microcontrollers like Arduino and ESP32 [14,16,28,60]. Thanks to this accessibility, it is possible to implement systems with multiple sensors, allowing for the coverage of large monitoring areas and resulting in more detailed and representative data, thereby enhancing the effectiveness of water resource management. The main characteristics of the described capacitive sensors are summarized in Table 4.

Table 4. The table compares and summarizes different capacitive sensor technologies for measuring soil moisture, highlighting their characteristics, strengths, and weaknesses.

Sensor Type	Characteristics	Strengths	Weakness
Commercial capacitive sensor [55]	Measures the electrical capacity, i.e., the potential difference between two conductors to determine VWC.	- Provides real-time moisture change data. - Large measuring range. - Fast response. - Chemical resistant. - Small and compact. - Low maintenance.	Calibration. - Strong influence of T. - High costs and possible extra costs for assistance.
SKU: SEN0193-Capacitive sensor [57]		- Inexpensive prototype cost USD 45.7. - Low operating current 5mV. - Corrosion resistant.	- Specific soil calibration required. - Variability between devices makes a specific calibration for each sensor appropriate. - Sensitivity to the effects of salinity and soil structure.
Capacitive sensor [58]	Intelligent monitoring system with an operating frequency 430 kHz.	- High performance in moisture content estimation (CV < 25%). - Accurate and robust system. - Energy autonomy. - Real-time monitoring of soil and environmental conditions. - Salinity-insensitive probes.	- Variability between sensor and sensor; CV = 0.045 implies a specific calibration per sensor and soil type.
SKU: SEN0193-capacitive sensor [59]		- System's ability to measure daily and seasonal humidity variations. - Low voltage (3.3 to 5.5 V). - Isolated system not sensitive to the presence of salts. - Economic system (total cost USD 162.56). - Minimal temperature dependence. - Low energy consumption due to low-voltage operation that reduces energy demand by 40%.	- Medium accuracy. - Individual calibration, requiring time and specialized labor. - Low sampling volume. - Sensitive to interference and short life expectancy.

2.1.7 Time-Domain Reflectometry (TDR) and Frequency-Domain Reflectometry (FDR)

TDR is an accurate and established measurement method for soil dielectric permittivity and moisture content. These consist of a transmission line, i.e., metal probes, placed in the soil, as shown in Figure 4. TDR sensors estimate the VWC by determining the bulk dielectric constant, K, of the soil through the measurement of the propagation time of an electromagnetic pulse along the sensor [61]. An average of the water content in the examined volume is therefore performed; therefore, such techniques do not give precise information on water content. These systems are characterized by their high accuracy, with precision within 1–2% of the volumetric water content [62], and they require minimal calibration. Additionally, they enable fast, simple, and continuous measurements, providing excellent spatial and temporal resolution [62]. It has become popular in soil-water content determination due to its simplicity, speed of acquisition, accuracy, and high resolution; it can be used up to a frequency of 1 GHz [63]. However, as well as the high initial costs, salinity affects the signal, causing a loss of reflection, and the increase in conductivity due to the rise in soil moisture is one of the main factors that makes these systems little used by farmers [63]. The authors [64] describe the TDR 20/20 sensor (supplied by AEA). This consists of two parallel probes for measuring the strength of soil with a predetermined

volumetric water content. Good accuracy in determining the moisture content of sandy and clayey soils has been demonstrated. In particular, the TDR maintains its accuracy down to a water content of less than 30 per cent for clayey soils. As soil moisture increases, the sensor tends to overestimate moisture content, reducing performance accuracy. Other authors [65] attest to the effectiveness of the TDR-315L sensor in moisture determination for various soil types, using the factory calibration function.

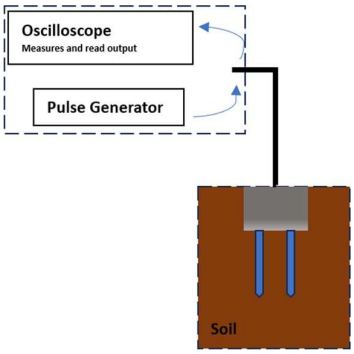

Figure 4. The image illustrates the principle of Time-Domain Reflectometry (TDR). A generator sends an electromagnetic pulse along a probe inserted into the soil, while the oscilloscope records the pulse reflection time. This measurement allows the calculation of the soil's dielectric constant, enabling the determination of the soil's water content.

Ecosearch (Montone, Italy) offers multiple solutions for soil studies, including several TDR sensors that are easy to use and available for limited budgets. The TDR 300 is a next-generation instrument that is portable and powered by AAA batteries. It offers the possibility of integrating a GPS to georeferenced points of measurement and interest. Data are stored by a data logger and easily viewed via the display on the instrument; this can be displayed as raw data, VWC and relative water content (RWC). It offers precise calibrations for different soil types; however, high clay content, EC > 2 ds/m, and high organic content effect sensor performance and device reading [66]. FDR provides an estimation of soil moisture based on the variation in the frequency of a signal, which reflects the dielectric properties of the soil [67]. FDR probes are accurate methods for soil moisture measurements, presenting a good correlation (R^2 = 0.99) between moisture values estimated by FDR and values estimated by the gravimetric method [68]; in addition, more precise and accurate measurements are obtained after specific soil calibration (±0.01 $ft^3 ft^{-3}$) [67]. These systems have various applications in agriculture [69–71], but the high costs, the demand for specialized personnel, and the sensitivity of sensors to influences make such systems uncommon. The main disadvantage of FDRs is temperature sensitivity: they tend to overestimate soil moisture with increasing temperature [72], but it is possible to significantly reduce measurement errors and improve measurement accuracy through specific calibration, considering the impact of temperature as proposed by [72]. The performance and response of the sensor can vary based on the type of sensor and substrate, bulk density, electrical conductivity

(EC), and soil temperature. Therefore, it is essential to consider these factors during the calibration phase [73–75]. The advantages and disadvantages of TDR and FDR are summarized in Table 5.

Table 5. The table compares two sensor technologies for measuring soil moisture: Time-Domain Reflectometry (TDR) and Frequency-Domain Reflectometry (FDR).

Sensor Type	Characteristics	Strengths	Weakness
TDR	The TDR sends an electromagnetic pulse along a probe inserted into the soil. It measures the time of reflection of the pulse to calculate the dielectric constant of the soil, which is influenced by the water content.	- High accuracy (within 1–2% of volumetric water content). - Minimal calibration requirements - Fast, continuous, and precise measurements - Excellent spatial and temporal resolution.	- High initial costs, exceeding USD 100 per sensor. - Sensitivity to soil salinity, which can cause loss of signal reflection. - May require complex equipment and a solid technical understanding for installation and use.
FDR	Measures soil moisture through the variation in the frequency of a signal that reflects the dielectric properties of the soil.	- Rapid and continuous measurements. - Low maintenance. - Good accuracy when properly calibrated.	- Sensitive to soil salinity and temperature. - Requires specific calibrations for different soil types. - Lower accuracy compared to TDR in certain applications - .

2.1.8 Cosmic Ray Neutron Sensor (CRNS)

These are among the most accurate tools for determining soil moisture, particularly utilizing the properties of hydrogen nuclei present in water. Through thermalization, a dispersion or slowing of these nuclei is induced [31], enabling the precise measurement of moisture content. They consist of a neutron source connected to a detector. When neutrons are released from the radioactive source, they disperse into the soil and collide with hydro- gen atoms they encounter, causing a change in their speed. The detector then measures the density of thermalized neutrons in the system, allowing for an accurate assessment of soil moisture content [31]. It has been demonstrated that, through careful calibration, it is possible to achieve an accuracy of 0.02 in VWC [36], making them reliable and precise tools for monitoring soil moisture. The suitability of this technique for the implementation of automated irrigation systems has been evaluated, as it has many advantages over other methods. This is a non-invasive and easy-to-use method; in addition, the neutrons integrate naturally in an area with a radius of about 150 m and a depth typically of 2–4 dm [76], allowing an assessment of soil moisture distribution at different depths and offering a representative moisture measurement of a large area. The measurement can take place by means of stationary or itinerant CRNS. The first provides average SWC measurements on a hectare scale, ensuring continuity without the need for maintenance over time. In contrast, the vehicle-mounted CRNS can reveal spatial patterns of SWC on a mean scale but only on survey days [77]. In their work, the authors [78] show the good roving capability of CRNS, proposing a mobile system for the continuous monitoring of SWC on larger scales and at different depths. However,

its technical implementation, data processing, and interpretation are complex [77]. They are also versatile and reliable tools for obtaining a high spatial resolution mapping of soil surface moisture by aerial over flight, as proposed by GNSS-R measurements were taken, and using the proposed model, moisture maps were created with a spatial resolution of 100 m, illustrating large differences between irrigated and non-irrigated areas, with good accuracy, an RMSE of 0.07 m^3/m^3. The advantages and disadvantages of CRNS are summarized in Table 6.

Table 6. The table compares two sensors for measuring soil moisture, CRNS and the Finapp Probe, outlining their main characteristics, advantages, and weaknesses.

Sensor Type	Characteristics	Strengths	Weakness
CRNS	It uses a radioactive source and measures soil moisture by exploiting the properties of hydrogen nuclei; the neutrons collide with hydrogen atoms, changing their speed.	- Efficient, fast, and reproducible. High accuracy, better ±0.02 in volumetric water content, with correct calibration. - Non-invasive.	- Radiation hazard. - Skilled operators. - Laborious and expensive method. - Long calibration times.
FinApp Probe (FinApp start-up, Pavpva) [48]	Uses CRNS technology for soil moisture measurement.	- Non-invasive. - Large-scale measurement (1–20 ha). - Independence from soil properties. - No calibration, easy to use and install. - Compact and lightweight instrument. - Obtaining detailed soil moisture maps. - Decision support for irrigation.	- The sensor is unable to control irrigation.

This section provided an analysis of various low-cost soil moisture monitoring systems, emphasizing their crucial role in agricultural irrigation management. The different sensor technologies discussed—including tensiometers, granular matrix sensors, thermal probes, capacitive sensors, TDR, FDR, and neutron moisture sensors—each offer distinct principles, components, advantages, and limitations. Tensiometers effectively measure soil matrix potential, while granular matrix sensors utilize electrical resistance to assess water tension. Thermal probes and capacitive sensors provide alternative methods for evaluating moisture content, with capacitive sensors known for their high accuracy and ease of use following calibration. TDR and FDR are well-established techniques that offer precise soil moisture measurements, although TDR is often associated with higher costs. Neutron moisture sensors stand out for their non-invasive capabilities, allowing extensive assessments of soil moisture distribution over larger areas. Each sensor type has unique characteristics, making them particularly suitable for specific agricultural applications. In conclusion, these low-cost soil moisture monitoring solutions are essential for improving irrigation efficiency. By enabling the real-time monitoring of soil moisture levels, they play a crucial role in optimizing water resource management and promoting sustainable agricultural practices. As technology advances, these systems will become increasingly accessible and effective, further supporting farmers in their efforts to maximize productivity and avoid the depletion of water resources.

2.1.9 Soil Nutrient Monitoring Technologies

It is well known that monitoring humidity and temperature is crucial for an optimal irrigation plan, while monitoring soil properties, such as pH, nutrients, salinity, electrical conductivity helps to understand soil characteristics and health to

optimize fertilization management. The use of fertilizers and pesticides is necessary for the growth and protection of crops. However, excessive and inappropriate use has negative repercussions on the environment, soil and crop health, water resources, and, consequently, on human health. Indeed, when in excess, unused nutrients are retained in the soil and contaminate soil and water through leaching and runoff [79]. Conversely, their deficiency negatively affects crop growth and productivity. Therefore, it is important to emphasize the significance of automated and accurate monitoring systems that take into account the spatial and temporal variability of nutrient concentrations. These systems are essential for avoiding unnecessary and inefficient applications, promoting an optimal and localized application of nutrients, and thereby contributing to the reduction in agronomic and economic losses [79]. Nitrogen is the principal nutrient for plant growth, it is primarily found in the soil, where its concentration depends on the soil type, microbiological and physico-chemical interactions, environmental conditions, and, during the growing season, mineralization, immobilization, and uptake [5]. Plants cannot utilize atmospheric nitrogen directly, so adding chemical nitrogen makes it available and usable for plants; however, overdosing decreases the chlorophyll content, and the plant dries out [78]. Phosphorus and potassium deficiencies also affect plant development and yield. Their deficiency or excessive concentrations cause significant yield losses and toxicity problems in plants [31]. Analytical determinations, while being highly accurate traditional techniques, have significant limitations in terms of cost, analysis time, and sample destruction. To overcome these limitations, the scientific community is focusing on the development of smart agricultural practices. Real-time monitoring through the use of sensors and precision agriculture technologies allows for the collection of valuable data on nutrient concentrations without compromising the integrity of the sample. The authors [80] propose a high-precision automated system for monitoring soil nutrients, consisting of a pH sensor, a soil moisture sensor, and a fiber-optic NPK sensor. The data collected by the sensors are transmitted to an Arduino UNO microcontroller and sent to a web server via a GSM module. The system compares the acquired data against a reference dataset and sends real-time notifications to the farmer. Through a specific predictive algorithm, the system was able to accurately determine the type and quantity of fertilizer to be used, ensuring an accuracy of 90% [80]. With the IoT configuration, the data are transmitted to the cloud and compared against the threshold values for each measured parameter. This allows for a comprehensive soil analysis, with data easily viewable on the website, enabling the selection of the best crop based on the detected soil characteristics and facilitating timely and informed intervention when necessary. Sensors for monitoring soil nutrients are based on various sensing techniques, ranging from spectroscopic and electrochemical systems to electromagnetic methods. Each approach will be discussed individually, focusing on the positive aspects and potential gaps to be filled. This aims to assess the effectiveness of various technologies and identify aspects for improvement to optimize soil nutrient monitoring.

2.1.10 Electrical and Electromagnetic Sensors

Electrical and electromagnetic sensors operate based on the determination of the apparent electrical conductivity (Eca) of the soil [17] by measuring the soil's ability to accumulate or conduct an electrical charge. These sensors can be categorized into two types based on their need to make contact with the soil and their configuration (Figures 5 and 6). Systems that measure electrical conductivity consist of a transmitter that induces a magnetic field in the soil and a receiver that measures conductivity. These sensors do not require direct contact with the soil and operate at relatively low frequencies [79] to generate an electric current. As a result, the magnitude of conductivity is determined by the generated magnetic field [79], enabling non-invasive and continuous measurements. Electrical resistivity measurement sensors require direct contact with the soil and con- sist of two electrodes. One is used to generate an electric current in the soil, while the other measures the potential difference, which represents the soil's resistivity [79]. Both types of sensors allow for continuous and non-invasive measurements, providing accurate monitoring of the soil's electrical properties.

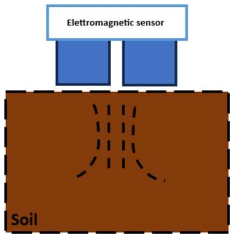

Figure 5. Electromagnetic sensor, composed of a generator that creates an electromagnetic field in the soil and a detector that detects the induced variations to determine the soil's electrical conductivity.

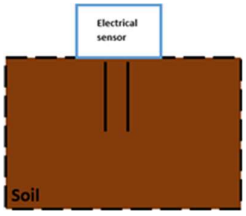

Figure 6. Electrical sensor, composed of two electrodes, one of which generates an electric current in the soil, while the other acts as a receiving electrode, detecting the variation in electric potential. This measurement allows for determining the soil's electrical resistance, which is closely related to its electrical conductivity.

Additionally, by varying the magnetic field strength in the first case and the distance between the electrodes in the second, it is possible to determine the apparent electrical conductivity (Eca) at different soil depths [12,79]. Changes in the soil's chemical and physical makeup affect how well it conducts electricity and, consequently, the EC detected by the sensor [81]. The type and amount of fertilizer, texture, soil moisture, irrigation system, and pH significantly influence soil EC, and thus the response of the EC sensor; so, when applying EC sensors

to monitor nutrient levels, several factors must be considered [82]. METER Group, USA, offers a next-generation CE probe. The Teros 12 sensor measures soil moisture, temperature, and electrical conductivity. It is small and compact, easy to install, and inexpensive and has a maximum measuring volume of about 1 liter. Gives accurate measurements as it works with low frequency (70 MHz), minimizing the effects of salinity and soil structure [83]. The authors [82] indicate the suitability of the Teros 12 sensor in monitoring soil nutrients. In particular, the addition of inorganic fertilizers was observed to increase the soil EC response, showing a strong positive correlation with soluble nutrients [82]. Nitrogen, in particular, had a significant impact on the sensor's response, suggesting that the Teros 12 is an effective commercial tool for monitoring soil nutrients and supporting crop development. However, its high cost (USD 300–500) makes it less accessible for many farmers. The study [81] demonstrates the suitability of these instruments for monitoring soil nutrients, highlighting the correlation between the apparent electrical conductivity (Eca) of the sensor and the nutrients, with excellent confirmation for nitrogen. However, while the sensor is useful for identifying the presence of nutrients, it does not provide precise determinations of their concentrations, thus limiting its practical application. The authors [84] propose an effective method for performing ion-selective measurements. The study was conducted on a soil paste enriched with known concentrations of electrolytes. By utilizing frequencies ranging from 20 to 250 kHz, an accurate identification of cations was achieved. In particular, these frequencies proved useful for the determination of K + (R^2 > 0.85) and Ca^2 + (R^2 > 0.86) [84]. Electric and electromagnetic sensors provide non-invasive soil monitoring, particularly those systems that measure conductivity, which do not require direct contact with the soil. This minimizes alterations to both the soil and the instrument used. Their versatility allows them to be used in different soil types, facilitating the determination of Eca at various depths. However, these sensors are complex and have a high sensitivity to electromagnetic interference and soil salinity, which can compromise the reliability of measurements. Furthermore, the high costs associated with these sensors make their implementation in low-cost IoT systems difficult. These aspects are summarized in Table 7. The implementation of this technology in low-cost monitoring systems is still limited, but given their importance in performance, it is desirable to integrate them into economical solutions and improve their effectiveness. The market offers various components at affordable prices, starting from just a few dollars, up to more expensive sensors with prices exceeding USD 100. For example, the Teros 12 sensor costs between USD 300 and USD 400. Greater accessibility to these technologies would support more sustainable soil monitoring, promoting more responsible and productive agricultural practices.

Table 7. The table compares various types of sensors for soil monitoring, including non-contact sensors, contact sensors, and the TEROS12 sensor. It details the key characteristics of each type.

Sensor Type	Characteristics	Strengths	Weaknesses
Non-contact soil sensor	They measure electrical conductivity through the magnetic field generated in the soil. These systems consist of a generator and a detector.	- Low frequencies. - Not invasive.	- Not ion-selective. - Sensor reading influenced by soil structure and moisture.
Contact soil sensor	It measures the electrical resistivity of the soil. The system consists of two electrodes.	- Low frequencies. - Not invasive.	- Not ion-selective. - Sensor reading influenced by soil structure and moisture.
TEROS12	The sensor measures soil moisture, temperature, and electrical conductivity.	- Non-invasive measurements. - Continuous monitoring. - Versatility in use for various soil types. - Accuracy in measuring moisture and temperature. - Accuracy in measuring nutrients, with excellent confirmation for nitrogen.	- High cost (USD 300–500). - Sensitivity to external interference. - Does not provide precise measurements of nutrients like NPK.

2.1.11 Electrochemical Sensors

Electrochemical sensors use electrodes to detect and quantify nutrients in the soil. These sensors include ion-selective electrochemical sensors (ISEs) and ion-sensitive field- effect transistors (ISFETs) [79], both capable of selectively detecting specific ions. The sensors are equipped with a selective element to recognize the ion to be detected, such as using a selective membrane, and a reference electrode to measure the electrical potential difference between the soil and the reference solution expressed in mV [79]. ISEs are commonly used because of their excellent performance and ability to measure soil quality directly. They can be placed in direct contact with the soil, allowing for fast and accurate measurements. These sensors can operate either in direct contact with a wet soil sample or in soil solution. The miniaturized electrochemical sensor developed by the authors [85] represents an important advancement in the monitoring of nitrates in the soil. Its design for direct contact with the ground allows for more precise and timely measurements. The use of a nanocomposite of molybdenum disulfide (POT–MoS2) and poly(3-octyl-thiophene) is an innovation that leverages the unique properties of these materials, enhancing the sensor's sensitivity due to their excellent electrical characteristics and stability. The working electrode uses a patterned gold electrode coated with a selective membrane for nitrates. This method enhances selectivity towards nitrates and ensures specific and reliable results while reducing the risk of interference from other ions in the soil. Calibrating the sensor with standard solutions and extracted soil solutions ensures its versatility and reliability. The results show the ability to detect nitrates in a range of 1–1500 ppm NO_3^- [85], highlighting the sensor's importance for agricultural applications. The authors [86] analyzed the performance of various membranes for measuring soil nutrients using a real-time ISFET sensor. The study revealed that the response of nitrate membranes, using tetradodecylammonium nitrate (TDDA) or methyltridodecylammonium chloride (MTDA), and valinomycin-based potassium membranes is influenced by both the type of membrane and the nature of the soil extractor. The nitrate membrane based on TDDA has shown remarkable ability to detect low concentrations of nitrate in the soil, reaching up to approximately 10^{-5} mol/L NO_3^- [86]. On the other hand, the

valinomycin-based membranes have demonstrated satisfactory selectivity performance in measuring potassium, even in the presence of interfering cations. These results emphasize the importance of optimizing the membranes to develop more sensitive and reliable sensors. These sensors should be capable of operating effectively even in complex environments where the presence of other ions can strongly influence and cause interference in measurements. An ISE sensor has been developed in [87] for the determination of nitrate in soil, utilizing electrochemical impedance spectroscopy (EIS). This device allows for direct and continuous real-time measurements, eliminating the need for soil pretreatment, and has demonstrated excellent reliability, particularly within the nitrate range of 5 to 512 ppm. During a continuous monitoring period of 7 days, the sensor conducted hourly measurements and required a stabilization time ranging from 12 to 24 h. The results confirmed the sensor's stability and reliability, highlighting an error rate of less than 5% and a coefficient of variation below 20% in long-term nitrate concentration measurements [87]. An IoT device was developed in [88] for the quantification of nutrients in soil. The system comprises an ISFET pH sensor, a soil moisture sensor, and an RGB color sensor, all integrated into the Arduino MEGA 2560 microcontroller board, which is responsible for data acquisition and processing. The integration of machine learning algorithms has made it possible to measure macronutrient levels in the soil with a high degree of precision. In particular the predictive models achieved high accuracies: 95.83% for nitrogen, 98.10% for phosphorus, and 93.75% for potassium [88]. Electrochemical sensors are sophisticated devices that monitor the chemical composition of soil by detecting specific nutrients such as nitrates, potassium, and phosphorus. These sensors are crucial for optimizing agricultural management due to their high sensitivity and fast response times. However, the high costs of the electrodes, which range from USD 300 to over USD 1000 [89], can pose a barrier to broader adoption. Though accurate and portable, further studies are required to improve their accuracy, durability, and selectivity. Their main limitations include high costs, susceptibility to environmental factors, and the need for a good understanding of soil conditions, as well as careful selection of the membrane to avoid inaccurate readings. The strengths and weaknesses of electrochemical methods are summarized in Table 8, highlighting the positive aspects and areas that require further development.

Table 8. The table provides an overview of electrochemical sensors used for the detection and quantification of nutrients in the soil. It outlines the main characteristics of these sensors, along with their strengths and weaknesses.

Sensor Type	Characteristics	Strengths	Weaknesses
Electrochemical sensors	The sensors utilize electrodes to selectively detect and quantify nutrients in the soil. They require a selective element and a reference electrode. The most common types are ion-selective electrodes (ISEs) and ion-sensitive field-effect transistors (ISFETs). Additionally, they can operate in direct contact with the soil or in solution.	- Ion selective. - Measurement of pH and NKP. - High sensitivity. - Rapid measures. - Real time.	- High cost (USD 300–1000). - Minimal sample preparation required. - Requesting specific membranes for each nutrient.

2.1.12 Optical Sensor

Multiple and diverse technologies are employed in the implementation of optical sensors. Reflectance spectroscopy is used in optical sensing to determine how much energy is absorbed or reflected. The main spectroscopic methods used in soil monitoring are based on ultraviolet (UV), visible (VIS), and infrared (IR), enabling rapid and non-destructive measurements [90]. NIR systems are based on the theory of harmonic oscillations, which analyzes the molecular vibrations of the bonds between atoms [90]. When the soil is irradiated with frequencies similar to the vibration frequencies of the bonds, part of the radiation is absorbed while the rest is reflected (see Figure 7). The reflectometer measures the reflectance, generating a spectrum that shows the energy absorbed as a function of the radiation wavelength. This spectrum enables the rapid identification of molecules, as each molecule has a characteristic absorption peak. Research [91] has identified specific wavelengths capable of detecting potassium (K) and phosphorus (P) content with good sensitivity. In particular, the 420–480 nm band has proven sensitive to K content, while the 620–660 nm band has shown notable sensitivity to P content. The authors [92] confirm the reliability of these wavelengths and describe an optical NPK sensor that uses an LED as a transmission system and two photodiodes to measure nutrient intensity in the soil. This system has been able to detect NPK nutrients at the respective wavelengths of interest: 950 nm, 660 nm, and 470 nm. These results highlight the importance of Vis–NIR spectroscopy as an effective tool for monitoring soil nutrients.

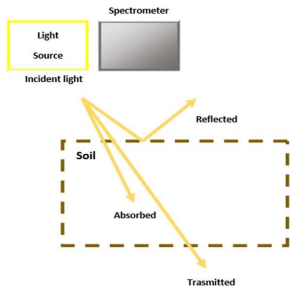

Figure 7. Simplified diagram of the operating principle of a VIS–NIR spectrophotometric system: incident light strikes the sample, and the sensor detects the reflected or transmitted light, analyzing the intensity at different wavelengths to determine the soil composition.

Raman spectroscopy measures the change in wavelengths and interaction of scattered light after interacting with a soil sample. Specifically, photons are re-emitted at different frequencies, known as the Raman effect [90]. This process generates a frequency spectrum that provides detailed information about the chemical structure of the molecule, aiding in its identification. The authors [93] analyzed the effectiveness of Raman spectroscopy for determining phosphorus in soils, operating at a wavelength of 785 nm. This wavelength proved particularly advantageous as it allows for enhanced sensitivity in the detection of phosphate compounds. The study conducted by other authors [94] confirms the effective- ness of Raman spectroscopy for phosphorus analysis in soils. The relationship between phosphorus concentration in sandy soil and the corresponding Raman spectra was examined. The calibration results demonstrated excellent accuracy, highlighting the potential of Raman spectroscopy as a promising method for phosphorus detection. Attenuated Total Reflectance (ATR) spectroscopy operates similarly to infrared techniques, but with some key differences. Instead of directly illuminating the samples, it utilizes a crystal that receives the incident energy [95]. This crystal, placed in direct con- tact with the sample, creates an evanescent field between them due to the reflection of the energy [95]. The energy then propagates from the crystal to a spectrometer, where a specific spectrum for the analyzed sample is generated. ATR spectroscopy allows for an accurate determination of various soil properties, including nitrogen content, moisture, and organic content [90]. However, direct determination using ATR spectroscopy requires minimal sample preparation but can be affected by potential interferences from water and soil constituents. Additionally, it is crucial to carefully select the type of crystal to be used, as this choice can influence the sensitivity and accuracy of the measurements. The characteristics of optical sensors are summarized in Table 9. A nutrient detection system for soil is proposed [96], utilizing an optical sensor designed for monitoring macronutrients in an IoT context. The data recorded by the sensor re processed by an Arduino UNO board, which allows the conversion of the information into the corresponding values of macronutrients through a dedicated program. The obtained values are transmitted to the cloud via a pair of LoRa units interfaced with ESP8266. The system has demonstrated an error rate of between 1% and 2%, thereby highlighting its accuracy in determining soil macronutrients such as nitrogen (N), potassium (K), phosphorus (P), and soil pH. Several sensor technologies used in soil nutrient monitoring have been examined, with a particular focus on electrical, electrochemical, and optical sensors. Electrical and electro- magnetic sensors, such as the Teros 12, provide non-invasive, continuous measurements of the soil's apparent electrical conductivity (Eca), making them suitable for various agricul- tural applications. Electrochemical sensors, including ion-selective electrodes (ISEs) and ion-sensitive field-effect transistors (ISFETs), offer rapid and

precise nutrient detection capabilities, although their cost may limit accessibility. Optical sensors, which utilize techniques such as Vis–NIR and Raman spectroscopy, enable quick, non-destructive assessments of soil properties and nutrient concentrations. Each type of sensor has specific advantages and limitations. For example, electrical sensors are effective for Eca and nutrient monitoring but are sensitive to electromagnetic interference. Electrochemical sensors excel in nutrient specificity, but they are often costly and can be influenced by environmental factors. Optical sensors provide high accuracy and non-destructive analysis, yet they may require sophisticated calibration and can be sensitive to soil conditions. Overall, although these sensor technologies have proven useful for agricultural management, their integration into low-cost IoT systems requires further development. Future efforts should focus on improving affordability and reliability to enable broader adoption. This approach would promote sustainable agricultural practices and optimize resource management, encouraging more efficient and responsible agriculture.

Table 9. The table presents a comparison of different types of sensors used for soil analysis, highlighting their characteristics, strengths, and weaknesses. It includes NIR systems, Raman spectroscopy, and ATR spectroscopy, each with specific methodologies and applications in measuring soil composition.

Sensor Type	Characteristics	Strengths	Weaknesses
NIR systems	They use the reflectance of light in the visible and infrared bands to analyze Soil composition. Typically Operate in the 400 nm to 2500 nm.	- Detailed information on nutrient availability. - Fast and non-destructive measurement. - Minimal sample preparation Required. - Good sensitivity for detection of specific nutrients.	- Possible interference from Moisture and other soil components.
Raman spectroscopy	It is based on the inelastic scattering of light, mainly by A laser, which causes changes in the frequency of Photons. It operates in the Near infrared (NIR) and infrared (IR) range but can also cover the visible.	- Non-destructive. - Provides detailed information on molecular structure. - Can be used for in situ analysis with portable devices.	- Strong dependence on excitation wavelength. - It can be affected by optical interference.
ATR spectroscopy	It uses an ATR crystal that receives incident infrared energy, creating an Evanescent field that penetrates the sample in direct contact. It typically Operates in the medium to	- High accuracy in measurements, provided appropriate calibration techniques are adopted. - Requires minimal sample preparation. - Non-destructive analysis. - Possibility of rapid and direct	- Sensitivity to interference from water and soil Components. - The crystal must be chosen Carefully to optimise Sensitivity.

2.1.13 IoT Systems for Soil Monitoring

IoT (Internet of Things) systems represent a network of interconnected physical de- vices that collect, share, and analyze data via an Internet network [95]. These systems, equipped with sensors and software, operate autonomously without the need for human intervention, ensuring real-time monitoring and efficient information management. IoT systems follow a general architecture composed of various interconnected layers, each playing a fundamental role in ensuring the entire process of data collection, processing, and action automation. This structure is outlined in Figure 8 and includes elements ranging from physical sensors to digital services and automation tools, which together enable the development of advanced applications. The physical layer is responsible for the data collection phase. It consists of sensors used to detect specific data, such as temperature, soil moisture, and NPK concentration. Each sensor node is equipped with a microcontroller, such as the ESP8266 and ESP32, by Espressif Systems (Shanghai, China), and Arduino UNO, Arduino Mega manufacted by Arduino (Monza, Italy), to which sensors and actuators are connected via digital interfaces and includes wireless or wired transceivers for com- munication between individual nodes. The actuators include transducers and electronic circuits that are activated in response to commands sent by the microcontroller [97]. Each sensor and device in the system are equipped with an identification code, such as digital codes or labels, which facilitate recognition and communication with the cloud, enabling real-time data visualization and sharing [95]. Furthermore, IoT systems require a power source connection, such as a battery, USB, or direct electrical grid connection, and may also be supported by a photovoltaic panel.

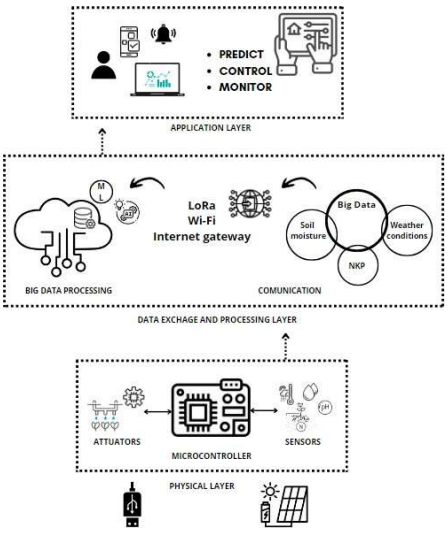

Figure 8. Schematic diagram of the IoT monitoring sensor system.

Data transfer occurs via an Internet connection, which enables the collection and trans- mission of data from sensors and the sending of commands to actuators. Depending on the type of network used, data exchange can occur in two ways: through direct communication, where sensors and actuators have an integrated Internet module that connects them directly to the cloud, or through an Internet gateway system that links the individual components of the physical layer to the network [97]. The first configuration is preferred in contexts where energy conservation is essential, such as battery-powered IoT systems. Conversely, a direct network may be more advantageous in situations where rapid and immediate communication is required. In the cloud, big data are stored, analyzd, and processed, representing one of the most critical phases of the IoT system. Using advanced algorithms, machine learning (ML), and artificial intelligence (AI), raw data are transformed into useful, understandable, and easily accessible information for farmers. This process enables them to make informed decisions based on accurate data. The characteristics of an optimal data processing layer are described in [98] and include the following: interoperability: to facilitate collaboration and information exchange between heterogeneous nodes; scalability management: the layer should automatically apply necessary adjustments when the system undergoes changes; data protection and privacy: ensuring data protection through encryption and safeguarding privacy. The application layer is responsible for the interaction between the system and the end user. It offers digital services for managing and utilizing the acquired and processed information. It relies on a user interface, which can be a mobile app or a website, through which operators can easily view real-time data, send commands, and access historical details. This layer manages notifications and alerts, informing the user in case of detected anomalies. However, a simple and intuitive user interface is essential to enhance the usability and effectiveness of the IoT system. One of the key aspects of IoT systems concerns the choice of communication technologies. These must ensure high-speed, reliable, and efficient data transmission. Additionally, since the process involves significant energy consumption, the chosen technologies should also enable low-power communication, such as that facilitated through Internet gateways. Wireless networking represents a communication technology that uses radio waves to facilitate data exchange between devices. Wi-Fi offers high transmission speeds and supports the rapid transfer of large amounts of data. Although it was not specifically designed to optimize energy consumption or cover long distances, it is still widely used in IoT application. The applicability and reliability of Wi-Fi in IoT systems for the agricultural sector have been demonstrated through numerous implementations of low-cost IoT solutions [13–16]. Thanks to its ability to transmit large amounts of data quickly, this technology proves useful for monitoring and optimizing agricultural operations. However, Wi-Fi is not particularly suited for applications that require wide coverage or low-energy devices, as its limited range and relatively high energy consumption can pose challenges in rural contexts or expansive areas. Wireless sensor networks

(WSNs) consist of a series of distributed nodes that collect and transmit data related to various environmental parameters, such as temperature, humidity, and pressure, to a central node. Each node is equipped with a wireless module, enabling direct communication between the sensors and a gateway, which acts as the central node for data management and processing [98]. This architecture allows for the continuous, real-time monitoring of the environment, enhancing operational efficiency and facilitating the collection of critical information for informed decision-making. In [18], the authors developed an autonomous fertirrigation system that utilizes the WSN protocol for communication. This communication technology is characterized by low costs and reduced energy consumption, thanks to its decentralized architecture. WSN, therefore, proves suitable for implementing low-cost IoT systems, especially for large-scale monitoring, as demonstrated in the study [18]. Furthermore, it is particularly well suited for use in remote rural areas, making it an effective solution even in contexts where access to energy resources is limited [28]. Long Range (LoRa) is a wireless communication technology designed for long-distance data transmission [26]. LoRa uses spread spectrum modulation (Frequency Modulation, FM) to transmit audio or data signals via radio waves. This technique enables LoRa to facilitate long-range communication, covering distances of up to approximately 8–15 km, depending on environmental conditions, as highlighted by [25,26]. In studies [25–27], the authors developed IoT systems for soil moisture monitoring using LoRa communication technology. The research demonstrates that it is possible to effectively and cost-efficiently monitor soil temperature and moisture levels by leveraging LoRa. This technology proves to be a powerful and versatile solution for IoT applications, thanks to its ability to enable long-distance communication with low energy consumption. Additionally, LoRa's flexibility and scalability make it particularly suitable for large-scale applications, facilitating the coverage of extensive areas without the need for complex infrastructure. Table 10 summarizes the characteristics of the described IoT systems, which utilize various communication technologies. Additionally, communication can also occur via Bluetooth for devices without a Wi-Fi module. However, the primary limitation of this technology is its reduced range, covering only a few meters [98]. This characteristic limits Bluetooth's suitability for monitoring large areas, such as an agricultural field, where it is essential to maintain a stable and continuous connection over longer distances.

Table 10. Overview of the features of the different analyzed low-cost IoT systems, highlighting the main components, monitoring functionalities, and user interface functionalities.

Ref.	Proposed System	Components	Control System	User Interface	Internet Connection	Activation Conditions	Power Supply
[13]	Irrigation system	Micro controller: Arduino UNO by Arduino (Monza, Italy) Sensors: Soil	Arduino Uno programs irrigation based on soil moisture,	16 × 2 LCD display for data visualization. Data sent and displayed on ThingSpeak,	Wi-Fi module.	Irrigation is activated based on the detected moisture levels and temperature,	Power supply with a 12 V transformer and relay circuit; board

		moisture sensor, temperature sensors: LM35 by Texas Instruments (Dallas, Texas), pH, and air humidity Sensors. Attuators: Water pump controlled via relay.	activating the pump if necessary.	with updates every 5 min. Notification system not specified; access to data via online dashboard.		starting the pump if the soil is too dry.	powered via DC jack, USB Connector, or VIN pin.
[14]	Irrigation system	Micro controller: ESP32 by Espressif (Shanghai, China). Sensors: Soil moisture sensor SEN0308 by DFRobot (Shanghai, China), temperature sensors DS18320 by DFRobot (Shanghai, China), pH, and air Humidity sensors DHT22 by AZ Delivery (Deggendorf, Germany). Water flow sensor: Mod FS300 by SEA (Guangdong, China). Attuators: Solenoid valve controlled via relay for irrigation: Hunter PGV-100G by Hunter (San Marcos, USA).	ESP32 controls automatic Irrigation based on soil moisture and temperature, activating the solenoid valve during ideal time windows; Blynk allows for manual management and remote monitoring.	Blynk app for remote control and monitoring. Real-time data updates on Blynk, logging the date and time of irrigation, soil temperature, and water flow.	Wi-Fi connectivity.	If the soil Moisture is low And the temperature is adequate, and the ESP32 controls automatic irrigation within A specific time; the user can intervene manually.	Powered via battery, micro-USB connection for ESP32.
[16]	Irrigation system	Micro controller: ESP32 by Espressif (Shanghai, China). Sensors: Soil moisture sensor YL-69by Jiexing (Guangdong, China) and temperature and humidity sensor DHT11 by AZ Delivery (Deggendorf, Germany). Attuators: Water pump controlled via relay for irrigation.	ESP32 automatically Activates the pump if the soil moisture is below the threshold; the Blynk app allows for manual control of the pump and the receipt of notifications.	Blynk app for monitoring and remote control. Irrigation data updated on Blynk with continuous logging; includes date and time of irrigation, soil temperature, and humidity. Email notifications or via The Blynk app.	Wi-Fi connectivity.	Irrigation is Automatically Activated if the soil moisture drops below the threshold; the pump remains off if the threshold is not exceeded; manual control is available via Blynk.	Direct power via laptop through a micro-USB cable for ESP32.
[18]	Automated fertigation system that processes the water Requirements of crops.	Weather sensor. Soil sensor (moisture, T, pH/EC). Plent sensor (leaf wetners sensor). Crop database.	Ability to make intelligent irrigation decisions for crops based on Etc.	Data transmission and display on a Web Platform.	Wireless sensor network (WSN).	Strategy that takes into Account different irrigation schedules and weather Conditions. Daily irrigation quantity and	Battery, implemented with a photovoltaic panel.

[26]	Air temperature And soil moisture monitoring systems	Micro controller: ESP32 by Espressif (Shanghai, China). Sensors: Soil moisture sensor FC-28 by and temperature and humidity sensor DHT11 by AZ Delivery (Deggendorf, Germany).	Continuous monitoring System of environmental conditions and soil moisture levels.	Cayenne iot Platform for storage and visualization.	The data then transmitted using lora. Data from Source Node will receive by The Sink Node.	The system is designed to Continuously monitor environmental conditions and Soil moisture, without explicitly specifying whether it is equipped with The functionality to activate irrigation.	Power source not specified.
[27]	Soil health monitoring system	Host micro-controller: Atmega 2560 from Atmel (San Jose, USA). Sensors: Soil moisture and temperature Teros12 by Meter Group (Washington, USA). Soil CO_2 GMP251, by Vaisala (Vanta, Finland. GPS module for geo-location. Radio module RN2930. Solar panel.	Continuous monitoring of soil health.	IoT-SHM server every 10 min. On The IoT-SHM server, these measurements have been recorded for long-term storage and visualized in Real-time using the dashboard.	LoRa commu-nication.	The system is Designed to continuously monitor various soil parameters, such as temperature, humidity, electrical conductivity (EC), CO_2 levels, and location information. It is configured to send soil Measurements to The server every 10 min. However, the system is not integrated with automated irrigation or fertigation systems.	2500 mAh battery and photovoltaic panel.
[28]	Irrigation system	Microcontroller: Arduino NANO From Arduino (Monza, Italia). Sensors: DHT11by AZ Delivery (Deggendorf, Germany). Light-dependent resistor (LDR) for light levels. YL-83 sensor for rainfall Levels. YL-69 sensor for soil Moisture. Actuator: pump.	Arduino Uno programs irrigation Based on soil moisture, activating the pump if Necessary.	ThingSpeak, used for the visualization and analysis of collected data. Provides intuitive dashboards for the User, with graphs and reports to monitor field conditions. Allows for the storage of historical data for future analysis.	LoRa commu-nication.	Irrigation is Activated when the current time falls within the Predefined time windows, and the environmental and soil conditions are favorable for irrigation. estimated fertilization nutrients based on environmental factors, crop specifications, and soil conditions.	Solar cell and a lithium battery.

In conclusion, the various IoT communication technologies offer distinct advantages and disadvantages based on key parameters such as distance,

energy consumption, and data transmission capacity. LoRa stands out for its ability to cover long distances, making it ideal for large-scale applications, while WSN occupies a middle ground. Wi-Fi, although offering the highest data transmission capacity, is limited to shorter distances and has higher energy consumption. Table 11 provides a comparison between the IoT technologies LoRa, WSN, and Wi-Fi, considering parameters such as coverage range, energy consumption, and operational capacity. Therefore, the choice of the most appropriate technology depends on the specific requirements of the application, such as battery life, range, and the volume of data to be transmitted.

Table 11. Comparison between the technologies LoRa, WSN, and Wi-Fi based on distance, energy consumption, and communication capacity.

Technology	Range	Energy Consumption	Data Transmission Capacity
LoRa	High (8–15 km)	Low	Moderate
WSN	Moderate (approx. 10 m per node)	Low	Low
Wi-Fi	Shortest (around 100 m)	Higher	Highest

2.1.14 Conclusions and Future Prospects

An adequate and efficient management of the soil is essential not only for environ- mental sustainability but also for increasing productivity, both in terms of quality and maximizing yields. Recognizing potential stressors and critical situations for crops in advance allows for preventive and specific actions to be taken. In this context, the sensors described in the article prove to be promising, offering concrete solutions to address cur- rent challenges in agriculture. The adoption of soil monitoring technologies emerges as a key factor in promoting sustainable agricultural practices and optimizing resource use. Soil moisture and nutrient sensors offer significant advantages, enabling more targeted irrigation and fertilization, reducing water consumption, and facilitating a conscious use of fertilizers. The variety of available sensors, including tensiometers, thermal probes, capacitive sensors, TDR, FDR, and neutron moisture sensors, allows for responses to different agricultural needs and conditions. While each of these tools has its advantages and limitations, their integration enables precise and real-time monitoring of soil moisture, greatly improving water efficiency. Additionally, electrical, electrochemical, and optical sensors provide accurate and non-invasive measurements of nutrients. However, the costs associated with these technologies can hinder their widespread adoption. Regarding data transmission, technologies such as Wi-Fi, WSN, and LoRa present various solutions, each suited to specific coverage and energy consumption needs. While Wi-Fi guarantees high transmission speeds, its limited range and high energy consumption make it impractical for rural areas. In contrast, WSN and LoRa are more suitable for large-scale agricultural applications due to their ability to cover vast areas with low energy consumption. The future of soil monitoring and sustainable

agriculture appears promising, thanks to continuous technological advancements and the integration of IoT practices. The adoption of cutting-edge systems and the implementation of AI and ML have the potential to radically transform resources management, increasing the efficiency and sustainability of agricultural practices. To fully leverage the potential of these sensors, it is crucial to undertake further research and improvements in various areas, such as sensor calibration, the improvement of connection system, and energy reliability. Developing increasingly accurate predictive models that can improve crop yields, anticipate plant diseases, and optimize the use of fertilizers and pesticides is a critical objective. It is essential to develop AI models specific to different crops, climates, and soil characteristics, making these tools understandable even for farmers without technical expertise. Despite significant progress in data collection, managing that data remains a significant challenge. Future information management systems will need to store, analyze, and show data clearly and accessibly while ensuring ethical protection of information, with particular attention to farmers' privacy. There is also an expected expansion in the use of intelligent systems for the continuous monitoring of soil parameters. These systems should leverage advanced and reliable connectivity technologies, such as 5G and edge computing, ensuring immediate processing and greater precision in corrective actions over large areas.

Such efforts by the scientific community must be accompanied by agricultural policies that adapt to promote the adoption of precision agriculture, encouraging investments in technology and supporting farmers' training. It is fundamental to develop more affordable and durable sensors, improving their reliability and precision through the use of innovative materials and technologies so that they can operate effectively in challenging agricultural environments and be accessible to small enterprises and developing countries. This integrated approach will help make agriculture more sustainable and efficient in the long term, promoting a future in which innovative technologies will benefit all farmers and preserve natural resources.

2.1.15 References

1. Simão, L.M.; Cruppe, G.; Michaud, J.P.; Schillinger, W.F.; Ruiz Diaz, D.; Dille, A.J.; Rice, C.W.; Lollato, R.P. Beyond grain: Agronomic, ecological, and economic benefits of diversifying crop rotations with wheat. In *Advances in Agronomy*; Elsevier: Amsterdam, The Netherlands, 2024; Volume 186, pp. 51–112. ISBN 978-0-443-29528-7.
2. FAO. *Water for Sustainable Food and Agriculture: A Report Produced for the G20 Presidency of Germany*; FAO: Rome, Italy, 2017; pp. 1–27.
3. Ingrao, C.; Strippoli, R.; Lagioia, G.; Huisingh, D. Water scarcity in agriculture: An overview of causes, impacts and approaches for reducing the risks. *Heliyon* **2023**, *9*, e18507. [CrossRef] [PubMed]
4. Qin, Y.; Horvath, A. What contributes more to life-cycle greenhouse gas emissions of farm produce: Production, transportation, packaging, or food loss? *Resour. Conserv. Recycl.* **2022**, *176*, 105945. [CrossRef]
5. FAO. *The Future of Food and Agriculture: Trends and Challenges*; Food and Agriculture Organization of the United Nations: Rome, Italy, 2017; ISBN 978-92-5-109551-5.

6. Tara, N.; Uddin, M.; Hyder, K.S.; Sharmin, S. A Survey on the Inclusion of IoT in Agriculture for Soil Monitoring. 2022. Available online: https://www.researchgate.net/publication/361115512 (accessed on 20 June 2024).
7. Kalambukattu, J.G.; Kumar, S.; Arya Raj, R. Digital soil mapping in a Himalayan watershed using remote sensing and terrain parameters employing artificial neural network model. *Environ. Earth Sci.* **2018**, *77*, 203. [CrossRef]
8. Zeyada, A.M.; Al-Gaadi, K.A.; Tola, E.; Madugundu, R.; Alameen, A.A. Sentinel-2 Satellite Imagery Application to Monitor Soil Salinity and Calcium Carbonate Contents in Agricultural Fields. *Phyton* **2023**, *92*, 1603–1620. [CrossRef]
9. Gerardo, R.; De Lima, I.P. Sentinel-2 Satellite Imagery-Based Assessment of Soil Salinity in Irrigated Rice Fields in Portugal. *Agriculture* **2022**, *12*, 1490. [CrossRef]
10. Thomas, S.; Kuska, M.T.; Bohnenkamp, D.; Brugger, A.; Alisaac, E.; Wahabzada, M.; Behmann, J.; Mahlein, A.-K. Benefits of hyperspectral imaging for plant disease detection and plant protection: A technical perspective. *J. Plant Dis. Prot.* **2018**, *125*, 5–20. [CrossRef]
11. Pane, C.; Manganiello, G.; Nicastro, N.; Cardi, T.; Carotenuto, F. Powdery Mildew Caused by Erysiphe cruciferarum on Wild Rocket (*Diplotaxis tenuifolia*): Hyperspectral Imaging and Machine Learning Modeling for Non-Destructive Disease Detection. *Agriculture* **2021**, *11*, 337. [CrossRef]
12. Viscarra Rossel, R.A.; Adamchuk, V.I.; Sudduth, K.A.; McKenzie, N.J.; Lobsey, C. Proximal soil sensing: An effective approach for soil measurements in space and time. In *Advances in Agronomy*; Elsevier: Amsterdam, The Netherlands, 2011; Volume 113, pp. 243–291. ISBN 978-0-12-386473-4.
13. Abba, S.; Wadumi Namkusong, J.; Lee, J.-A.; Liz Crespo, M. Design and Performance Evaluation of a Low-Cost Autonomous Sensor Interface for a Smart IoT-Based Irrigation Monitoring and Control System. *Sensors* **2019**, *19*, 3643. [CrossRef]
14. Pereira, G.P.; Chaari, M.Z.; Daroge, F. IoT-Enabled Smart Drip Irrigation System Using ESP32. *IoT* **2023**, *4*, 221–243. [CrossRef]
15. Tamil Malar, J.E.; Vaishnavi, M. IoT based Smart Irrigation System using ESP32. In Proceedings of the 2022 3rd Interna- tional Conference on Electronics and Sustainable Communication Systems (ICESC), Coimbatore, India, 17–19 August 2022; pp. 1751–1755.
16. Gunawan, T.S.; Kamarudin, N.N.; Kartiwi, M.; Effendi, M.R. Automatic Watering System for Smart Agriculture using ESP32 Platform. In Proceedings of the 2022 IEEE 8th International Conference on Smart Instrumentation, Measurement and Applications (ICSIMA), Melaka, Malaysia, 26–28 September 2022; pp. 185–189.
17. Toselli, M.; Baldi, E.; Ferro, F.; Rossi, S.; Cillis, D. Smart Farming Tool for Monitoring Nutrients in Soil and Plants for Precise Fertilization. *Horticulturae* **2023**, *9*, 1011. [CrossRef]
18. Ahmad, U.; Alvino, A.; Marino, S. Solar Fertigation: A Sustainable and Smart IoT-Based Irrigation and Fertilization System for Efficient Water and Nutrient Management. *Agronomy* **2022**, *12*, 1012. [CrossRef]
19. Umpi. La Conclusione del Progetto Overgreen (H2020 Vida). Available online: https://www.umpi.it/la-conclusione-del- progetto-overgreen-h2020-vida/ (accessed on 20 June 2024).
20. 50% Water Savings in Tuscan Pears. Sentek Technologies. Available online : https ://sentektechnologies.com/case-studies/50 -water-savings-in-tuscan-pears (accessed on 20 June 2024).
21. Sentek Probes & Strawberries: A Money-Saving Marriage. Sentek Technologies. Available online : https ://sentektechnologies. com/case-studies/sentek-probes-strawberries-a-money-saving-marriage/ (accessed on 20 June 2024).
22. Loures, L.; Chamizo, A.; Ferreira, P.; Loures, A.; Castanho, R.; Panagopoulos, T. Assessing the Effectiveness of Precision Agriculture Management Systems in Mediterranean Small Farms. *Sustainability* **2020**, *12*, 3765. [CrossRef]
23. Adeyemi, O.; Norton, T.; Grove, I.; Peets, S. Performance evaluation of three newly developed soil moisture sensors. In Proceedings of the CIGR-AgEng Conference, Aarhus, Denmark, 26–29 June 2016.
24. Payero, J.O.; Qiao, X.; Khalilian, A.; Mirzakhani-Nafchi, A.; Davis, R. Evaluating the Effect of

Soil Texture on the Response of Three Types of Sensors Used to Monitor Soil Water Status. *J. Water Resour. Prot.* **2017**, *9*, 566–577. [CrossRef]
25. Adi, P.D.P.; Siregar, V.M.M. A Soil moisture sensor based on Internet of Things LoRa. *Internet Things Artif. Intell. J.* **2021**, *1*, 120–132. [CrossRef]
26. Aji Purnomo, F.; Maulana Yoeseph, N.; Alim Tri Bawono, S.; Hartono, R. Development of air temperature and soil moisture monitoring systems with LoRA technology. *J. Phys. Conf. Ser.* **2021**, *1825*, 012029. [CrossRef]
27. Ramson, S.R.J.; León-Salas, W.D.; Brecheisen, Z.; Foster, E.J.; Johnston, C.T.; Schulze, D.G.; Filley, T.; Rahimi, R.; Soto, M.J.C.V.; Bolivar, J.A.L.; et al. A Self-Powered, Real-Time, LoRaWAN IoT-Based Soil Health Monitoring System. *IEEE Internet Things J.* **2021**, *8*, 9278–9293. [CrossRef]
28. Rodríguez-Robles, J.; Martin, Á.; Martin, S.; Ruipérez-Valiente, J.A.; Castro, M. Autonomous Sensor Network for Rural Agriculture Environments, Low Cost, and Energy Self-Charge. *Sustainability* **2020**, *12*, 5913. [CrossRef]
29. Bathre, M.; Das, P.K. Water supply monitoring system with self-powered LoRa based wireless sensor system powered by solar and hydroelectric energy harvester. *Comput. Stand. Interfaces* **2022**, *82*, 103630. [CrossRef]
30. Yu, L.; Gao, W.; Shamshiri, R.R.; Tao, S.; Ren, Y.; Zhang, Y.; Su, G. Review of research progress on soil moisture sensor technology. *Int. J. Agric. Biol. Eng.* **2021**, *14*, 32–42. [CrossRef]
31. Kashyap, B.; Kumar, R. Sensing Methodologies in Agriculture for Soil Moisture and Nutrient Monitoring. *IEEE Access* **2021**, *9*, 14095–14121. [CrossRef]
32. De Almeida, W.S.; Panachuki, E.; De Oliveira, P.T.S.; Da Silva Menezes, R.; Sobrinho, T.A.; De Carvalho, D.F. Effect of soil tillage and vegetal cover on soil water infiltration. *Soil Tillage Res.* **2018**, *175*, 130–138. [CrossRef]
33. Rasheed, M.W.; Tang, J.; Sarwar, A.; Shah, S.; Saddique, N.; Khan, M.U.; Imran Khan, M.; Nawaz, S.; Shamshiri, R.R.; Aziz, M.; et al. Soil Moisture Measuring Techniques and Factors Affecting the Moisture Dynamics: A Comprehensive Review. *Sustainability* **2022**, *14*, 11538. [CrossRef]
34. Zhang, J.; Zhou, Z.; Yao, F.; Yang, L.; Hao, C. Validating the Modified Perpendicular Drought Index in the North China Region Using In Situ Soil Moisture Measurement. *IEEE Geosci. Remote Sens. Lett.* **2015**, *12*, 542–546. [CrossRef]
35. Abdelmoneim, A.A.; Khadra, R.; Derardja, B.; Dragonetti, G. Internet of Things (IoT) for Soil Moisture Tensiometer Automation. *Micromachines* **2023**, *14*, 263. [CrossRef]
36. Hunduma, S.; Kebede, G. Indirect Methods of Measuring Soil Moisture Content Using Different Sensors. *Afr. J. Basic Appl. Sci.* **2020**, *12*, 37–55. [CrossRef]
37. Smith, J.B.; Kean, J.W. Long-Term Soil-Water Tension Measurements in Semiarid Environments: A Method for Automated Tensiometer Refilling. *Vadose Zone J.* **2018**, *17*, 180070. [CrossRef]
38. Home|Ecosearch. Available online: https://www.ecosearch.info/ (accessed on 20 June 2024).
39. IRROMETRO Home. Available online: https://www.irrometer.com/ (accessed on 20 June 2024).
40. Soil Moisture Monitoring: A Selection Guide. Available online: https://www.agric.wa.gov.au/horticulture/soil-moisture- monitoring-selection-guide (accessed on 20 June 2024).
41. Markovic, M.; Josipovic, M.; Sostaric, J.; Zebec, V.; Rapcan, I. Effectiveness of granular matrix sensors in different irrigation treatments and installation depths. *J. Agric. Sci. Belgrade* **2016**, *61*, 257–269. [CrossRef]
42. Salman, A.K.; Aldulaimy, S.E.; Mohammed, H.J.; Abed, Y.M. Performance of soil moisture sensors in gypsiferous and salt-affected soils. *Biosyst. Eng.* **2021**, *209*, 200–209. [CrossRef]
43. De Morais Franca, M.B.; Morais, F.J.O.; Carvalhaes-Dias, P.; Duarte, L.C.; Siqueira Dias, J.A. A Multiprobe Heat Pulse Sensor for Soil Moisture Measurement Based on PCB Technology. *IEEE Trans. Instrum. Meas.* **2019**, *68*, 606–613. [CrossRef]
44. Dias, P.C.; Roque, W.; Ferreira, E.C.; Siqueira Dias, J.A. A high sensitivity single-probe heat pulse soil moisture sensor based on a single npn junction transistor. *Comput. Electron. Agric.* **2013**, *96*, 139–147. [CrossRef]
45. Carvalhaes-Dias, P.; Morais, F.J.O.; Duarte, L.F.C.; Cabot, A.; Siqueira Dias, J.A. Autonomous Soil

Water Content Sensors Based on Bipolar Transistors Encapsulated in Porous Ceramic Blocks. *Appl. Sci.* **2019**, *9*, 1211. [CrossRef]
46. Morais, F.; Carvalhaes-Dias, P.; Zhang, Y.; Cabot, A.; Flosi, F.S.; Duarte, L.C.; Dos Santos, A.; Dias, J.A.S. Low-Cost Control and Measurement Circuit for the Implementation of Single Element Heat Dissipation Soil Water Matric Potential Sensor Based on a $SnSe_2$ Thermosensitive Resistor. *Sensors* **2021**, *21*, 1490. [CrossRef]
47. Jorapur, N.; Palaparthy, V.S.; Sarik, S.; John, J.; Baghini, M.S.; Ananthasuresh, G.K. A low-power, low-cost soil-moisture sensor using dual-probe heat-pulse technique. *Sens. Actuators A Phys.* **2015**, *233*, 108–117. [CrossRef]
48. Rugged Monitoring—Measurement and Control Instrumentation for Any Application. Available online: http://www.campbellsci. eu// (accessed on 20 June 2024).
49. Ravazzani, G. Open hardware portable dual-probe heat-pulse sensor for measuring soil thermal properties and water content.
Comput. Electron. Agric. **2017**, *133*, 9–14. [CrossRef]
50. Pal, P.; Tripathi, S.; Kumar, C. Single Probe Imitation of Multi-Depth Capacitive Soil Moisture Sensor Using Bidirectional Recurrent Neural Network. *IEEE Trans. Instrum. Meas.* **2022**, *71*, 9504311. [CrossRef]
51. Hrisko, J. *Capacitive Soil Moisture Sensor Theory, Calibration, and Testing*; Maker Portal LLC: New York, NY, USA, 2020. [CrossRef]
52. Huan, Z.; Wang, H.; Li, C.; Wan, C. The soil moisture sensor based on soil dielectric property. *Pers. Ubiquitous Comput.* **2017**, *21*, 67–74. [CrossRef]
53. Bhat, A.M.; Hanumantha, B.; Singh, D.N. A Generalized Relationship for Estimating Dielectric Constant of Soils. *J. ASTM Int.*
2007, *4*, 1–17. [CrossRef]
54. Kulmány, I.M.; Bede-Fazekas, Á.; Beslin, A.; Giczi, Z.; Milics, G.; Kovács, B.; Kovács, M.; Ambrus, B.; Bede, L.; Vona, V. Calibration of an Arduino-based low-cost capacitive soil moisture sensor for smart agriculture. *J. Hydrol. Hydromech.* **2022**, *70*, 330–340. [CrossRef]
55. Pinpoint Accurate Farming|Farming Sensors—Farm21. Available online: https://www.farm21.com/ (accessed on 20 June 2024).
56. Adla, S.; Rai, N.K.; Karumanchi, S.H.; Tripathi, S.; Disse, M.; Pande, S. Laboratory Calibration and Performance Evaluation of Low-Cost Capacitive and Very Low-Cost Resistive Soil Moisture Sensors. *Sensors* **2020**, *20*, 363. [CrossRef]
57. Nagahage, E.A.A.D.; Nagahage, I.S.P.; Fujino, T. Calibration and Validation of a Low-Cost Capacitive Moisture Sensor to Integrate the Automated Soil Moisture Monitoring System. *Agriculture* **2019**, *9*, 141. [CrossRef]
58. Okasha, A.M.; Ibrahim, H.G.; Elmetwalli, A.H.; Khedher, K.M.; Yaseen, Z.M.; Elsayed, S. Designing Low-Cost Capacitive-Based Soil Moisture Sensor and Smart Monitoring Unit Operated by Solar Cells for Greenhouse Irrigation Management. *Sensors* **2021**, *21*, 5387. [CrossRef] [PubMed]
59. Schwamback, D.; Persson, M.; Berndtsson, R.; Bertotto, L.E.; Kobayashi, A.N.A.; Wendland, E.C. Automated Low-Cost Soil Moisture Sensors: Trade-Off between Cost and Accuracy. *Sensors* **2023**, *23*, 2451. [CrossRef] [PubMed]
60. Numbi, N.H.; Mbuyu, S.; Hlahlele, T.S. Development of an ESP32 Smart and Safe Outdoor Plant Watering System. In Proceedings of the 2024 32nd Southern African Universities Power Engineering Conference (SAUPEC), Stellenbosch, South Africa, 24–25 January 2024; pp. 1–6.
61. Wyseure, G.C.L.; Mojid, M.A.; Malik, M.A. Measurement of volumetric water content by TDR in saline soils. *Eur. J. Soil Sci.* **1997**,
48, 347–354. [CrossRef]
62. Skierucha, W.; Wilczek, A.; Szypłowska, A.; Sławiński, C.; Lamorski, K. A TDR-Based Soil Moisture Monitoring System with Simultaneous Measurement of Soil Temperature and Electrical Conductivity. *Sensors* **2012**, *12*, 13545–13566. [CrossRef]
63. Su, S.L.; Singh, D.N.; Shojaei Baghini, M. A critical review of soil moisture measurement. *Measurement* **2014**, *54*, 92–105. [CrossRef]
64. Abdullah, N.H.H.; Kuan, N.W.; Ibrahim, A.; Ismail, B.N.; Majid, M.R.A.; Ramli, R.; Mansor, N.S. Determination of soil water content using time domain reflectometer (TDR) for clayey soil. In Proceedings of the Advances in Civil Engineering and Science Technology, Penang, Malaysia, 5–6 September 2018; p. 020016.
65. Jia, J.; Zhang, P.; Yang, X.; Zhen, Q.; Zhang, X. Comparison of the accuracy of two soil moisture

sensors and calibration models for different soil types on the loess plateau. *Soil Use Manag.* **2021**, *37*, 584–594. [CrossRef]
66. TDR 200|Ecosearch. Available online: https://www.ecosearch.info/tdr-200 (accessed on 22 July 2024).
67. Sharma, P.K.; Kumar, D.; Srivastava, H.S.; Patel, P. Assessment of Different Methods for Soil Moisture Estimation: A Review. *J. Remote Sens. GIS* **2018**, *9*, 57–73.
68. Shukla, A.; Panchal, H.; Mishra, M.; Patel, P.R.; Srivastava, H.S.; Patel, P.; Shukla, A.K. Soil Moisture Estimation using Gravimetric Technique and FDR Probe Technique: A Comparative Analysis. *American International Journal of Research in Formal, Applied & Natural Sciences* **2014**, *8*, 89–92.
69. Ahmed, Z.; Gui, D.; Murtaza, G.; Yunfei, L.; Ali, S. An Overview of Smart Irrigation Management for Improving Water Productivity under Climate Change in Drylands. *Agronomy* **2023**, *13*, 2113. [CrossRef]
70. Choi, K.-Y.; Choi, E.-Y.; Kim, I.S.; Lee, Y.-B. Improving water and fertilizer use efficiency during the production of strawberry in coir substrate hydroponics using a FDR sensor-automated irrigation system. *Hortic. Environ. Biotechnol.* **2016**, *57*, 431–439. [CrossRef]
71. Wang, Q.; Jia, Y.; Pang, Z.; Zhou, J.; Scriber, K.E.; Liang, B.; Chen, Z. Intelligent fertigation improves tomato yield and quality and water and nutrient use efficiency in solar greenhouse production. *Agric. Water Manag.* **2024**, *298*, 108873. [CrossRef]
72. Chen, L.; Zhangzhong, L.; Zheng, W.; Yu, J.; Wang, Z.; Wang, L.; Huang, C. Data-Driven Calibration of Soil Moisture Sensor Considering Impacts of Temperature: A Case Study on FDR Sensors. *Sensors* **2019**, *19*, 4381. [CrossRef] [PubMed]
73. Kizito, F.; Campbell, C.S.; Campbell, G.S.; Cobos, D.R.; Teare, B.L.; Carter, B.; Hopmans, J.W. Frequency, electrical conductivity and temperature analysis of a low-cost capacitance soil moisture sensor. *J. Hydrol.* **2008**, *352*, 367–378. [CrossRef]
74. Rhie, Y.H.; Kim, J. Changes in Physical Properties of Various Coir Dust and Perlite Mixes and Their Capacitance Sensor Volumetric Water Content Calibrations. *HortScience* **2017**, *52*, 162–166. [CrossRef]
75. Qin, A.; Ning, D.; Liu, Z.; Duan, A. Analysis of the Accuracy of an FDR Sensor in Soil Moisture Measurement under Laboratory and Field Conditions. *J. Sens.* **2021**, *2021*, 6665829. [CrossRef]
76. Francke, T.; Heistermann, M.; Köhli, M.; Budach, C.; Schrön, M.; Oswald, S.E. Assessing the feasibility of a directional cosmic-ray neutron sensing sensor for estimating soil moisture. *Geosci. Instrum. Methods Data Syst.* **2022**, *11*, 75–92. [CrossRef]
77. Altdorff, D.; Oswald, S.E.; Zacharias, S.; Zengerle, C.; Dietrich, P.; Mollenhauer, H.; Attinger, S.; Schrön, M. Toward Large-Scale Soil Moisture Monitoring Using Rail-Based Cosmic Ray Neutron Sensing. *Water Resour. Res.* **2023**, *59*, e2022WR033514. [CrossRef]
78. Franz, T.E.; Wang, T.; Avery, W.; Finkenbiner, C.; Brocca, L. Combined analysis of soil moisture measurements from roving and fixed cosmic ray neutron probes for multiscale real-time monitoring. *Geophys. Res. Lett.* **2015**, *42*, 3389–3396. [CrossRef]
79. Molin, J.P.; Tavares, T.R. Sensor systems for mapping soil fertility attributes: Challenges, advances, and perspectives in 61razilian tropical soils. *Eng. Agríc.* **2019**, *39*, 126–147. [CrossRef]
80. Akhil, R.; Gokul, M.S.; Menon, S.; Nair, L.S. Automated Soil Nutrient Monitoring for Improved Agriculture. In Proceedings of the 2018 International Conference on Communication and Signal Processing (ICCSP), Chennai, India, 3–5 April 2018; pp. 0688–0692.
81. Kim, H.N.; Park, J.H. Monitoring of soil EC for the prediction of soil nutrient regime under different soil water and organic matter contents. *Appl. Biol. Chem.* **2024**, *67*, 1. [CrossRef]
82. Vyavahare, G.D.; Lee, Y.; Seok, Y.J.; Kim, H.N.; Sung, J.; Park, J.H. Monitoring of Soil Nutrient Levels by an EC Sensor during Spring Onion (*Allium fistulosum*) Cultivation under Different Fertilizer Treatments. *Agronomy* **2023**, *13*, 2156. [CrossRef]
83. TEROS 12—METER Group. Available online: https://metergroup.com/products/teros-12/?gad_source=1&gclid=CjwKCAjwydSzBhBOEiwAj0XN4NT9XlDEsbQlHpzo6ZHFMCvT1R47i9aFjkbLwzJ6O75J9tV8eoKRFRoCtQ4QavD_BwE (accessed on 21 June 2024).
84. Horváth, J.; Kátai, L.; Szabó, I.; Korzenszky, P. An Electrical Conductivity Sensor for the Selective Determination of Soil Salinity. *Sensors* **2024**, *24*, 3296. [CrossRef] [PubMed]
85. Ali, M.A.; Wang, X.; Chen, Y.; Jiao, Y.; Mahal, N.K.; Moru, S.; Castellano, M.J.; Schnable, J.C.; Schnable, P.S.; Dong, L. Continuous Monitoring of Soil Nitrate Using a Miniature Sensor with

Poly(3-octyl-thiophene) and Molybdenum Disulfide Nanocomposite. *ACS Appl. Mater. Interfaces* **2019**, *11*, 29195–29206. [CrossRef]

86. Kim, H.J.; Hummel, J.W.; Birrell, S.J. Evaluation of nitrate and potassium ion-selective membranes for soil macronutrient sensing. *Trans. ASABE* **2006**, *49*, 597–606. [CrossRef]
87. Eldeeb, M.A.; Dhamu, V.N.; Paul, A.; Muthukumar, S.; Prasad, S. Electrochemical Soil Nitrate Sensor for In Situ Real-Time Monitoring. *Micromachines* **2023**, *14*, 1314. [CrossRef]
88. Amado, T.M.; Alvarez, A.E.D.; Ocampo, A.; Paz, V.A.F.; Punongbayan, A.J.N.; Lemuel, M.; Yumena; Padilla, M.V.C.; Madrigal, G.A.M.; Tolentino, L.K.S.; et al. Development of an IoT-Based Soil Macronutrient Analysis System Utilizing Electrochemical Sensors and Machine Learning Algorithms. In Proceedings of the 2023 International Conference on Network, Multimedia and Information Technology (NMITCON), Bengaluru, India, 1–2 September 2023; pp. 1–6.
89. Elettrodi ISE Professionali. Hanna Instruments. Available online: https://hanna.it/./ise/ise-elettrodi-ise/ (accessed on 25 September 2024).
90. Laskar, S.; Mukherjee, S. Optical Sensing Methods for Assessment of Soil Macronutrients and other Properties for Application in Precision Agriculture: A review. *ADBU J. Eng. Technol.* **2016**, *4*, 208–209. Available online: https://journals.dbuniversity.ac.in/ ojs/index.php/AJET/article/view/181 (accessed on 24 June 2024).
91. Mukherjee, S.; Laskar, S. Vis–NIR-based optical sensor system for estimation of primary nutrients in soil. *J. Opt.* **2019**, *48*, 87–103. [CrossRef]
92. Masrie, M.; Rosli, A.Z.M.; Sam, R.; Janin, Z.; Nordin, M.K. Integrated optical sensor for NPK Nutrient of Soil detection. In Proceedings of the 2018 IEEE 5th International Conference on Smart Instrumentation, Measurement and Application (ICSIMA), Songkhla, Thailand, 28–30 November 2018; pp. 1–4.
93. Bogrekci, I.; Lee, W.S. Effects of soil moisture content on absorbance spectra of sandy soils in sensing phosphorus concentrations using UV-VIS-NIR spectroscopy. *Trans. ASABE* **2006**, *49*, 1175–1180. [CrossRef]
94. Zheng, L.; Lee, W.S.; Li, M.; Katti, A.; Yang, C.; Li, H.; Sun, H. Analysis of soil phosphorus concentration based on Raman spectroscopy. In Proceedings of the Multispectral, Hyperspectral, and Ultraspectral Remote Sensing Technology, Techniques and Applications IV, Kyoto, Japan, 30–31 October 2012; SPIE: Bellingham, WA, USA, 2012; pp. 203–210.
95. Burton, L.; Jayachandran, K.; Bhansali, S. Review—The "Real-Time" Revolution for In situ Soil Nutrient Sensing. *J. Electrochem. Soc.* **2020**, *167*, 037569. [CrossRef]
96. Jain, N.; Awasthi, Y.; Jain, R.K. An IoT-based soil analysis system using optical sensors and multivariate regression. *Int. J. Exp. Res. Rev.* **2023**, *31*, 23–32. [CrossRef]
97. Balestrieri, E.; De Vito, L.; Lamonaca, F.; Picariello, F.; Rapuano, S.; Tudosa, I. Research challenges in Measurement for Internet of Things systems. *Acta IMEKO* **2019**, *7*, 82. [CrossRef]
98. Sethi, P.; Sarangi, S.R. Internet of Things: Architectures, Protocols, and Applications. *J. Electr. Comput. Eng.* **2017**, *2017*, 9324035. [CrossRef]

3 MATERIALS AND METHODS

The present chapter describes the main phases that led to the design, implementation, and characterization of the developed low-cost monitoring system.
From the preliminary study, it emerged that soil monitoring represents a key element for the sustainable management of water resources, particularly in contexts such as Basilicata, where recurring water crises, the complex morphology of the territory, and the small farm sizes make the adoption of efficient, adaptable, and low-cost technologies indispensable. The review of the main existing solutions highlighted a growing interest in low-cost devices and architectures, laying the foundations for the definition of the selection criteria adopted in the choice of the prototype components. In the following sections, the details are described: i) the selection criteria for sensors and electronic components; ii)the description of hardware and software; iii)the phase of assembly and system configuration; iv)calibration phase; v)the experimental validation of the prototype. The development began with a proof of concept, aimed at verifying technical feasibility. Subsequently, the complete prototype was realized, following a sequence of phases that allowed its implementation, configuration, and technical characterization. The calibration was carried out through gravimetric measurements, used to construct the conversion equations between the electrical signal and the VWC in the soil. Subsequently, the system validation phase was conducted in order to evaluate the accuracy and stability of the device after the integration of the calibration equation.

Finally, the acquired data were integrated into an Application Programming Interface (API) with the aim of testing the scalability and interoperability of the system in view of the future design of a platform for the management and real-time visualization of the data.

3.1 SYSTEM COMPONENTS

The selection of components for the implementation of the environmental and soil monitoring prototype was guided by key criteria such as technical specifications, reliability, resistance to interference and environmental factors (corrosion, humidity, temperature fluctuations), as well as cost. The main objective was to develop a low-cost, robust, accessible, and easily integrable and adaptable solution, capable of operating effectively in real agricultural contexts.

3.1.1 Key requirements

- **Robustness and Durability**

The robustness of a sensor refers to its ability to withstand environmental stresses and mechanical shocks, while durability relates to its longevity and reliability over time. To ensure stable and continuous operation, even under harsh environmental conditions, sensors with high mechanical and chemical resistance were selected. In particular, capacitive-based devices were preferred, recognized for their long-term reliability and lower susceptibility to interference. Moreover, protection with corrosion and moisture resistant materials facilitates their use in agricultural environments and in close proximity to the soil.

- **Accuracy and Reliability**

The accuracy of a sensor refers to its ability to provide measurements close to the true value, while reliability relates to the consistency and repeatability of readings over time and under varying operational conditions. Both aspects are influenced by factors such as calibration, non-linearity, hysteresis, noise, environmental conditions, and device resolution. Therefore, measurement quality represents an essential requirement, as it affects both the reliability of statistical analyses and the validity of agronomic decisions based on the collected information. In this regard, sensor selection focused on devices with high accuracy, low measurement error, and good repeatability, capable of minimizing uncertainties and supporting reliable monitoring.

- **Efficientcy in data management and transmission**

Although not yet implemented in the current prototype, the system was designed with the use of technologies such as Wi-Fi and/or Bluetooth for the automatic transmission of acquired data. Integration with real-time data collection and processing platforms will enable timely and informed agronomic decisions, such as irrigation optimization. In the future, this functionality could enhance operational efficiency and the sustainability of agricultural management.

- **Low energy consumption and autonomy**

The selected components primarily operate at a supply voltage of 3.3 V, which helps reduce energy consumption and extend the system's autonomy. Energy efficiency is a crucial aspect in field applications, where access to stable power sources is often limited or unavailable. To further increase autonomy, the system has been designed for integration with solar charging modules, a solution that enables prolonged and sustainable operation even in remote agricultural settings. This combination of low power consumption and renewable energy sources makes the prototype particularly suitable for long-term installations, reducing the need for frequent maintenance interventions.

- **Cost**

Another key criterion adopted in the system design concerns cost containment, both for individual components and for the prototype as a whole. In the development of technologies aimed at the agricultural sector, particularly for small- and medium-sized producers, cost often represents a limiting factor in the adoption of digital monitoring solutions. For this reason, the selection focused on low-cost sensors and electronic modules, capable of providing adequate performance while maintaining a limited investment.

3.1.2 Hardware and Software components

- **ESP32:** The ESP32-WROOM-32 microcontroller, developed by Espressif Systems, constitutes the central component of the designed monitoring system. It is a compact, cost-effective, and efficient solution, designed for applications requiring wireless connectivity, operational reliability, and low power consumption—key features in environmental and agricultural monitoring projects. Based on a System-on-a-Chip (SoC), the ESP32 integrates a 32-bit dual-core Tensilica Xtensa LX6 processor, operating up to 240 MHz, capable of simultaneously handling sensor readings, data processing, and network communication. The integrated Wi-Fi, Bluetooth, and Bluetooth Low Energy (BLE) modules enable wireless data transmission, making the device particularly suitable for distributed and interconnected systems without the need for complex wiring. Its 4 MB flash memory allows storage of complex sketches, libraries, and temporary data, while 512 KB of RAM is sufficient for real-time operations typical of embedded systems. The board also offers 38 input/output pins (GPIO), enabling interfacing with a wide range of sensors, actuators, and external modules, making the system highly flexible and adaptable to multiple application scenarios *(Figure 3.1)*.

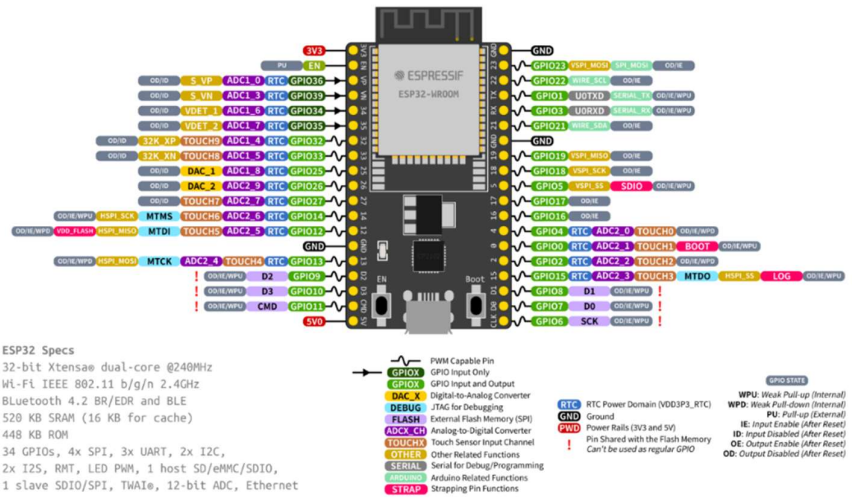

Figure 3.1 Pin layout of the ESP32-WROOM-32 development board: compact, high-performance microcontroller with 38 GPIO pins, allowing interfacing with sensors, actuators and external modules [30].

The device can be powered either via a 5 V USB connection or directly through a 3.3 V pin, making it compatible with various power configurations. *Table 3.1* summarizes its main technical specifications. Its low energy consumption, combined with the possibility of using batteries or solar panels, makes it ideal for applications in remote contexts, where electricity availability may be limited or unstable. This autonomy allows continuous monitoring of soil and microclimate without frequent maintenance or recharging interventions. Thanks to the combination of versatility, energy efficiency, and integrated wireless communication functionalities, the ESP32 represents an optimal solution for IoT applications, with particular effectiveness in environmental and agricultural monitoring. The ability to create autonomous, scalable, and low-power sensor networks makes it a strategic tool in the development of technologies for precision agriculture and sustainable management of environmental resources, as demonstrated in various applications [31], [32], [33], [34], [35], [36], [37].

Table 3.1 Main technical specifications of the ESP32 development board [38] and features of screw terminal board [39].

Model: ESP32-WOOM-32	**Main Processor:** dual-core Tensilica Xtensa LX6 a 32 bit	**Module interfaces:** SD card, UART, SPI, SDIO, I2C, LED PWM, Motor PWM, I2S, IR, pulse counter, GPIO, capacitive touch sensor, ADC, DAC, Two-Wire Automotive Interface (TWAI®), compatible with ISO11898-1 (CAN Specification 2.0)	**Module Communication :** Wi-Fi + Bluetooth® + Bluetooth LE
Arduino IDE compatibility	**Pin tot**: 38	**Operating Voltage:** 3.0V-3.6V	**Integrated SPI flash**: 4 MB **Integrated RAM**: 512 KB
Recommended operating: T = -40°C to +85°C	**Input Voltage/Power Supply**: 3.3V-5V	**Operating current**: Average 80 mA **Minimum current delivered by power supply**: 500 mA	**Cost**: 12€
Model: ESP32-DevKitC	Pin tot: 38	ESP32-WROOM-32 compatibility	Cost: 12,50€

- **Screw Terminal Board**: The terminal screw board for the ESP32-DevKitC (38 pins) is an expansion board designed to simplify the connection of sensors and peripherals *(Figure 3.2)*. Thanks to the screw terminals, it ensures stable, secure, and reliable electrical contacts, reducing the risk of accidental disconnections. As such, it provides a practical and organized method for managing connections in embedded projects.

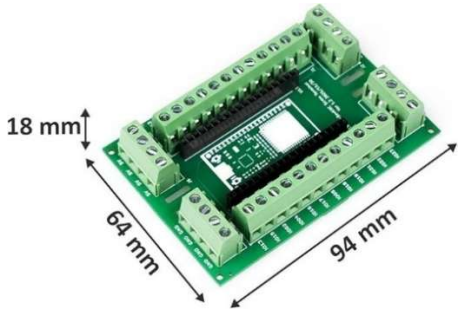

Figure 3.2 Expansion board designed to facilitate the connection of sensors and peripherals via screw terminals[39].

- **Modulo RTC (Real Time Clock):** The SD2405AL, produced by DFROBOT, is a high-precision RTC module with an I²C interface, designed for applications in industrial and outdoor environments *(Figure 3.3).* One of its most significant features is the integrated rechargeable battery, which allows the device to maintain accurate date and time even in the event of a main power interruption. The module features an automatic dual-power system: when the input voltage falls below a defined threshold, the SD2405AL automatically switches to the internal battery, ensuring uninterrupted operation. This feature makes it ideal for integration into autonomous systems, such as those used in environmental or agricultural monitoring, where electrical power may be intermittent or unavailable.

Figure 3.3 SD2405 RTC module with I²C interface and integrated rechargeable battery, for accurate date and time maintenance even without external power supply [40].

The module's time registers are stored in BCD (Binary-Coded Decimal) format and support full calendar and clock management, including seconds, minutes, hours (12h or 24h mode), day, month, year, and day of the week. Thanks to its compactness, energy efficiency, and reliability, the SD2405AL represents an ideal solution for low-power embedded applications requiring precise time synchronization, such as microcontroller-based environmental monitoring systems. Its main technical specifications are summarized in *Table 3.2.*

Table 3.2 Main features of RTC [40] and SD module and SD card [41].

Model: Module RTC SD2405AL	**Operation voltage range:** 3.3V~5.5V	**Communication protocol:** I^2C Interface	Countdown timer interrupt
Low-power: typical 1uA (inner battery, Ta=25°C)	**Power Supply:** 4.5V-5V	Real-Time Clock Counts Seconds, Minutes, Hours, Day, Date, Month, and Year with Leap Year Compensation Valid Up to 2100.	ROHS Recognized
High precision time trimming circuit.	**Accuracy :** ±5ppm from -40°C to +85°C	CMOS logic	**Cost**: 10€
Model: Module SD + Card SD	**Capacity card SD:** 32 GB	**Cost Module SD:** 4,50€ **Cost SD card:** 10€	

- **MicroSD module and memory card:** Serial Peripheral Interface (SPI) readers are modules that enable communication between a microcontroller and a memory card via the SPI protocol. The microSD card module from AZDelivery (*Figure 3.4*) is compact and reliable, designed for memory expansion. Powered at 5 V, it ensures efficient data management, with small dimensions and compatibility with various development boards. The selected 32 GB microSD card provides sufficient storage capacity to accommodate a large number of acquisitions generated by the monitoring system.

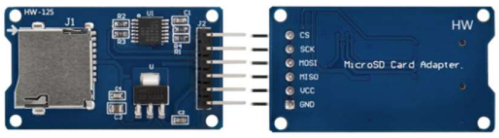

Figure 3.4 AZDelivery microSD card adapter, compatible with ESP32[41].

- **DHT22:** Also known as the AM2303, it is a digital sensor for measuring air temperature and relative humidity (RH) *(Figure 3.5)*, widely appreciated for its reliability, accuracy, and ease of use. It integrates a capacitive humidity sensor and a thermistor, providing data in digital format through a single communication line based on a proprietary protocol similar to 1-Wire, which requires approximately 5 ms per transmission cycle and facilitates integration with microcontrollers operating at both 3.3 V and 5 V *Table3.3*.

Figure 3.5 DHT22 digital sensor for precise measurement of air temperature and humidity.

Compared to the previous version (DHT11), the DHT22 offers superior performance, providing a wider measurement range (1%–99% for humidity and –40 °C to +80 °C for temperature) and higher accuracy [42] [43]. These characteristics make it particularly suitable for applications requiring stable, continuous, real-time acquisitions with low energy consumption. The sensor is now widely used in environmental monitoring systems and smart farming, where the availability of reliable data is a fundamental requirement for resource management and optimization. Recent studies [35] [37] [44] [45] [46] [47], have confirmed its reliability even in critical operational contexts, consolidating its role as the de facto standard in low-cost sensing systems.

Table 3.3 Main technical specifications of DHT22 [48].

Model: DHT22	**Operating range:** humidity 0-100%RH; **temperature** -40~80°C	**Resolution or sensitivity:** humidity 0.1%RH; temperature 0.1°C	**Sensing element:** Polymer capacitor
Output signal: digital signal via single-bus	**Power Supply**: 3.3V-6V	**Repeatability:** humidity ±1%RH; temperature ±-0.2°C	**Current supply:** 1.5 mA
Sensing period: 2s	**Accuracy :** humidity ± 2%RH(Max ± 5%RH); temperature <+-0.5°C	**Humidity hysteresis**: ±0.3%RH	**Cost:** 5€

- **SHT10:** Produced by Sensirion and belonging to the SHT1x series, it is a digital sensor for measuring RH and temperature. It integrates both the sensing elements and the processing circuitry in a compact format, providing a pre-calibrated digital output. The module combines the SHT10 chip with a porous stainless steel using (*Figure 3.6)*, designed to ensure corrosion resistance and protection against water and dust, while allowing proper air circulation.

Figure 3.6 SHT10 sensor based on CMOSens® technology (left) and version integrated into a probe with porous metal casing for field applications (right).

This configuration makes it particularly suitable for outdoor applications or harsh environmental conditions, where stable and continuous measurements of temperature and humidity are required. The sensor measures humidity via a capacitive element and temperature via a band-gap sensor. Thanks to CMOSens® technology, it ensures high

reliability, long-term stability, fast response times, and resistance to electromagnetic interference. With an accuracy of ±4.5% for humidity and ±0.5 °C for temperature (*Table 3.4*), the SHT10 represents a robust and effective solution for monitoring [33] [49] [50] [51] [52] [53] [54], proving particularly reliable in long-term applications .

Table 3.4 . Main technical specifications of the SHT10 sensor as reported in the official datasheet[55].

Model: SHT10	**Operating range:** moisture 0-100%RH; temperature -40 + 123.8°C	**Resolution or sensitivity:** humidity 0.05%RH; temperature 0.01°C	**Communication protocol:** I^2C
Output signal: digital	**Power Supply**: 3.3V-5V	**Repeatability:** humidity ±0.1%RH; temperature ±0.1°C	**Power Consumption**: 3 mW
Sensing period: 8s	**Accuracy :** humidity ± 1.8 – 4.5%RH; temperature ±0.3 – 0.5°C	**Humidity hysteresis**: ±1%RH	**Cost:** 15€

- **DS18B20:** Produced by Dallas Semiconductor, it is a digital temperature sensor based on the 1-Wire protocol, which allows multiple devices to be connected to a single pin. Each sensor is equipped with a unique 64-bit ID, enabling the microcontroller to identify it individually, thus allowing simultaneous monitoring of multiple measurement points through a single communication line. The DS18B20 covers a wide temperature range (–55 °C to +125 °C) with a typical accuracy of ±0.5 °C within the –10 °C to +85 °C range. It operates with a supply voltage between 3 V and 5 V, making it compatible with most microcontrollers, including the ESP32. Its main characteristics are summarized in *Table 3.5.*

Table 3.5 . Main technical specifications of temperature soil sensor [56].

Model: DS18B20	**Operating range:** -45 + 125°C	**Resolution (conversion time):** 93.75 ms (at 9 bits) to 750 ms (at 12 bits)	**Communication protocol:** 1-Wire
Output signal: digital	**Power Supply**: 3.3V-5V	**Accuracy :** ± 0.5°C (-10 to +85°C)	**Cost:** 6,50€

Particularly relevant feature is the availability of the sensor in a waterproof version, sealed in a metal casing that protects it from weather and corrosion (*Figure 3.7*). The DS18B20 represents a versatile, robust, low-cost, and low-power (typical standby current of 1–1.5 µA and peaks up to 1.5 mA during temperature conversion) solution for digital temperature measurement. Thanks to its precision, ease of use, and flexibility, the sensor has become a reference standard in environmental and agricultural monitoring systems [35] [57] [58] [59].

Figure 3.7 DS18B20 temperature probe in waterproof version.

- **SKU SEN0308:** The SEN0308 is a capacitive probe with an analog output, produced by DFRobot, designed for the indirect measurement of soil moisture. Its operating principle is based on detecting changes in capacitance caused by variations in the dielectric material in the presence of moisture. Consequently, the sensor does not directly measure the water content of the soil, but detects the ions present, converting these variations into an analog signal sent to the microcontroller, which, once properly calibrated, translates it into a soil moisture measurement. DFRobot capacitive probes have been widely used over the years in soil monitoring systems. The first version, SKU SEN0193, already stood out for good accuracy in estimating soil moisture, especially after soil-specific calibration [4] [60] [61] [62] [63]. In the present project, the SKU SEN0308 model (*Figure 3.8*), the latest evolution introduced by DFRobot, was used. It can be inserted into the soil for long periods without damage, providing stable and reliable moisture measurements.

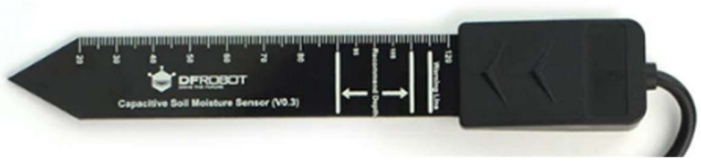

Figure 3.8 SKU: SEN 0308 capacitice soil moisture probe.

Compared to the previous model, the SEN0308 features enhanced characteristics, including superior waterproofing, increased corrosion resistance, an elongated probe for more accurate measurements, and an optimized circuit to improve reading precision, as highlighted in recent studies [35] [64] [65] . Additionally, it is equipped with a graduated scale engraved on the probe, which facilitates installation, making it simpler and more efficient. The sensor supports a supply voltage range of 3.3 to 5.5 V and is fully compatible with major development boards, including the ESP32. Its technical specifications are summarized in *Table 3.6*.

Table 3.6 Main features of soil moisture probe SKU SEN0308 [66].

Model: SEN0308	**Power Supply:** 3.3V-5.5V	**Communication protocol:** Analog-to-Digital Converter (ADC)
Output signal: Analogic	**Output voltage**: 0-2.9VDC	**Cost:** 20€
ADC value range: 0–1023 (10-bit resolution, 5 V power supply)		

In summary, the low-cost sensors analyzed represent an innovative and economically accessible solution for monitoring environmental and soil variables. Although their performance is lower than that of commercial devices, they are particularly suitable for research and experimental applications, where cost reduction and the possibility of implementing scalable systems represent added value. The use of such sensors allows for the acquisition of real-time data while containing economic investments, laying the groundwork for the development of practical and replicable solutions, even in contexts with limited resources. A bill of materials for the construction of monitoring system units has been provided in *Table 3.7*.

Table 3.7 List of the components used for the development of the monitoring system, unit cost and the corresponding function. The table provides an overall view of the required resources, useful for assessing the economic sustainability and replicability of the system.

ITEM NUMBER	COMPONENT	NUMBER REQUIRED	COST UNIT^{-1} (€)	TOTAL COST (€)	SCOPE OF APPLICATION
1	SKU SEN0308	1	20	20	Soil moisture measurement
2	DS18B20	1	6,50	6,50	Soil temperature measurement
3	SHT10	1	15	15	Air monitoring
4	DHT22	1	5	5	Air monitoring
5	Module MICROSD	1	4,50	4,50	Connection to SD
6	MICRO SD 32GB	1	10	10	Data storage
7	Module RTC	1	10	10	Date and time maintenance
8	ESP32	1	12	12	Development board
9	SCREW TERMINAL BOARD	1	12,50	12,50	Connecting facilitator
10	BREABOARD	1	5	5	Sensor and ESP32 connection
11	RESISTOR 10 KΩ	2	0,05	0,10	limit the current and regulate the voltage
12	RESISTOR 4.7 KΩ	1	0,05	0,10	limit the current and

					regulate the voltage
13	JUMPER WIRE	1 pack (40pz)	0,12	5	Electrical connection of components
14	CABLE USB	1	5	5	ESP32 connection and power supply
15	POWERBANK (20.000mAh)	1	25	25	Power supply
			Tot €	**135,70**	

- **Arduino IDE:** Arduino IDE 2 (Integrated Development Environment) represents the official development environment for the Arduino platform and is an evolution of the classic IDE, offering improved performance and a more modern structure. It is a cross-platform application, available for Windows, macOS, and Linux, written in Java. The IDE is open-source, free, lightweight, and benefits from a large developer community and extensive online documentation, which are particularly useful during program development. The IDE is used to write, compile, and upload programs to Arduino-compatible boards, including boards based on different microcontrollers, such as the ESP32. The primary programming language is C/C++, adapted with simplified code structuring rules. Each program, referred to as a sketch, requires two fundamental functions:
  - void setup(): a function executed only once at the microcontroller startup, necessary for system initialization.
  - void loop(): a function containing the main program cycle, executed continuously as long as the board remains powered.

    The IDE interface (*fig 3.9*) integrates several essential tools for writing and executing sketches.

Figure 3.9 Arduino IDE interface [67].

- **Verify/Upload**: compile and transfer the sketch to the Arduino or ESP32 board;
- **Select board e port**: allows you to select the connected card and its serial port. These are usually detected automatically;
- **Sketchbook**: collects sketches written and saved locally on the computer;
- **Boards Manager**: manages official Arduino packages and third-party packages; for example, to use the ESP32, you need to install the esp32 package by Espressif Systems;
- **Library Manager**: allows you to explore and install thousands of open source libraries developed by Arduino and the community;
- **Debugger**: allows programmes to be tested and corrected in real time;
- **Search**: facilitates code navigation using keywords;
- **Serial Monitor**: tool that displays data sent by the card in real time (for example, using Serial.print() function);
- **Serial Plotter**: useful for graphically displaying the trend of data acquired by sensors.

  Thanks to these features and the support of a considerable number of open-source libraries, Arduino IDE 2 represents a versatile and comprehensive tool, capable of effectively supporting the development, testing, and integration of the various sensors and electronic modules that make up the system under study in the present research work.

- **MongoDB:** MongoDB is an open-source, document-oriented NoSQL database, widely used for managing and storing heterogeneous and dynamic data. Unlike traditional relational databases, which organize information in rigidly structured tables, MongoDB uses a flexible document-based structure in BSON (Binary JSON) format [68]. This allows data to be represented hierarchically and intuitively, facilitating the integration of information from different sources. From an architectural perspective, MongoDB adopts a hierarchical logical structure in which data are organized into databases, further divided into collections containing BSON/JSON documents:
  - **Database**: logical sets containing one or more collections;
  - **Collection**: groups of documents, equivalent to tables in relational databases;
  - **Document**: the fundamental storage unit, structured as key-value pairs and easily convertible to JSON format.

  This architecture ensures high flexibility in managing large volumes of data and remarkable scalability. In the present project, MongoDB was adopted to efficiently handle the heterogeneous data streams generated by the sensors, which are characterized by variable frequency and potential structural evolution over time. Its compatibility with programming languages such as Python, along with the availability of official drivers,

facilitated the integration between the database, the ESP32 microcontroller, and the subsequent data analysis phases. For the management and analysis of the collected data, ***MongoDB Compass***, the official graphical interface provided by MongoDB, was used. This tool allows:

- Visually explore databases and collections;
- Execute queries and apply filters to the data without writing code;
- Analyze statistics, indexes, and value distributions;
- Monitor database performance in real time.

MongoDB Compass proved to be an essential tool during the experimental phase, as it allowed for the rapid verification of the accuracy and consistency of the data acquired from the sensors, simplifying debugging and the optimization of data acquisition pipelines. *Figure 3.10* shows the MongoDB Compass environment, highlighting the main sections:

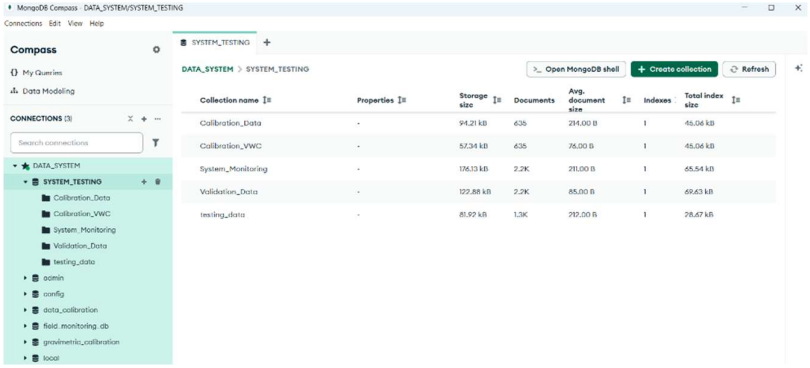

Figure 3.10 MongoDB Compass graphical interface: used to explore databases and collections, execute queries, analyse data, and monitor performance. Database and collection browser (on the left), display of documents and related fields (in the centre) and tools for queries, analysis and export (at the top).

- **FastAPI:** It is a next-generation web framework designed for developing modern application programming interfaces (API) using Python (version 3.6 or higher). Developed in 2018 by Sebastián Ramírez, FastAPI has quickly become one of the most widely used and appreciated open-source solutions due to its combination of high performance, ease of use, and architectural flexibility. From an architectural perspective, FastAPI is built on three fundamental components:
  - **Starlette**: an asynchronous framework that manages HTTP (Hypertext Transfer Protocol), requests and responses, WebSocket connections, and the core functionalities needed to build high-performance web applications. Using Starlette ensures low response times and high scalability.
  - **Pydantic**: a library dedicated to data validation and serialization. It leverages type hints introduced in Python 3.6 to declaratively define data models, ensuring consistency and correctness of information

exchanged between client and server, as well as automatic conversion between formats such as JSON and Python objects.

- **Uvicorn**: a lightweight, high-performance ASGI (Asynchronous Server Gateway Interface) server that runs the FastAPI application. Developed in Python and based on uvloop and httptools, Uvicorn ensures low response times and efficient handling of numerous simultaneous connections, making it particularly suitable for real-time applications, IoT systems, and cloud-native architectures.

Thanks to this modular architecture, FastAPI natively supports the development of RESTful APIs, i.e., interfaces that adhere to the architectural principles of REST (Representational State Transfer), ensuring interoperability and ease of integration with other systems. A distinctive feature of FastAPI is the automatic generation of interactive API documentation based on the OpenAPI and Swagger UI standards, allowing users to explore and test functionalities directly from a web browser. Additionally, the ReDoc interface is available, providing an alternative, detailed view of the API specifications.
In conclusion, FastAPI stands out as one of the most advanced and reliable tools for building APIs in Python, thanks to its distinctive features and capabilities [69]:

- **Fast:** among the fastest Python frameworks ever, thanks to Starlette and Pydantic.
- **Fast to code**: enables new features to be implemented more quickly.
- **Fewer bugs**: automatic input validation and strict typing reduce human errors during development by up to 40%.
- **Intuitive and Easy**: provides advanced support for editors (auto-completion, typing suggestions), which simplifies code writing.
- **Short**: minimises code duplication, allowing you to achieve greater functionality with fewer lines of code and, consequently, fewer bugs.
- **Robust**: includes native interactive documentation generation features.
- **Standards-based**: is fully based on the open standards OpenAPI (formerly Swagger) and JSON Schema, ensuring compatibility and interoperability.

In this project, the integration of data with FastAPI took place in the final phase, enabling the connection with the MongoDB database and serving as the main application interface. The framework does not merely transfer data but manages the entire information flow in a structured manner: on one side, it receives data generated by the ESP32-based monitoring system (which are stored in MongoDB), while on the other, it makes them available through RESTful endpoints (*Figure 3.11*). These standardized access points allow external software, visualization tools, and predictive models to query the system and retrieve data either in real time or on demand. In this way, FastAPI not only ensures secure and efficient interaction with the database

but also acts as a central hub supporting analysis, operational decision-making, and future model integrations.

Figure 3.11 FastAPI interactive interface via Swagger UI: allows you to automatically explore, test, and document the RESTful endpoints exposed by the framework.

3.2 SYSTEM IMPLEMENTATION AND CONFIGURATION

The implementation phase of the prototype involved both the hardware assembly of the sensors and the software configuration for data collection and storage. The main objective was to develop a reliable, modular, and easily replicable system for measuring soil and air temperature and humidity in agri-food contexts.

3.2.1 System implementation

The system was developed using low-cost components, described in detail in the previous paragraph. The sensors were connected to the ESP32 following the wiring diagram shown in *Figure 3.12*, , in compliance with the power supply and communication specifications:

- **SHT10:** communicates via a proprietary 3.3 V digital bus with a 10 kΩ pull-up resistor.
- **DHT22:** connected to a digital pin with a 10 kΩ pull-up resistor.
- **SEN0308:** uses an analogue output with internal ADC conversion of the ESP32.
- **DS18B20:** connected to a digital pin with a 4.7 kΩ pull-up resistor.
- **MicroSD card:** connected via SPI interface and powered at 5 V.

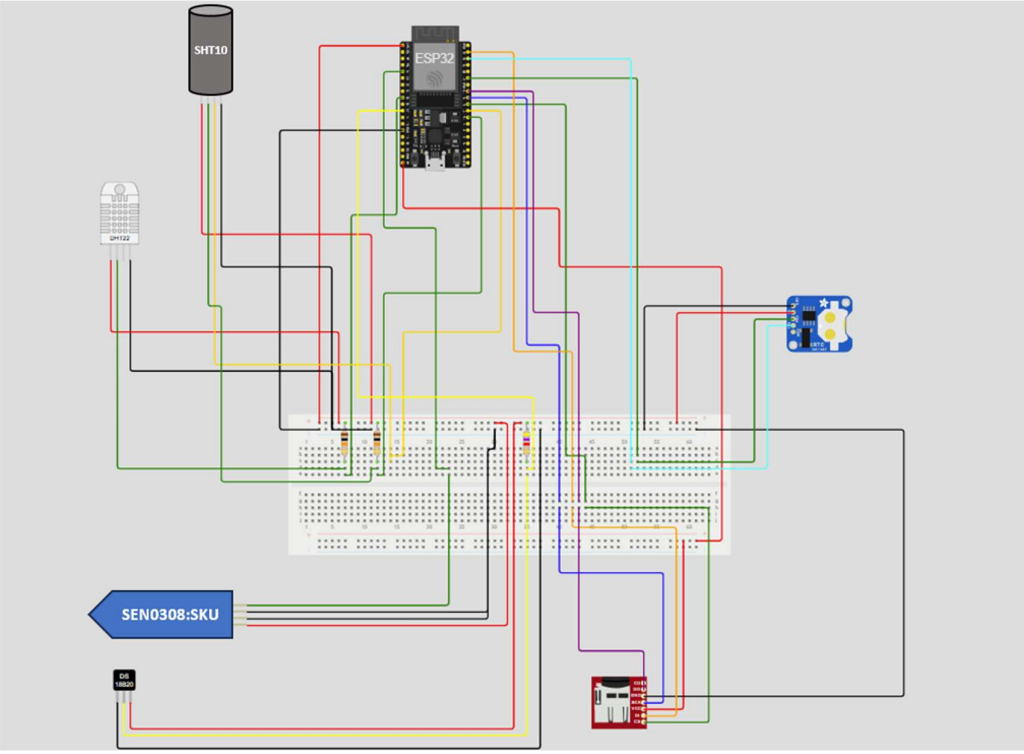

Figure 3.12 Schematic representation of the implemented system, created using https://wokwi.com/.

Table 3.8 shows the correspondence between the sensor pins and those of the ESP32, highlighting the necessary connections for data acquisition. The analog pins were assigned to the SEN0308 sensor, which provides a voltage signal to be converted through the integrated ADC; the digital pins were used for the SHT10, DHT22, and DS18B20 sensors, each with the corresponding pull-up resistor to ensure signal stability; meanwhile, the SPI interface was dedicated to managing the microSD card for data storage. This configuration ensures proper power supply and communication among all components of the monitoring system.

Table 3.8 The table shows the correspondence between the sensor and components pins and those of the ESP32, highlighting the connections required for data acquisition.

Sensor	Pin Sensor	Pin ESP32
SKU SEN0308	▪ VCC ▪ DATA ▪ GND	▪ 3V3 ▪ I34 ▪ GND
DS18B20	▪ VCC ▪ DATA ▪ GND	▪ 3V3 ▪ IO027 ▪ GND
SHT10	▪ VCC ▪ DATA ▪ CLK ▪ GND	▪ 3V3 ▪ IO016 ▪ IO017 ▪ GND
DHT22	▪ VCC ▪ DATA ▪ GND	▪ 3V3 ▪ IO025 ▪ GND
RTC module	▪ VCC ▪ ATA ▪ SCL ▪ GND	▪ 3V3 ▪ IO021 ▪ IO022 ▪ GND

Module SD	▪ VCC ▪ CS ▪ SCK ▪ MOSI ▪ MISO ▪ GND	▪ 5V ▪ IO05 ▪ IO018 ▪ IO023 ▪ IO019 ▪ GND

3.2.2 System configuration

The system configuration was carried out using the Arduino IDE, a development environment suitable for programming the ESP32. The first step involved setting up the board in the IDE through the installation of the CP210x driver, which enables the USB connection to be converted into a standard serial port. This allows the computer to establish direct communication with the microcontroller, making it ready for programming and data exchange. Next, the main libraries needed for managing the sensors and external peripherals were imported:

- SD.h and SPI.h for writing data to the microSD card;
- Wire.h for communication with devices based on the I^2C protocol;
- GravityRtc.h for interfacing with the RTC module;
- DHT.h for managing the DHT22 sensor;
- SHT1x-ESP.h for managing the SHT10 sensor;
- OneWire.h e DallasTemperature.h for managing the DS18B20 sensor.

This phase constitutes the first lines of the sketch in Arduino IDE (*Figure 3.13*), in which the libraries are initialised and the connection pins of the various components are configured.

sketch_lowCost_sensor.ino

```
// === Inclusion libraries ===
#include <SPI.h>
#include <SD.h>
#include <Wire.h>
#include "GravityRtc.h"
#include "DHT.h"
#include <SHT1x-ESP.h>
#include <OneWire.h>
#include <DallasTemperature.h>


// === Pin definition ===
#define DHTPIN 25
#define DHTTYPE DHT22
#define SHT10_DATA_PIN_1 16
#define SHT10_CLOCK_PIN_1 17
#define CSPIN 5
#define SOIL_PIN 34
#define ONE_WIRE_BUS 27

```

Figure 3.13 First lines of the sketch in Arduino IDE, with initialization of the libraries and configuration of sensor connection pins.

3.3 SYSTEM CHARACTERISATION AND CALIBRATION

The purpose of this phase was to evaluate the performance of the individual low-cost sensors, analyze the overall reliability of the implemented system, and calibrate the soil moisture probe through gravimetric measurements. The objective was to ensure more accurate estimation and establish a solid correlation between the values returned by the capacitive probe and the actual soil water content, expressed as volumetric water content in $cm^3\backslash cm^3$. This procedure was necessary to reduce systematic errors typical of low-cost sensors and to improve the overall quality of the acquired data. Furthermore, calibration represents a fundamental step for the integration of sensors into agronomic monitoring models, where accuracy in soil water content measurement is crucial for sustainable water resource management and for optimizing agricultural practices.

3.3.1 Capacitive soil moisture

Capacitive sensors for soil moisture measurement exploit the dielectric contrast between water and the solid matrix, since the different components exhibit distinct permittivity values: dry soil generally has a relative permittivity between 2 and 6, water has a value of about 80 at standard pressure and temperature, while air is equal to 1 [70]. Capacitance is defined as the amount of energy stored in a capacitor. The latter is an electrical device consisting of two conductive plates, one positive and one negative, separated by a dielectric medium, namely the space between them. The shape and geometry of the capacitor significantly influence the detection and measurement of capacitance [57], [70]. The classical reference model is represented by the parallel-plate capacitor, which allows for a simplified calculation of capacitance through the following equation [57], [71], [72] (*eq. 3, eq.4*):

Equation 3

$$q = CV$$

Equation 4

$$C = \varepsilon_0 \frac{A}{d}$$

where:

- C= capacity;
- q = charge;
- V = tension;
- ε_0 = absolute permittivity of vacuum;
- A = plate area;
- d = distance between plates.

From the equation it is evident that the capacitance of the capacitor depends closely both on the area of the plates and on the permittivity of the dielectric medium. Soil moisture capacitive probes exploit this property by measuring capacitance variations caused by dielectric changes generated by water content. Specifically, as the amount of water in the soil increases, the permittivity of the medium changes and, consequently, so do the capacitance and the voltage value detected by the sensor. An important theoretical reference for the relationship between soil dielectric constant and volumetric water content is represented by the equation proposed by Topp et al [73], developed from measurements carried out using the TDR technique. This equation empirically describes the polynomial relationship between the dielectric constant (ε) and the VWC *(θv),* and has become widely used as a scientific standard (*eq.5*):

Equation 5

$$\theta v = -5.3 \times 10^{-2} + 2.92 \times 10^{-2}\, \varepsilon - 5.5 \times 10^{-4}\, \varepsilon^2 + 4.3 \times 10^{-6}\, \varepsilon^3$$

- θv= VWC (%),
- ε= relative dielectric constant of soil.

Although originally conceived for TDR sensors, Topp's equation can also be considered a conceptual reference for other types of sensors, including low-cost capacitive ones, which exploit variations in electrical capacitance as a function of the soil's dielectric contrast.

3.3.2 Gravimetric soil moisture content and Volumetric soil moisture content

The gravimetric soil moisture content allows determining the mass of water present in a soil sample. Although the gravimetric method is the most widely used for determining soil moisture, it is time-consuming and requires the destruction of the sample. In this approach, the soil is considered as consisting of two components: the dry solid fraction and the water contained in the pore spaces. The formula can be expressed as the ratio between the mass of the wet soil (*ms*) and that of the dry soil (*md*), representing the most common definition of water content, which is generally reported as a percentage (*eq.1*).

Another method for determining soil water content is VWC (θ*v*), which represents the volume of water present within a given volume of soil. It is derived from the gravimetric water content, taking into account the soil's density and mass (*eq. 2*), where:

ρω = water density (often neglected, as it is close to 1);

ρd,s = Bulk density of sample soil.

VWC plays a central role in agriculture, soil science, and soil physics, as it influences fundamental properties such as water retention capacity,

compressibility, infiltration, and soil reactivity [74]. In recent years, the use of capacitive sensors to estimate VWC has become widespread in many agricultural applications. However, the accuracy of measurements provided by these devices may not always reflect actual conditions, making it necessary to preliminarily assess sensor performance and perform soil-specific calibration. Several authors [74] [75] [76] [77] have highlighted how pedological properties, such as soil structure and texture, significantly affect the sensor's electromagnetic response and, consequently, the estimated water content values. In particular, soil texture has been shown to have a notable impact not only on sensor response but also on determining the irrigation activation point, with direct effects on water resource management [75].

3.3.3 Calibration

The calibration of the sensor was conducted in two main phases. In the first phase, soil samples with a predominantly clay-loam texture (37.3% clay, 34.4% silt, and 28.3% sand), neutral pH (7.65; 1:2.5 H_2O), and low electrical conductivity (0.164 $dS \cdot m^{-1}$; 1:5 H_2O)[78] were collected from the experimental site at the Rabanales University Campus in Córdoba (Andalusia, southern Spain; 37.87° N, 4.58° W in the WGS84 datum, elevation 238 m a.s.l.) in May 2025. This area is characterized by mild winters and extremely hot, dry summers, typical of the Mediterranean climate, where recurrent periods of water scarcity significantly limit irrigation water availability, making efficient water management essential for sustainable agricultural production [78]. The purpose of this first calibration phase was to accurately determine the ADC values recorded by the sensor at specific, known levels of soil moisture. The samples were air-dried for 24 hours, as reported in [57], and subsequently reprocessed. This step involved sieving the soil through a mesh ≤ 2 mm and removing coarse fragments and impurities (stones, roots, leaves, woody debris, etc.). This procedure was necessary as it improves calibration accuracy, as highlighted in [57], [62]. The prepared soil was further dried in an oven at 105 °C for 24 hours. The dried samples, characterized by a GWC of 5%, were transferred into 1 L plastic containers, for which the bulk density had been preliminarily determined. The first calibration phase involved acquiring ADC values from the SEN:SKU0308 sensor at known moisture concentrations to define the device's response range. To achieve the different moisture levels, water was added to the samples according to the following formula:

Equation 6

$$m_{H2O} = \frac{(U_f - U_i)}{100} * m_{soil}$$

where U_f represents the desired moisture content, U_i is the initial moisture content of the dried sample, and m_{soil} is the mass of soil contained in the pot. Two series of tests were conducted (between May and June 2025) at

moisture levels of 5%, 15%, 25%, 45% and 50%, at which point the soil was already saturated. The sensor was inserted vertically to a depth of approximately 15 cm, and before recording the ADC value, a waiting period of 20 minutes was observed to allow the system to reach equilibrium, as suggested by [57], [62]. Table 3.9 reports the parameters used to determine the amount of water (mH_2O, in grams) added to the different samples, along with the corresponding ADC values recorded by the sensor, calculated as the average of the two trials, and the respective values measured in air and water.

Table 3.9 Parameters used for the preparation of soil samples at different moisture levels and corresponding ADC values recorded by the SEN:SKU0308 sensor during the calibration phase.

Soil weight (g)	**Mass of h_2o to be added (g)**	**Weight of added h_2o (g)**	**Soil volume (l)**	**Ui %**	**Uf %**	**U% range**	**ADC**	**Classification**
1100	0	0	1	5	5	0-5	3532	Soil very dry
1100	110	110	1	5	15	6-15	2855	Soil dry
1105	221	219	1	5	25	16-25	1816	Soil moist
1102	385	380	1	5	45	26-45	1226	Soil very moist
1098	494	490	1	5	50	46-50	735	Soil satured
						ADC in air	3750	
						ADC in water	320	

The second phase focused on the calibration of the system. In this stage, the soil moisture sensor was calibrated in relation to the soil water content [4], [70], [79], [62]. a 1 L volume of soil, previously air-dried, cleaned of impurities, sifted, and oven-dried, was brought to full saturation with water. The moisture sensor was inserted vertically to a depth of 15 cm and kept in position for the entire natural drying period of the soil, which lasted approximately ten days. Readings were recorded automatically every 10 minutes, with the aim of obtaining a continuous and detailed curve of moisture variation over time. At the same time, a temperature sensor was placed vertically at 5 cm depth to monitor synchronous thermal changes of the soil during the drying process (Figure 3.14). For calibration purposes, soil samples were collected at approximately 15 cm depth, close to the probe, obtaining one sample per day of about 10 g.

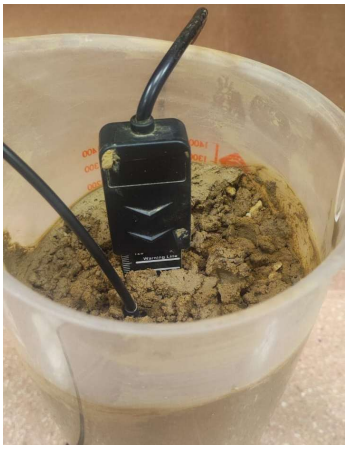

Figure 3.14 Placement of moisture and temperature probes in the soil sample: The SEN0308 probe is inserted vertically at a depth of 15 cm, while the DS18B20 sensor is positioned at 5 cm depth. This arrangement allows synchronous monitoring of soil moisture and temperature parameters during the natural soil drying process.

The fresh samples were immediately weighed with an electronic balance and then oven-dried at 105 °C for 24 hours to determine GWC, from which the VWC was subsequently calculated. Environmental thermo-hygrometric conditions (minimum and maximum temperatures of 21–30 °C and relative humidity of 35–60%) were monitored using a thermostat. Additionally, sensors dedicated to ambient condition monitoring were placed approximately 1 m above the soil sample to simulate field installation recommendations (*Figure 3.15*). This phase had a dual purpose: on one hand, to calibrate the sensor with respect to the soil's volumetric water content, and on the other, to test the overall system performance under real operational conditions. Specifically, aspects such as durability, continuity of measurements, and reliability of the data-saving process were evaluated, aiming to highlight the strengths of the proposed solution and identify potential areas for improvement.

Figure 3.15 Placement of the complete monitoring system: sensors for soil and environmental parameters are installed, with ambient sensors positioned at 1 meter height. The system is powered via a power bank, ensuring continuous operation, and all components are connected to enable real-time data acquisition and storage.

3.4 SYSTEM VALIDATION AND INTEGRATION WITH FASTAPI

After obtaining the calibration equation for the direct estimation of the VWC from the sensor, a new monitoring phase was initiated in June and July 2025 to validate the low-cost system under controlled conditions.

For this test, a sandy-loam soil sample was collected from the experimental site in Córdoba. The sample underwent a standard preparation process: air-drying for 24 hours, sieving and removal of impurities, followed by oven-drying to ensure a minimal water content. Subsequently, 1 liter of soil (dry weight 1108 g) was placed in a pot, and the moisture probe and the temperature probe were inserted vertically, at depths of 15 cm and 5 cm, respectively. The experiment started with a soil initial moisture content of 8%. Then, 440 g of water (corresponding to 50% GWC) were added, and the monitoring phase was initiated. The test lasted for approximately 20 days, during which variable amounts of water were periodically added to assess the sensor's response under different soil moisture conditions. Acquisitions took place every 10 minutes and, once daily, 10 g samples were taken to determine the actual VWC.

During this phase, beyond data acquisition, the functional performance of the low-cost system was assessed, verifying:

- the correct operation of the Arduino (.ino) code;
- the stability of the system and possible software or hardware failures;
- and the durability of the power supply throughout the monitoring period;
- system validation;
- development of a multi-factor DSS.

Following calibration, a rigorous statistical analysis was conducted to evaluate the accuracy of the low-cost system. This analysis compared the VWC values estimated by the sensor with reference data obtained through gravimetric determination. This study verified the effectiveness of the polynomial calibration process and the stability of the measurements over time.

At the end of the experimental monitoring phase, and following validation, the recorded data were centralized and integrated into a simulated platform using FastAPI, through the development of a Python code. This integration was essential to simulate a low-cost Decision Support System (DSS) environment, thereby demonstrating the practical applicability of the system. The approach adopted for the DSS is multifactorial, based on combining critical variables: integrating soil data (VWC and Temperature) with environmental data, for which the SHT10 sensor was employed. This choice is

motivated by the results of the preceding descriptive analysis, which clearly demonstrated that the SHT10 provided significantly better performance and reliability compared to the DHT22 model. The developed decision architecture is entirely accessible through the FastAPI interface, which allows for the real-time visualization of the analysis of every single sensor reading and the consequent decision or recommendation alert.

To provide a clearer understanding of the system's development logic and organization, *Figure 3.16* illustrates the general architecture of the monitoring system. It is structured into three main functional levels:

i) **Data acquisition layer:** this represents the foundation of the system and includes the low-cost sensors dedicated to measuring environmental and soil parameters (temperature, relative humidity, and soil water content). The ESP32 microcontroller serves as the operational core of this section, managing the processes of data reading, preliminary processing, and transmission.

ii) **Data storage and management layer:** the acquired data are transmitted and organized within the MongoDB database, which ensures scalable, structured, and secure storage. The NoSQL nature of MongoDB allows efficient management of large and heterogeneous data sets originating from multiple sensors, providing flexibility for querying and integration with other software tools.

iii) **Interface and visualization layer:** this is the user access point. Through the FastAPI framework and its Swagger UI interface, users can connect from any device to visualize real-time data, access the analytical results, and interact with the system intuitively.

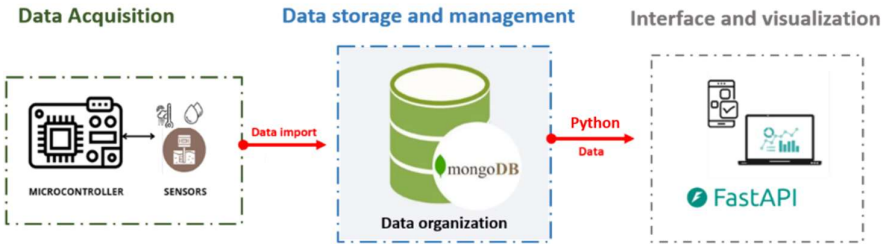

Figure 3.16 Diagram of the low-cost monitoring system.

4 DISCUSSION OF RESULTS

This chapter analyzes and discusses the results obtained from the implementation of the monitoring system, with particular focus on the physical and technical performance of the sensors used. Data processing was performed using RStudio, allowing the calculation of descriptive statistics, verification of measurement normality, and analysis of correlations between variables, as well as the evaluation of the effectiveness of the developed calibrations. The results are interpreted in the context of the experimental conditions and their practical implications for soil monitoring and integration into smart farming systems. Finally, a critical analysis of the main issues encountered during the experimentation is presented, including power supply through power banks and the challenges related to data transmission and management, with the aim of highlighting the current limitations and the possible perspectives for system improvement.

4.1 PROBE CALIBRATION PHASE

The first phase of the work involved a linear calibration specific to the soil, with the aim of identifying the ADC values corresponding to the actual soil water content. According to the manufacturers' guidelines, the calibration procedure is based on two boundary conditions:

- **Value 1 (dry soil):** obtained by exposing the probe to air, representing 0% moisture. Under standard conditions, this value should fall within the range 520–640, depending on atmospheric humidity.
- **Value 2 (saturated soil):** obtained by immersing the probe in water until reaching the limit value of 0, corresponding to soil saturation.

However, during the experimental tests, an anomalous behavior was observed: under conditions of genuinely dry soil, the sensor returned values outside the expected range. This outcome highlighted the need to perform a rigorous, soil-specific gravimetric calibration, as widely suggested in the literature [57], [61], [62], [79], [80], in order to obtain reliable soil moisture measurements. Another important aspect to consider concerns the supply voltage. The sensor datasheet reports values based on a 5 V supply, whereas in this project the sensors were powered at 3.3 V. This choice was motivated by the need to reduce energy consumption and increase overall system efficiency from a low-power perspective. It is well known that variations in supply voltage can affect the sensor's response, shifting the ADC range. Therefore, this calibration phase made it possible to define the different experimental ADC value ranges, reported in Table *3.10*, which represent the reference points for dry and saturated soil conditions. Based on these values, the first sketch was developed in the Arduino IDE environment. Figure 4.1 shows the definition of constants using the **#define** directive, employed to implement the sensor calibration. This procedure allows the ADC values to be uniquely associated with the corresponding soil moisture conditions.

```
19
20  // === Soil Sensor Calibration: GWC ===
21  #define ADC_VERYDRY 3532                                    //0%-5% MOISTURE: 5%
22  #define ADC_DRY 2855                                       //6-15% MOISTURE
23  #define ADC_MOIST 1816                                     //16-25% mOISTURE
24  #define ADC_VERYMOIST 1226                                 //26-45% moisture
25  #define ADC_SATURATED 735                                  //50% mOISTURE
26  #define ADC_WATER 320                                      //100% MOISTURE
27
```

Figure 4.1 Extract from the code developed in the Arduino IDE (sketch_Calibration_lowcost_sensor) to define the sensor reference values.

The relevant function in the *.ino* code is calcSoilMoisture() (*Figure 4.2*), which converts the raw reading from the soil moisture sensor **(*int soil_adc*)** into an estimated soil moisture content value, expressed as a percentage. To achieve this, the function uses a series of predefined soil moisture thresholds, each associated with a specific range of ADC values. The internal logic is based on an **if–else if** conditional structure that divides the sensor's value range into several bands corresponding to different moisture conditions. Within each range, the **mapFloat()** function is used to perform a linear mapping between two known extremes: the ADC values and the corresponding percentage values of soil moisture (GWC%). This approach is particularly useful for low-cost sensors, whose electrical response is not always perfectly linear across the entire measurement range. Moreover, since the ADC thresholds are defined based on real measurements (e.g., very dry, moist, or saturated soil), the function ensures a realistic and representative calibration of the sensor's actual behavior. The final output is a percentage value that is easy to interpret, providing the basis for subsequent data processing phases and for the application of the calibration equation.

```
182  // === calculation of moisture content, using defined GWC thresholds ===
183  float calcSoilMoisture(int soil_adc) {
184    float soil_moisture;
185    if (soil_adc >= ADC_VERYDRY) {
186      soil_moisture = 5.0;
187    }
188    else if (soil_adc >= ADC_DRY) {
189      soil_moisture = mapFloat(soil_adc, ADC_VERYDRY, ADC_DRY, 5.0, 15.0);
190    }
191    else if (soil_adc >= ADC_MOIST) {
192      soil_moisture = mapFloat(soil_adc, ADC_DRY, ADC_MOIST, 15.0, 25.0);
193    }
194    else if (soil_adc >= ADC_VERYMOIST) {
195      soil_moisture = mapFloat(soil_adc, ADC_MOIST, ADC_VERYMOIST, 25.0, 45.0);
196    }
197    else if (soil_adc >= ADC_SATURATED) {
198      soil_moisture = mapFloat(soil_adc, ADC_VERYMOIST, ADC_SATURATED, 45.0, 50.0);
199    }
200    else if (soil_adc > ADC_WATER) {
201      soil_moisture = mapFloat(soil_adc, ADC_SATURATED, ADC_WATER, 99.0, 100.0);
202    }
203    else {
204      soil_moisture = 100.0;
205    }
206
```

Figure 4.2 Arduino function calcSoilMoisture() used to convert the raw ADC readings from the soil moisture sensor into percentage values (GWC%), based on predefined calibration thresholds.

4.2 SYSTEM PERFORMANCE AND OPERATION

This section analyzes the performance and correct operation of the monitoring system over time. *Figures 4.3* and *4.4* show the continuous monitoring graphs, which highlight the system's ability to consistently acquire and record sensor data, ensuring sufficient temporal coverage for subsequent statistical analyses. The behaviour of the sensors was evaluated both in terms of signal stability and with respect to the consistency of the recorded values compared to the observed soil and environmental conditions. This analysis made it possible to detect potential anomalies, discontinuities, or instrumental drifts, providing useful insights into the actual performance of the system under operational conditions. Throughout the monitoring period, the system never interrupted data acquisition; the RTC module ensured accurate date and time tracking, while the data were regularly stored in .csv files. At the end of the monitoring days, the power bank still retained about 20% of residual charge: a positive result considering that it was not exposed to solar radiation and therefore could not benefit from any form of autonomous recharging.

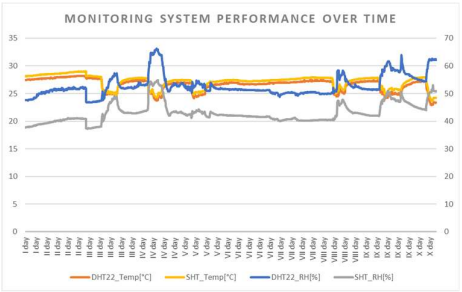

Figure 4.3 Trend of continuous monitoring of environmental parameters (air) recorded by DHT22 and SHT sensors.

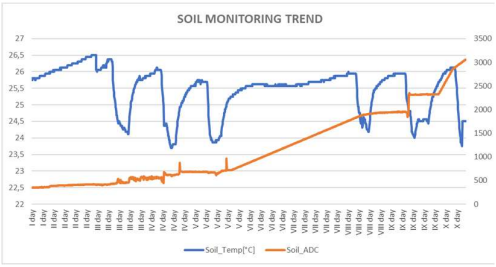

Figure 4.4 Continuous monitoring of soil parameters (temperature and ADC) recorded by sensors in the soil sample.

4.3 CHARACTERIZATION OF THE PROTOTYPE

A sensor characterization phase was subsequently carried out, aimed at providing a detailed description of the performance of each component. In this phase, descriptive analyses of the collected data were performed using the RStudio environment. The analyses allowed for the calculation of central tendency indices (mean, median, mode) and dispersion measures (standard deviation, variance), as well as the assessment of data distribution through skewness, kurtosis, and normality tests. This preliminary characterization provided essential information on the behavior of the sensors in terms of precision, variability, and statistical reliability, laying the groundwork for the gravimetric calibration procedure.

4.3.1 Descriptive analysis

To understand the behavior of the sensors and characterize the measurements obtained, a descriptive analysis of the collected data was carried out. This analysis makes it possible to summarize the main features

of the recorded values by evaluating central tendency (mean, median, mode), dispersion (standard deviation, variance), and the shape of the distribution (skewness and kurtosis). In addition, the minimum and maximum values were considered to assess the overall range of variation.

In support of the numerical parameters reported in *Table 4.1*, boxplots were produced for each sensor and type of measurement, allowing visualization of the data distribution and the presence of possible outliers. This step is essential to verify the stability and reliability of the sensors, to compare the different devices, and to provide preliminary insights useful for gravimetric calibration and subsequent statistical analyses.

Table 4.1 Summary of descriptive statistics for all sensors and measured variables: mean, median, mode, standard deviation, variance, skewness, kurtosis, minimum and maximum values, and number of observations (n).

Sensor	Variable	Mean	Median	Mode	Standard deviation	Variance	Skewness	Kurtosis	Min	Max	n
DHT22	RH	53.86	53.4	51.9	4.43	19.67	0.14	-0.65	46.7	63.9	635
DHT22	Temp	26.21	26.6	27.2	1.21	1.47	-0.36	-1.05	22.9	27.9	635
SHT	RH	44.49	44.18	42.95	3.96	15.65	-0.16	-0.50	37.28	54.34	635
SHT	Temp	26.64	27.04	27.89	1.25	1.57	-0.30	-1.41	23.66	28.25	635
Soil	ADC	1744.47	1774	2320	519.81	270.197.34	-0.13	-1.25	806	2583	635
Soil	Gravimetric	27.66	23.58	18.28	10.03	100.55	0.65	-1.02	16.67	49	635
Soil	Temp	25.26	25.44	26.06	0.76	0.58	-0.24	-1.45	23.75	26.37	635

4.3.1.1 *DHT22*

The DHT22 sensor, used for environmental monitoring of temperature and relative humidity, shows an overall stable behaviour consistent with the measured conditions. For RH, the mean (53.86%) and median (53.4%) are very close, indicating a well-balanced data distribution. The mode (51.9%) is also close to these values, confirming the absence of strong asymmetries. The skewness value (0.14) indicates an almost symmetric distribution, with only a slight positive tendency (a small right tail), while the negative kurtosis (-0.65) suggests a platicurtic distribution, flatter than the normal one and therefore showing slightly greater dispersion, though minimal, as the value is close to zero. The standard deviation (4.43) and variance (19.67) are moderate, confirming good stability of the measurements with limited variability. The range (46.7–63.9%) shows that the sensor recorded moderate fluctuations in humidity, consistent with normal environmental conditions.

For temperature, the mean (26.21 °C), median (26.6 °C), and mode (27.2 °C) are very close, indicating a centred and homogeneous distribution. The slightly negative skewness (-0.36) suggests a mild left asymmetry due to a few lower values that slightly decrease the mean, while the negative kurtosis (-1.05) indicates a platicurtic distribution, with greater dispersion compared to a normal curve. The standard deviation (1.21) and variance (1.47) are low,

highlighting high precision and stability in the measurements. The range (22.9–27.9 °C) confirms that the ambient temperature remained within realistic and stable limits during monitoring. Overall, the results of the descriptive analysis show that the DHT22 sensor provides consistent, stable, and undistorted data, making it reliable for environmental monitoring under the experimental conditions considered. Figure 4.5 shows the box plots for both measurements, providing a visual summary of the consistent and stable behavior of the sensor under the monitored environmental conditions.

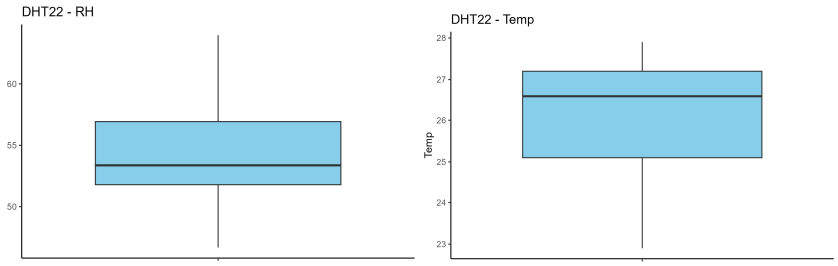

Figure 4.5 Boxplot of the measurements from the DHT22 sensor. The boxes represent the central 50% of the data, the internal line indicates the median, and points outside the whiskers represent outliers.

4.3.1.2 *SHT10*

The SHT10 sensor, used for environmental monitoring, showed consistent and stable measurements for both relative humidity (RH) and temperature. Regarding RH, the mean (44.49%) and median (44.18%) are very close to each other, indicating a well-centered data distribution. The mode (42.95%) is also close to these values, confirming a high level of homogeneity in the measurements. The standard deviation (3.96) and variance (15.65) are low, suggesting a limited dispersion of data around the mean. The skewness (–0.16) is slightly negative, indicating an almost symmetrical distribution with a slight left tail, meaning the presence of a few lower values that marginally reduce the mean. The kurtosis (–0.50) is also negative, indicating a platicurtic distribution, with a greater spread of values compared to a normal distribution, with a slightly flatter curve, but in this case contained. Overall, RH values range between 37.28% and 54.34%, confirming the sensor's stability and a realistic behavior consistent with field conditions.

As for soil temperature (T), the mean (26.64 °C) and median (27.04 °C) show good alignment, indicating a centreded distribution, while the mode (27.89 °C) is slightly higher, suggesting a mild concentration of higher values. The standard deviation (1.25) and variance (1.57) are low, confirming a high stability of temperature measurements. The skewness (–0.30) is slightly negative, indicating an almost symmetrical distribution with a minor tendency toward lower values. The kurtosis (–1.41) highlights a markedly

platicurtic distribution, meaning the curve is flatter than a normal distribution, with a somewhat wider spread of values around the mean, though still limited. The observed range, between 23.66 °C and 28.25 °C, confirms that the sensor recorded small thermal fluctuations, consistent with the stable laboratory conditions during the monitoring period. The results are visualized in the boxplot shown in *Figure 4.6*, which highlights the median, the central 50% of the data, and any outliers. Overall, the data confirm the consistency and reliability of the SHT10 sensor under the monitored environmental conditions.

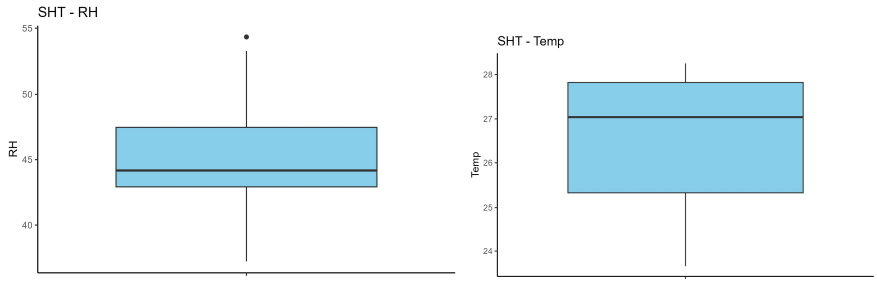

Figure 4.6 Boxplot of SHT10 sensor measurements: relative humidity (%) and temperature (°C).

4.3.1.3 *SKU SEN0308 and DS18B20*

The capacitive soil moisture sensor shows a strongly positively skewed distribution: the ADC values show an overall stable and consistent behaviour. The mean (1744.47) and median (1774) are very close, indicating a well-centered distribution, while the mode (2320), slightly higher, suggests the presence of a group of higher values that occur more frequently. The standard deviation (519.81) and variance (270.197.34) indicate a moderate dispersion of data around the mean, consistent with the variable nature of the ADC signal, which directly reflects fluctuations in soil moisture content during the drying process.

The skewness (–0.13) is slightly negative, indicating an almost symmetrical distribution with a minor tendency toward lower values. This means that most ADC readings are concentrated around the mean, with a few lower values that do not significantly affect the overall distribution. The kurtosis (–1.25) is negative, revealing a platykurtic distribution, i.e., flatter than a normal curve, characterized by greater dispersion around the mean and fewer pronounced peaks. The range of variation (806–2583) shows a wide spread of ADC values, consistent with the full soil moisture cycle, from saturation to near complete drying. Overall, the descriptive results confirm that the soil sensor consistently recorded the variability of the ADC signal

throughout the experiment, faithfully reflecting changes in soil moisture conditions and demonstrating good measurement sensitivity of the system.

These characteristics are clearly visible in the boxplot shown in *Figure 4.7*. where the median and the concentration of central data can be observed.

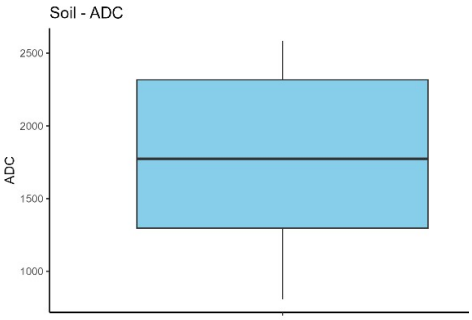

Figure 4.7 Boxplot of the capacitive soil moisture sensor measurements.

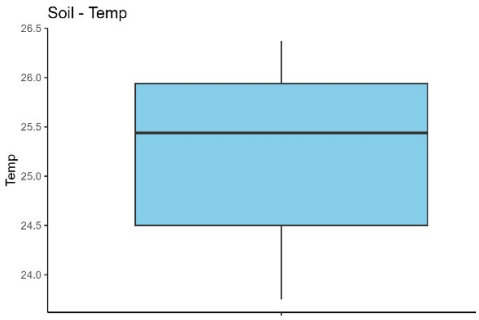

Figure 4.8 Boxplot of soil temperature sensor measurements.

The soil temperature values show an extremely stable and consistent behavior over time. The mean (25.26 °C) and median (25.44 °C) are very close, indicating a well-centered distribution of the data. The mode (26.06 °C), slightly higher, suggests the presence of a small group of higher values occurring more frequently, though without significantly affecting the overall symmetry of the distribution. The standard deviation (0.76) and variance (0.58) are very low, revealing a minimal dispersion of the values around the mean and confirming the high precision and stability of the sensor in recording soil temperature. The skewness (–0.24) is slightly negative, indicating an almost symmetrical distribution with a small tendency toward lower-than-average values. The kurtosis (–1.45) is negative, suggesting a greater dispersion of the data compared to a normal distribution. The range of variation, between 23.75 °C and 26.37 °C, shows a narrow thermal excursion, consistent with stable laboratory or controlled field conditions.

Overall, these results confirm that the soil sensor provided reliable, consistent, and low-variability measurements, accurately describing the temperature trend during the monitoring period. The distribution of data and the presence of outliers are clearly visible in the boxplot *(Figure 4.8*).

4.3.1.4 *Conclusions*

The analysis of environmental measurements highlighted that both DHT22 and SHT10 sensors provided consistent and relatively stable data, with relative humidity and temperature values generally well-centred around the mean. However, some differences emerge when examining the distributions in detail. The DHT22 sensor, designed for air monitoring, showed mean and median values that are very close to each other and low data dispersion, indicating good precision in measuring temperature and relative humidity. However, compared to the SHT sensors, the DHT22 tends to exhibit greater variability and slight asymmetry in the distributions, indicative of lower stability under conditions of wider temperature fluctuations. Moreover, the environmental values recorded by the DHT22 and SHT are consistent with those measured by the laboratory thermostat, whose variation ranges during the monitoring period were T = 21.5–30 °C and RH = 35–60 %. The capacitive soil moisture sensor shows high variability and an asymmetric distribution, recording elevated values and significant peaks, confirming its ability to cover a wide range of soil water content. Conversely, the DS18B20 sensor, used for soil temperature, exhibits very stable and well-centred measurements, with low dispersion and a near-normal distribution. Overall, while the moisture sensor effectively captures the full range of soil variation, the temperature sensor provides reliable and consistent readings.

4.3.2 Normality test

To study the distribution of data collected by the different sensors and for the various parameters, the Shapiro–Wilk test was applied, with a significance threshold set at 5%. All analyzed variables exhibited non-normal distribution, as in every test the p-value was below 0.05, leading to the rejection of the null hypothesis of normality (*Table 4.2*). This step is crucial for subsequent correlation analyses, since the choice between parametric and non-parametric tests depends on the underlying distribution of the data.

Table 4.2 Results of the Shapiro–Wilk test for the different sensors and parameters. The W column reports the test statistic, p-value, and the Normality column indicates whether the null hypothesis of data normality was accepted or rejected.

Sensor	**Variable**	**W**	**p_value**	**Normality**
DHT22	RH	0.96	2.89E-12	Rejected
DHT22	Temp	0.91	3.97E-19	Rejected
SHT	RH	0.96	1.65E-12	Rejected
SHT	Temp	0.88	1.91E-21	Rejected
DS18B20	Temp	0.90	1.92E-19	Rejected
SKU SEN0308	ADC	0.93	3.49E-16	Rejected

4.3.2.1 *DHT22*

For this sensor, neither relative humidity nor temperature follow a normal distribution, as confirmed by the very low p-values ($p < 0.05$) obtained from the Shapiro–Wilk test. These results are consistent with the observations reported in the previous paragraph regarding the characteristics of the distribution: humidity shows a slight positive skewness, while temperature exhibits a slight negative skewness. In the corresponding Q-Q plots (*Figure 4.9 and 4.10)*, a deviation of the variables from the reference line of the normal distribution can be observed.

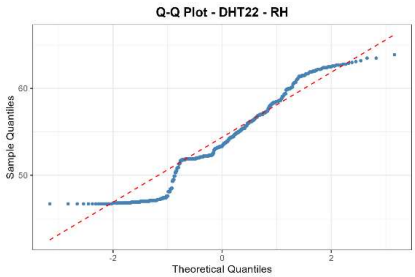

Figure 4.9 Q-Q plot of RH measured by the DHT22 sensor. The plot compares the quantiles of the observed data with those of a theoretical normal distribution. Deviations from the diagonal line indicate departures from normality.

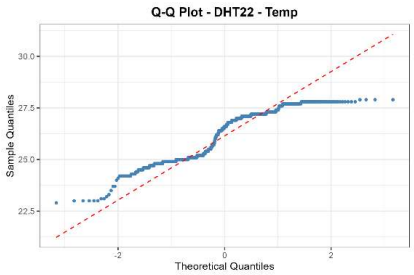

Figure 4.10 Q-Q plot of T measured by the DHT22 sensor. The plot compares the quantiles of the observed data with those of a theoretical normal distribution. Deviations from the diagonal line indicate departures from normality.

4.3.2.2 *SHT10*

For the SHT sensor, the Shapiro–Wilk test also indicates that neither RH nor T follow a normal distribution. Although the W statistic is close to 1 (0.96 for RH and 0.88 for T), the p-value remains well below 0.05. These distribution characteristics are further confirmed by the corresponding Q-Q plots (*Figure 4.11 and 4.12).*

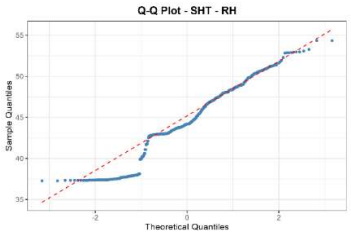

Figure 4.11 Q-Q plot of RH measured by the SHT sensor. Deviations from the diagonal line indicate departures from normality.

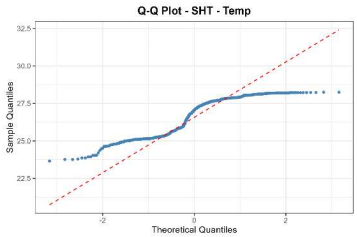

Figure 4.12 Q-Q plot of T measured by the SHT sensor. Deviations from the diagonal line indicate departures from normality.

4.3.2.3 *SKU:SEN0308 and DS18B20*

For soil measurements, the Shapiro–Wilk test indicates that the ADC values do not follow a normal distribution (w= 0.93 but p-value $\ll 0.05$), as also

evident from the Q-Q plot (*Figure 4.13-4.14*). Similarly, for soil temperature, the test confirms a non-normal distribution (w= 0.90, p-value ≪ 0.05). This tendency is clearly visible in the corresponding Q-Q plot, where the data deviate from the normal line.

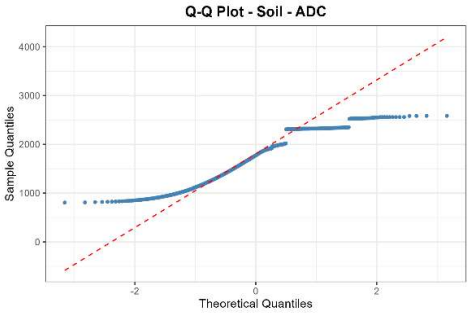

Figure 4.13 Q-Q plot of ADC. The plot compares the quantiles of the observed ADC data with those of a theoretical normal distribution. Deviations from the diagonal line indicate departures from normality.

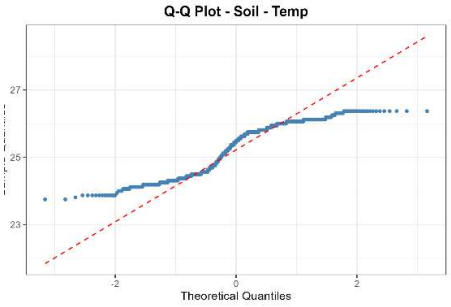

Figure 4.14 Q-Q plot of soil temperature. The plot compares the quantiles of the observed soil temperature data with those of a theoretical normal distribution. Deviations from the diagonal line indicate departures from normality.

4.3.2.4 *Conclusion*

For all the variables considered, the Shapiro–Wilk test, applied with a 5% significance threshold, highlighted a significant deviation from the normal distribution (p-value < 0.05). This result implies the rejection of the null hypothesis of normality, confirming what was already observed in the descriptive analysis regarding the presence of skewness and extreme values. This evidence is methodologically relevant, as the choice of statistical test to be applied, for correlation studies, strongly depends on the nature of the data distribution. For this reason, subsequent statistical and correlation analyses will be conducted using non-parametric methods, which are more robust and appropriate for handling the actual structure of the collected data.

4.3.3 Correlation study

From the preliminary normality analysis, it emerged that none of the distributions of the analyzed parameters are Gaussian. For this reason, correlation analyses were carried out using non-parametric methods, specifically adopting Spearman's rank correlation coefficient (ρ_s), which allows measuring the strength and direction of monotonic relationships between paired variables without assuming constraints on data distribution [81], [82]. This approach is also widely employed in sensor calibration studies [79]. In this work, correlation was investigated in three phases:

i. comparison between the two environmental sensors, in order to assess the consistency of their temperature and relative humidity measurements;
ii. internal analysis for each sensor, to explore the relationship between the monitored parameters;
iii. evaluation of soil-related relationships, fundamental for probe calibration, through the study of the correlation between the raw signal (ADC) and GWC, as well as between temperature and GWC, and between temperature and ADC.

4.3.3.1 *Correlation between air monitoring sensors (DHT22-SHT10)*

Spearman's correlation analysis shows that the RH and T measurements from the DHT22 and SHT sensors are both strongly correlated, with ρ_s =0,97 for RH and ρ_s =0,95 for T, both with p-value <<0.05 (*Table 4.3*). This indicates a positive correlation, that the two sensors follow the same trend in environmental parameters, confirming that the DHT22 readings are consistent with those of the SHT. This correlation is clearly represented in the scatterplots (*Figure 4.15a-b*).

Table 4.3 Results of the Spearman correlation analysis between DHT22 and SHT sensors for RH and T measurements. Reported values include the correlation coefficients (ρs) and the corresponding significance levels (p-values).

Misures	**ρ_s**	**p-value**
RH	0.97	<2.2e-16
Temp	0.95	<2.2e-16

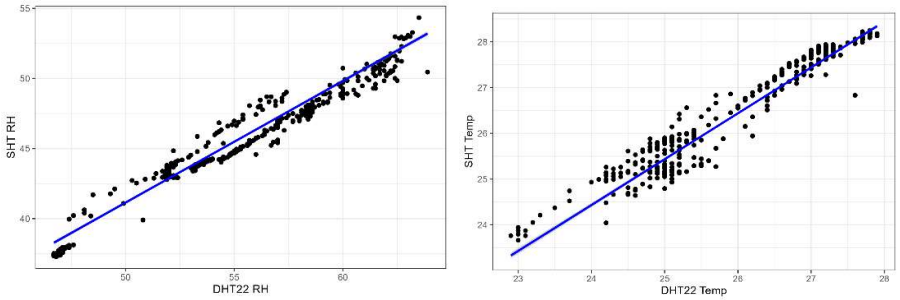

Figure 4.15a-b Scatterplots of relative humidity (RH) and temperature (T) measurements obtained from the DHT22 and SHT sensors. The trend line highlights the strong agreement between the two sensors, confirmed by the Spearman correlation analysis.

However, the slight differences observed can be attributed to instrumental variations, sensor positioning, external shielding, and differing response times. In summary, both sensors are reliable for simultaneously monitoring air RH and temperature.

4.3.3.2 *Internal correlation of environmental sensor parameters*

The internal correlation within each environmental sensor was also evaluated. The results are reported in *Table 4.4*, while the distribution of the data with respect to the trend line is shown in the corresponding scatterplots.

Table 4.4 Results of the Spearman correlation analysis between RH e T in different sensors.

Sensor	**ρ_s**	**p-value**
DHT22	-0.73	9.26E-107
SHT	-0.71	5.40E-99

For the DHT22 sensor, Spearman's correlation between relative humidity and temperature is $\rho_s = -0.73$, with p-value $\ll 0.05$, indicating a statistically significant negative correlation. This means that, as the temperature measured by the DHT22 increases, relative humidity tends to decrease. Also, for the SHT sensor, a strong significant negative correlation ($\rho_s = -0.71$, with p value $\ll 0.05$) was observed between temperature and relative humidity *(Figure 4.16a and 4.16b).*

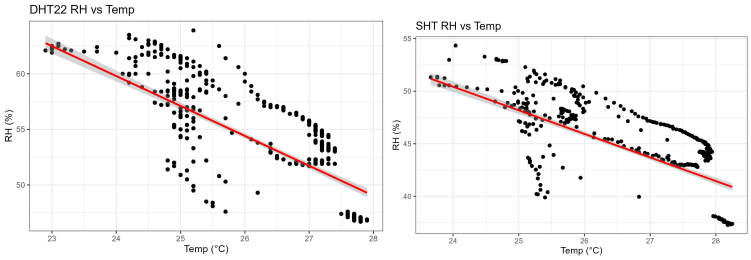

Figure 4.16a-b Scatterplot showing the relationship between relative humidity (RH) and temperature (T) within the DHT22 and SHT air sensors. Points represent individual measurements, and the line indicates the Spearman trend line.

4.3.3.3 *Soil correlation*

For the soil correlation analysis, the parameters T, ADC, and GWC were considered. The results of the Spearman test are reported in Table 4.5.

Table 4.5 Results of the Spearman correlation analysis in the soil.

Test	**ρ_s**	**P_value**
ADC vs Moisture	-0.99	0*
Temp vs Moisture	0.10	0.01
Temp vs ADC	-0.10	0.01

First, the correlation between ADC values and GWC was evaluated, showing an almost perfect negative correlation that is statistically significant. RStudio returns a p-value of 0 because the actual value is too small to be displayed. As the ADC value (the raw sensor output) increases, the gravimetric water content of the soil exhibits an almost perfectly monotonic decrease (*Figure 4.17*). This behaviour was expected, since the ADC indirectly reflects the

electrical resistance of the soil: drier soil exhibits higher resistance, which translates into higher ADC values and lower measured water content.

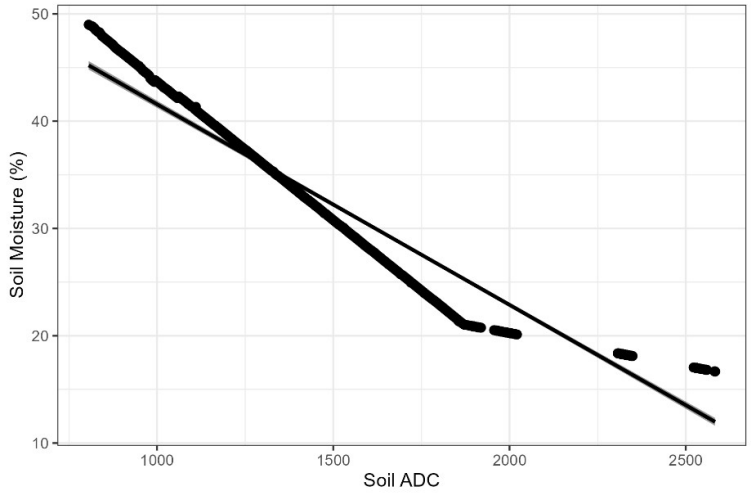

Figure 4.17 Scatterplot showing the relationship between the raw ADC values from the sensor and the gravimetric water content (GWC) of the soil.

The correlation between soil temperature and gravimetric water content is positive but weak ($\rho_s \approx 0.10$), although highly statistically significant (p-value < 0.05). This finding suggests that, on average, an increase in soil moisture is associated with a slight increase in temperature. However, in this specific case, the relationship is likely to be partially influenced by external factors, such as the temperature of the water present in the soil. Finally, the correlation between soil temperature and ADC values is negative and weak ($\rho_s \approx -0.10$), yet also highly significant. This indicates that, as temperature increases, ADC values tend to decrease slightly, in line with the weak positive relationship observed between temperature and gravimetric water content. Overall, this modest association confirms that soil temperature does not directly exert a substantial influence on ADC measurements, which remain primarily determined by soil water content.

4.3.3.4 *Conclusion*

In summary, the correlation analyses confirm the consistency and reliability of the sensors employed. The environmental sensors DHT22 and SHT provided consistent measurements of temperature and relative humidity, showing a parallel trend of the monitored parameters; in particular, the SHT sensor exhibits a stronger and more stable internal relationship between the two variables. With regard to the soil, the ADC values are strongly and negatively correlated with the GWC, confirming the sensor's ability to accurately detect moisture variations. The correlation with soil temperature, although weak yet statistically significant, suggests a secondary influence of this variable on the measurements. Overall, these results demonstrate the effectiveness of the monitoring system in providing reliable and coherent

data, thereby establishing a solid basis for subsequent calibration and analysis phases.

4.3.4 Regression analysis

The regression study allowed quantifying the relationship between the ADC values provided by the sensor and the soil water content, determined through gravimetric measurements and expressed in terms of VWC %. The literature reports various approaches to calibrate soil moisture sensors, depending on the type of sensor and the measured variable. For example,[79], employs piecewise linear regression equations, based on the least-squares method, between low-cost capacitive sensors to align dielectric constant readings. Other studies [70], [83] adopt a least-squares linear regression between the inverse of the sensor voltage and the gravimetrically estimated VWC, while, [44] and [48] apply both a second-order polynomial fit and a three-parameter exponential fit, flexibly modeling the relationship between sensor voltage and water content, which is useful in cases of nonlinear behavior. Alternative approaches [60], [62] are based on the output frequency of the sensor or integrate polynomial regressions with intermediate dielectric conversion steps.

In this work, the sensor used provides direct digital ADC values, acquired through continuous monitoring of soil from saturated to dry conditions. The actual water content was determined through gravimetric measurements and converted into VWC. The application of Topp's equation, was not necessary, since the sensor does not measure the dielectric constant but directly returns ADC values, consistent with [60], [61], [65]. Preliminary analysis using Spearman's rank correlation revealed a nearly perfect and statistically significant negative relationship between ADC and GWC, confirming the validity of ADC as a predictor of soil water content. Based on this evidence, two regression approaches were tested to model the relationship between ADC and VWC: a simple linear regression and a second-order polynomial regression. The results are presented in *Table 4.6*.

Table 4.6 Results of the regression models tested for sensor calibration. The table reports the coefficient of determination (R^2), mean absolute error (MAE), relative absolute error (RAE), root mean square error (RMSE), and the corresponding base regression equation.

Model	R2	MAE	RAE	RMSE	MSE	Equation
Linear	0.85	9.67	0.39	10.99	120.81	$Y = \beta_0 + \beta_1 * x1 + \varepsilon$
Polynomial (2°)	0.97	3.86	0.16	4.92	24.23	$Y = a + b_1 x + b_2 x^2$

The best-performing model was selected by evaluating the regression models using standard statistical indices, reported in *Table* 4.7 along with their corresponding references from the literature.

Table 4.7 reports the main model evaluation indices: the coefficient of determination (R^2), the Mean Absolute Error (MAE), the Relative Absolute Error (RAE), the Root Mean Squared Error (RMSE), and the Mean Squared Error (MSE), along with their corresponding ideal values.

Performance metric	Equation	Range	Ideal value
Coefficient of determination (R^2) [84]	$R^2 = \frac{\left(n\sum_{i=1}^{n}\hat{\theta}_i\theta_i\right) - \left(\sum_{i=1}^{n}\hat{\theta}_i\right)\left(\sum_{i=1}^{n}\theta_i\right)}{\sqrt{n\sum_{i=1}^{n}(\hat{\theta}_i)^2 - (\sum_{i=1}^{n}\hat{\theta}_i)^2}\sqrt{n\sum_{i=1}^{n}(\theta_i)^2 - (\sum_{i=1}^{n}\theta_i)^2}}$	0 to 1	1
Mean Absolute Error (MAE) [85]	$MAE = (\sum_{i=1}^{n}\lvert\theta_i - \hat{\theta}_i\rvert)/n$	0 to ∞	0
Relative Absolute Error (RAE) [85]	$RAE = \sum_{i=1}^{n}\lvert\theta_i - \hat{\theta}_i\rvert / \sum_{i=1}^{n}\lvert\hat{\theta}_i - \bar{\theta}\rvert$	0 to ∞	0
Root Mean Squared Error (RMSE) [85]	$RMSE = \sqrt{(\sum_{i=1}^{n}(\theta_i - \hat{\theta}_i)^2)/n}$	0 to ∞	0
Mean Squared Error (MSE) [85]	$\mathrm{MSE} = \frac{1}{n}\sum_{i=1}^{n}(Y_i - \hat{Y}_i)^2$	0 to ∞	0

From the analysis of the main goodness-of-fit indices of the tested regression models (*Table 4.6*), it emerges that the second-order polynomial model demonstrates the best performance. In particular, it explains 97% of the variability in the data (R^2 = 0.97), compared to 85% explained by the linear model (R^2 = 0.85). Moreover, the prediction errors are significantly lower: MAE = 3.86, RAE = 0.16, RMSE = 4.92, and MSE = 24.23, compared to the higher values observed for the linear regression. These results confirm the effectiveness of gravimetric calibration, which proves more accurate than calibration based on commercial sensors, as reported in [65], where the correlation SEN SKU0308 vs TDR reaches R^2 = 0.805. Figure 4.18 graphically illustrates the model's goodness-of-fit and the ability of the polynomial fit to more accurately follow the experimental trend of the data.

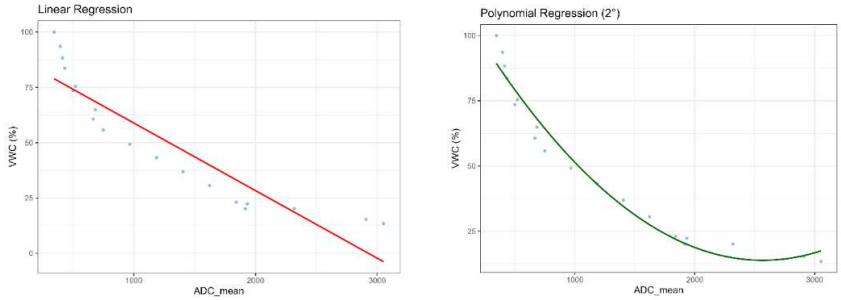

Figure 4.18 Comparison between linear and second-order polynomial regression models applied to the experimental data. The polynomial model shows a better ability to fit the observed points, describing more accurately the relationship between ADC values ADC values and the volumetric water content (VWC).

Starting from the calibration equation obtained from the second-order polynomial model (eq. 7), a simplified sketch (*sketch_Sensor_Calibrated*) was developed, in which the regression coefficients were implemented. This code allows for the direct estimation of the soil volumetric water content (VWC).

Equation 7

$$VWC = 114.536 - 0.078438 * ADC + 1.5278^{-05} * ADC^2$$

Figure 4.19 shows the main function of the code, **calcSoilVWC()**, which aims to convert the raw reading from the soil moisture sensor (*soil_adc*) into a VWC value, expressed as a percentage, using a polynomial regression equation derived from the experimental calibration phase.

```
43
44  // === Polinomial Calibration  ADC -> VWC ===
45  float calcSoilVWC(int soil_adc) {
46
47    const float a = 114.536;
48    const float b1 = -0.078434;
49    const float b2 = 0.000015278;
50
51    float VWC = a + (b1 * soil_adc) + (b2 * pow(soil_adc, 2));
52
53    // Limiti di sicurezza 0-100%
54    if (VWC < 0.0) VWC = 0.0;
55    if (VWC > 100.0) VWC = 100.0;
56
57    return VWC;
58  }
```

Figure 4.19 Excerpt of the Arduino code implementing the second-order polynomial calibration for soil volumetric water content (VWC). The coefficients used in the equation were obtained from the regression analysis conducted during the calibration study.

4.4 SYSTEM VALIDATION

To assess the behavior of the low-cost sensor after calibration, a descriptive statistical analysis was performed on the daily averaged volumetric water content (VWC) values measured by the sensor (Sensor_VWC) and on the corresponding reference values obtained from the gravimetric determinations (Real_VWC). The dataset consisted of measurements collected over 19 consecutive days. The sensor recorded VWC values every 10 minutes, while gravimetric samples were taken once per day, always around 18:00. For each day, the mean of the sensor's readings was computed and associated with the gravimetric measurement taken on the same date. The descriptive statistics included the calculation of mean, median, standard deviation, standard error of the mean, skewness, kurtosis for both datasets (Table 4.8). These parameters allowed for an initial understanding of the central tendency and dispersion of the measurements, as well as their distributional characteristics. In general, both datasets showed a similar range of variation, although the sensor data exhibited a slightly higher variability, as indicated by a larger standard deviation. The distribution of the values tended to be moderately skewed to the right, suggesting that higher VWC readings occurred more frequently. The negative kurtosis values indicated a relatively flatter

distribution compared to the normal curve, reflecting the presence of moderate variability across the monitoring period.

Table 4.8 Values from the descriptive analysis of VWC_sensor and VWC_real obtained from gravimetric measurements.

vars	mean	sd	median	se	skew	kurtosis
Sensor_VWC	34.22	19.06	22.49	4.62	0.62	-1.33
Real_VWC	32.58	18.79	22.70	4.56	0.68	-1.24

However, despite the greater variability observed in the sensor data, the VWC measurements provided by the low-cost system consistently follow the trend of the gravimetric determinations, confirming that the sensor, after calibration, is able to correctly reproduce the daily dynamics of the volumetric water content in the soil (*Figure 4.20*). This suggests a good level of reliability of the system for continuous monitoring, while taking into account some natural fluctuations due to the accuracy of the instrument.

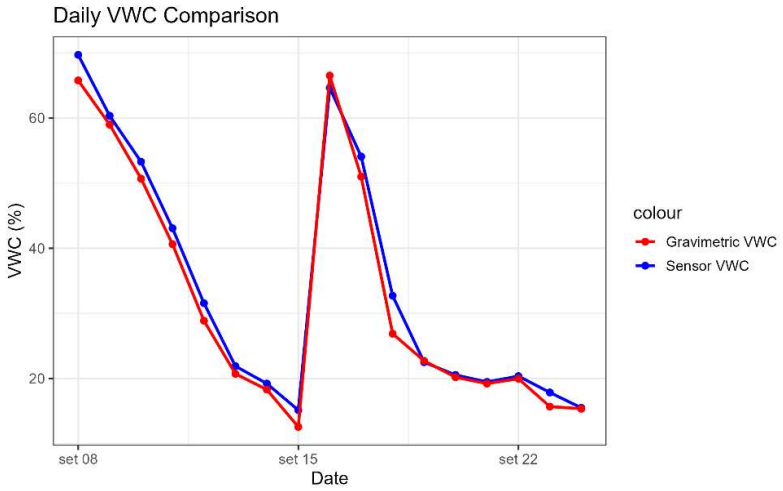

Figure 4.20 Visual comparison of the trend in gravimetric measurements and VWC returned by the sensor.

In this phase, the daily mean VWC values measured by the sensor were compared with the corresponding daily gravimetric determinations (Real VWC), allowing us to assess precision, accuracy, agreement, and correlation between the two datasets. *Table* 4.9 shows the accuracy parameters evaluated, while the results obtained are summarised below in *Table* 4.10:

Table 4.9 Accuracy Parameters Explained.

PARAMETER	DEFINITION	OPTIMAL VALUE
BIAS	Mean difference between sensor and reference	0 (no systematic over- or underestimation)
MAE	Mean absolute error	As low as possible (0 indicates perfect accuracy)

RMSE	Root mean squared error	As low as possible, penalizes large errors
MSE	Mean squared error	As low as possible
RAE	Relative absolute error	Close to 0 indicates minimal relative error
R^2	Coefficient of determination	1 → perfect linear correlation
CCC	Concordance Correlation Coefficient	1 → perfect agreement between sensor and reference

Table 4.10 Results obtained.

BIAS	MAE	RMSE	MSE	RAE	R2	CCC
1.638	1.883	2.405	5.784	0.116	0.991	0.991

Therefore, the slightly positive bias of 1.64% indicates that the sensor tends to slightly overestimate VWC, although the deviation is minimal. The low MAE and RMSE values suggest that both the mean and quadratic errors relative to the reference measurements are very small, while the RAE of 0.116 confirms that the relative error is smaller than the natural variability of the actual VWC values. An R^2 of 0.991 demonstrates that the sensor is capable of effectively reproducing the daily dynamics of actual volumetric water content. Furthermore, the CCC, which is very close to 1 (0.991), confirms the excellent agreement between the sensor and the reference, both in terms of correlation and absolute accuracy. Overall, these results indicate that, after calibration, the sensor provides reliable and accurate measurements of soil water content, making it suitable for continuous monitoring applications.

A correlation test was performed to evaluate the relationship between the average daily VWC values measured by the low-cost sensor and those obtained through gravimetric measurements. Initially, the normality of the two data sets was verified using the Shapiro-Wilk test, which revealed a deviation from normal distribution. Consequently, Spearman's correlation coefficient was chosen, as it is more suitable for non-normally distributed data and for measuring monotonic relationships. The results showed a very high correlation between the two data sets, with a Spearman coefficient of 0.995 and an extremely low p-value ($1.03*10^{-5}$), indicating that the observed relationship is highly significant. These results confirm that, after calibration, the sensor accurately reproduces the daily trend of the actual volumetric water content in the soil. The correlation test was further supported by a scatter plot with regression line (*Figure 4.21*), which visually highlighted how the daily values measured by the sensor follow those measured by gravimetry in a practically parallel manner. Overall, this analysis demonstrates the excellent ability of the low-cost system to monitor daily variations in VWC, providing reliable data consistent with reference measurements.

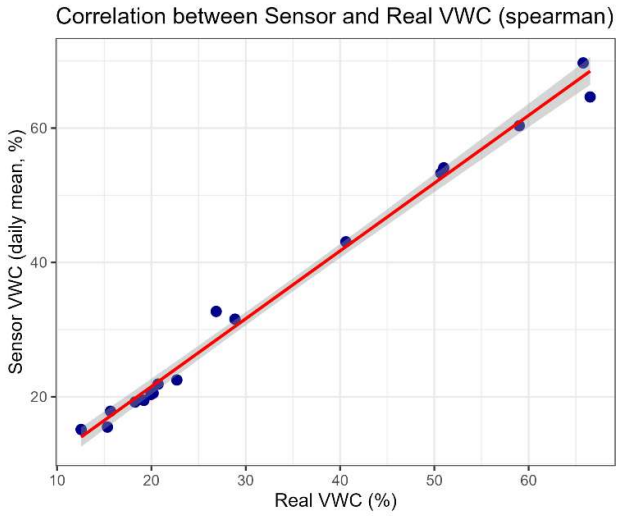

Figure 4.21 Scatterplot of the average daily VWC values measured by the low-cost sensor compared to the values obtained by gravimetric measurements. The red line represents the linear regression, highlighting the high correlation between the two data sets. The points show how the sensor accurately reproduces the trend of the actual volumetric water content in the soil.

4.4.1 Conclusion

The validation phase confirmed that the sensor, after calibration, is able to correctly reproduce the daily dynamics of VWC in the soil. The sensor showed a slight tendency to overestimate VWC, although the deviation was minimal. The low MAE and RMSE values indicate that both the mean and quadratic errors relative to the reference measurements are very small, while the RAE of 0.116 confirms that the relative error is smaller than the natural variability of the actual VWC values. An R^2 of 0.991 demonstrates that the sensor effectively reproduces the daily dynamics of real volumetric water content. From direct observation of the sensor behaviour, it was noted that the device responds rapidly to water additions, with a particularly high agreement between sensor and reference VWC values at low soil moisture levels. During the approximately 19 days of monitoring, some interruptions in data acquisition occurred: the first after 7 days due to the depletion of the power bank, requiring about half a day for full system restart, and a second interruption after 10 days, likely due to a system freeze. Despite these minor interruptions, the sensor demonstrated stable and consistent performance throughout the monitoring period. In particular, the RTC module reliably provided accurate date and time even after system restarts, confirming the sensor as a valid and reliable tool for continuous monitoring of soil VWC.

4.5 DSS SIMULATOR USING FASTAPI

The system is a Decision Support System (DSS) for precision agriculture, developed as a high-performance API using FastAPI in Python, connecting directly to a MongoDB database for sensor data acquisition. This DSS implements a complex multi-factor decision logic that transforms raw data into actionable agronomic information and, thanks to its foundation in Python, is perfectly adaptable to the specific needs of the crop and soil (Figure *4.22*).

```
13
14  # Example thresholds for the advanced DSS logic
15  # 1. Soil Moisture: Critical threshold.
16  CRITICAL_VWC_THRESHOLD = 30.0
17  # 2. Soil Temperature: Very hot soil (> 35°C) increases ET and requires attention.
18  HIGH_SOIL_TEMP_THRESHOLD = 35.0
19  # 3. Ambient Relative Humidity (RH): Low ambient humidity (< 40%) increases ET.
20  LOW_RH_THRESHOLD = 40.0
21  # 4. High Ambient Temperature (SHT): Drastically increases ET.
22  HIGH_AMBIENT_TEMP_THRESHOLD = 35.0
23
```

Figure 4.22 Definition of fundamental threshold values for DSS decision-making logic.

The DSS operates according to a hierarchical logic based on three main factors and their respective thresholds. In the experimental phase, the following were considered:

1. ***Volumetric Water Content (VWC): Primary Critical Factor***
   Experimentally, 30% VWC is considered the limit value; if VWC values below this threshold immediately trigger the status *"***IRRIGATION REQUIRED***"*, as they indicate a condition of water stress (*Figure 4.23*).

```
82
83      # 1. Multi-factor irrigation logic (Critical VWC is always prioritized)
84      if soil_vwc < CRITICAL_VWC_THRESHOLD:
85          decision_status = "IRRIGATION REQUIRED"
86          reasons.append(f"VWC ({soil_vwc:.1f}%) is below the critical threshold ({CRITICAL_VWC_THRESHOLD}%)")
87
```

Figure 4.23 Extract from the .py code showing the first condition for multi-factor irrigation logic.

2. ***Proactive Evapotranspiration (ET) Risk: Second Critical Factor***
   This factor uses environmental climate data to prevent excessive water loss. Irrigation is therefore flagged as *"***RECOMMENDED***"* if the ambient temperature exceeds 35 °C and the relative RH drops below 40%. This recommendation is applied only if the VWC is not already in a saturation or high-safety zone (VWC below 40%), ensuring that proactive action is truly necessary (*Figure 4.24*).

```
88      # 2. Evapotranspiration Stress (Low RH OR High Temp)
89      # Proactive irrigation recommended if climatic factors are extreme and soil is not saturated
90      elif (rh_ambient < LOW_RH_THRESHOLD or ambient_temp > HIGH_AMBIENT_TEMP_THRESHOLD) and soil_vwc < 40:
91          decision_status = "IRRIGATION RECOMMENDED"
92
```

Figure 4.24 Extract from the .py code, that shows the second condition of irrigation logic.

3. *Soil Thermal Stress: Third Critical Factor*

Soil temperature is monitored to detect conditions of root thermal stress. In this experimental phase, values above 35 °C contribute to the decision **"IRRIGATION RECOMMENDED"** (if VWC is below 45%), acknowledging that excessive soil heat accelerates the plant's water demand (*Figure 4.25).*

```
104
105     # 3. Soil Temperature Stress
106     elif soil_temp > HIGH_SOIL_TEMP_THRESHOLD and soil_vwc < 45:
107         decision_status = "IRRIGATION RECOMMENDED"
108         reasons.append(f"High Soil Temperature ({soil_temp:.1f}°C) observed, increasing water demand.")
109
```

Figure 4.25 Extract from .py code showing the thir condition for multi-factor irrigation logic.

The hierarchical and multifunctional decision logic is summarized in the flowchart shown in Figure XXX, which clearly illustrates the operational sequence and the interactions among the different decision modules.

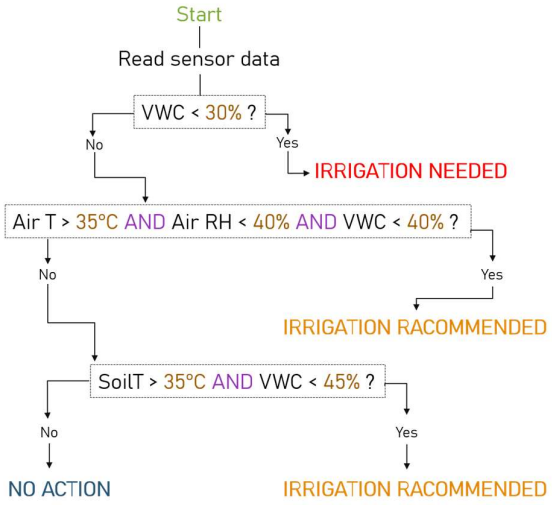

Figure 4.26 Flowchart illustrating the hierarchical and multifunctional decision logic implemented in the monitoring system.

The core logic of the DSS is exposed through a RESTful API developed with FastAPI, which serves as the operational interface of the system. The application, executed via the Uvicorn ASGI server, provides a set of essential endpoints for data management and analysis:

- ***Interactive Interface:*** The FastAPI Swagger UI (*Figure 3.11*), offers interactive API documentation and allows direct testing of the endpoints.
- ***Real-Time Data Access (GET /dati):*** this endpoint (Figure 4.27) enables immediate visualization and export of sensor values in JSON format. It loads the most recent data and returns the last five rows for quick inspection.

Figure 4.27 Interface of the FastAPI GET /dati endpoint showing the parameters monitored by the low-cost system and allowing data export in JSON format.

- ***DSS Analysis (GET /decision_maker or /irrigation_history):*** This endpoint applies the DSS multi-factor logic to all historical records, processing the data reading by reading. It returns the complete decision sequence generated by the system, providing a detailed overview of all decisions made throughout the monitoring period — including cases where irrigation was required (Figure 4.28), recommended (Figure 4.29), or not necessary (Figure 4.30).

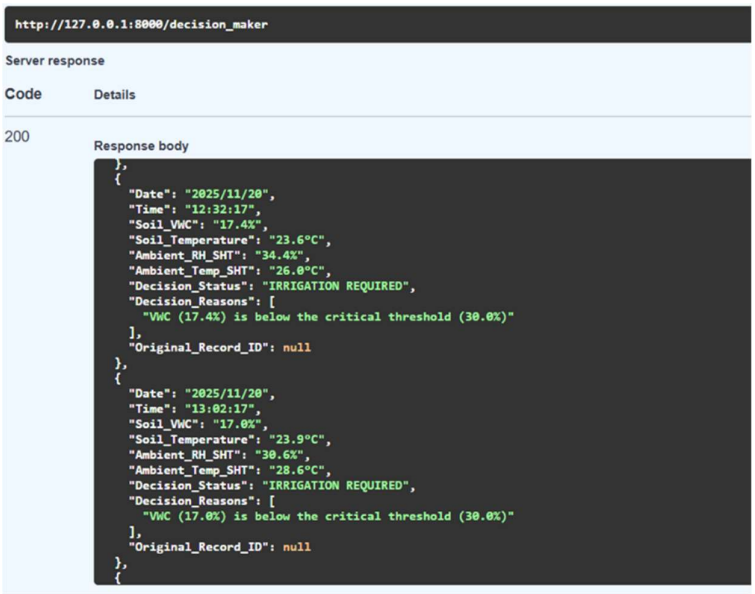

Figure 4.28 Interface of decision_maker: The system processed data from soil and environmental sensors and, upon detecting a volumetric water content (VWC) below the critical threshold of 30.0%, *generated an operational decision****: irrigation_required: True****. The interface allows the visualization and testing of the DSS logic, automatically translating raw sensor data into a clear and easily interpretable agronomic action.*

http://127.0.0.1:8000/decision_maker

Server response

Code	Details
200	Response body


```
    "Original_Record_ID": null
  },
  {
    "Date": "2025/11/22",
    "Time": "17:39:18",
    "Soil_VWC": "37.3%",
    "Soil_Temperature": "18.8°C",
    "Ambient_RH_SHT": "38.8%",
    "Ambient_Temp_SHT": "21.0°C",
    "Decision_Status": "IRRIGATION RECOMMENDED",
    "Decision_Reasons": [
      "High Evapotranspiration potential due to: Low Ambient RH (SHT: 38.8%)."
    ],
    "Original_Record_ID": null
  },
  {
    "Date": "2025/11/22",
    "Time": "18:09:18",
    "Soil_VWC": "38.7%",
    "Soil_Temperature": "18.8°C",
    "Ambient_RH_SHT": "38.9%",
    "Ambient_Temp_SHT": "20.9°C",
    "Decision_Status": "IRRIGATION RECOMMENDED",
    "Decision_Reasons": [
      "High Evapotranspiration potential due to: Low Ambient RH (SHT: 38.9%)."
    ],
    "Original_Record_ID": null
```


*Figure 4.29 FastAPI decision_maker interface: the system processed data from soil and environmental sensors, including VWC values. Since at least one of the evaluated parameters indicated sub-optimal conditions, the DSS generated the decision **irrigation_recommended**.*

http://127.0.0.1:8000/decision_maker

Server response

Code	Details
200	Response body


```
[
  {
    "Date": "2025/11/19",
    "Time": "01:02:19",
    "Soil_VWC": "49.4%",
    "Soil_Temperature": "20.2°C",
    "Ambient_RH_SHT": "47.1%",
    "Ambient_Temp_SHT": "22.8°C",
    "Decision_Status": "NOT irrigation required",
    "Decision_Reasons": [
      "Current VWC (49.4%) is adequate. No critical stress factors detected."
    ],
    "Original_Record_ID": null
  },
  {
    "Date": "2025/11/19",
    "Time": "01:32:19",
    "Soil_VWC": "49.4%",
    "Soil_Temperature": "20.2°C",
    "Ambient_RH_SHT": "47.4%",
    "Ambient_Temp_SHT": "22.6°C",
    "Decision_Status": "NOT irrigation required",
    "Decision_Reasons": [
      "Current VWC (49.4%) is adequate. No critical stress factors detected."
    ],
    "Original_Record_ID": null
  },
```


*Figure 4.30 Interface of the FastAPI decision_maker: the system processed data from soil and air sensors and, since the volumetric water content (VWC) was above the critical threshold and the other parameters were within normal ranges, it determined that no irrigation was required **(irrigation_required: False**).*

5 CONCLUSION AND FUTURE PERSPECTIVES

5.1 CONCLUSION

This research systematically addressed the challenges related to soil monitoring and the efficient management of water resources in agriculture, with the aim of developing, calibrating, and validating a low-cost measurement system capable of providing reliable, real-time data to support irrigation management decisions.

Starting from the analysis of the main issues of modern agriculture, characterized by the increasing demand for food, water scarcity, and the impacts of climate change, the study highlighted the need for innovative approaches based on the digitalization of production processes. The transition toward Agriculture 5.0 demonstrates how the integration of digital technologies, smart sensors, and automated systems can enhance productivity while reducing environmental impact. However, the high cost and technical complexity of commercial systems still represent a barrier to their widespread adoption, particularly among small and medium-sized farms.

In the specific context of Basilicata, a region facing increasing water scarcity and complex morphology, soil monitoring emerges as a strategic element for sustainable water management. The review of the main monitoring technologies highlighted the growing interest in low-cost solutions, especially capacitive sensors, which offer an excellent compromise between cost, stability, sensitivity, and compatibility with low-power IoT architectures.

Descriptive analyses confirmed the reliability and consistency of the selected sensors: the environmental sensors DHT22 and SHT10 exhibited stable and consistent measurements, with the SHT10 showing higher accuracy; the soil sensors SEN0308 and DS18B20 demonstrated, respectively, a good ability to capture the full range of soil moisture variation and a high degree of thermal stability. The Shapiro–Wilk normality test confirmed the non-normality of data distributions, thus justifying the use of non-parametric statistical methods in the subsequent correlation analyses.

Correlation analyses further validated the system's internal coherence: environmental sensors showed strong interrelationships between temperature and relative humidity, while the ADC values from the capacitive sensor were strongly and negatively correlated with the gravimetric water content, confirming the device's sensitivity to soil moisture variation.

The calibration process led to the development of a second-order polynomial equation, implemented directly in the Arduino IDE code, enabling the real-time estimation of VWC.

The validation phase confirmed the reliability and accuracy of the developed monitoring system. After calibration, the sensor demonstrated a high ability to accurately reproduce the daily dynamics of volumetric water content (VWC), with very low mean and quadratic errors (MAE and RMSE) and a determination coefficient (R^2) of 0.991. Despite some brief interruptions due to power depletion and system freezes, the sensor showed stable and consistent performance throughout the monitoring period.

The integration of data through the FastAPI-based API further enhanced the system, allowing visualization and export of the monitored parameters via the GET /dati command, and specific consultation of soil moisture levels through GET /decision_maker, which clearly indicates whether irrigation is required or not. This result represents a concrete step toward the development of a DSS for irrigation management based on real-time data flexible, scalable, and accessible.

In conclusion, the results demonstrate that low-cost sensors, when properly calibrated through gravimetric methods, can serve as reliable, affordable, and replicable tools for agro-environmental monitoring. The developed system provides a foundation for a more sustainable and digitally integrated approach to water resource management, contributing to the transition toward a more efficient, resilient, and data-driven agriculture.

5.2 FUTURE PERSPECTIVES

Based on the results obtained, the future perspectives of this research can be summarized in three main directions. First, the calibration phase should be expanded to include additional soil types, in order to assess the sensor's adaptability to different pedological conditions and improve the generalizability VWC estimation equation. Second, the sensor will need to be equipped with an autonomous power system, for example based on a lithium battery integrated with a power bank and a photovoltaic panel, to ensure continuous operation in the field. At the same time, the implementation of an IoT platform based on low-power architectures and long-range communication technologies (such as LoRa or NB-IoT) will allow the system to be scaled up, facilitating data collection, management, and sharing among farms, research institutions, and local authorities. Finally, the integration of the monitoring system with agronomic models such as AquaCrop represents a strategic objective for the future. This phase will need to be developed and refined through field tests and experimental validations, in order to create reliable predictive tools for real-time irrigation management, capable of adapting to dynamic climatic and crop scenarios.

In perspective, this work contributes to promoting increasingly intelligent, connected, and sustainable agriculture, providing concrete support for the digitalization of the agri-food sector and for the efficient and responsible management of water resources.

6 REFERENCE

[1] FAO, *The future of food and agriculture: trends and challenges*. Rome: Food and Agriculture Organization of the United Nations, 2017.

[2] «fao.org/aquastat/en/overview/methodology/water-use/». Consultato: 2 settembre 2025. [Online]. Disponibile su: https://www.fao.org/aquastat/en/overview/methodology/water-use/

[3] I. Charania e X. Li, «Smart farming: Agriculture's shift from a labor intensive to technology native industry», *Internet Things*, vol. 9, p. 100142, mar. 2020, doi: 10.1016/j.iot.2019.100142.

[4] S. Majumder *et al.*, «Assessing Low-cost Capacitive Soil Moisture Sensors: Accurate, Affordable, and IoT-ready Solutions for Soil Moisture Monitoring», *Int. J. Environ. Clim. Change*, vol. 13, fasc. 11, pp. 2233–2242, nov. 2023, doi: 10.9734/ijecc/2023/v13i113386.

[5] «pdf». Consultato: 8 settembre 2025. [Online]. Disponibile su: https://data.consilium.europa.eu/doc/document/ST-7085-2019-INIT/en/pdf

[6] «Digitalizzazione - Commissione europea». Consultato: 8 settembre 2025. [Online]. Disponibile su: https://agriculture.ec.europa.eu/overview-vision-agriculture-food/digitalisation_it

[7] «The State of the World's Land and Water Resources for Food and Agriculture – Systems at breaking points (SOLAW 2021)». Consultato: 5 settembre 2025. [Online]. Disponibile su: https://openknowledge.fao.org/server/api/core/bitstreams/bc8810ae-2a13-4cfe-b019-339158c7e608/content/cb7654en.html

[8] P. Saccon, «Water for agriculture, irrigation management», *Appl. Soil Ecol.*, vol. 123, pp. 793–796, feb. 2018, doi: 10.1016/j.apsoil.2017.10.037.

[9] M. Yadav *et al.*, «Improving Water Efficiencies in Rural Agriculture for Sustainability of Water Resources: A Review», *Water Resour. Manag.*, vol. 38, fasc. 10, pp. 3505–3526, ago. 2024, doi: 10.1007/s11269-024-03836-6.

[10] «Censimento Agricoltura 2020». Consultato: 7 settembre 2025. [Online]. Disponibile su: https://esploradati.istat.it/databrowser/#/it/censimentoagricoltura

[11] «REPORT-CENSIAGRI_2021-def.pdf». Consultato: 8 settembre 2025. [Online]. Disponibile su: https://www.istat.it/it/files/2022/06/REPORT-CENSIAGRI_2021-def.pdf

[12] «Statistiche sull'acqua_Anni 2020-2024».

[13] «IstatData». Consultato: 4 ottobre 2025. [Online]. Disponibile su: https://esploradati.istat.it/databrowser/#/it/dw

[14] «ANNUARIO DELL'AGRICOLTURA ITALIANA 2023 - Volume LXXVII».

[15] «focus-akis-agrifoglio.pdf». Consultato: 12 settembre 2024. [Online]. Disponibile su: https://www.innovarurale.it/sites/default/files/2023-07/focus-akis-agrifoglio.pdf

[16] M. D'Oronzio e C. Sica, «Innovation in Basilicata agriculture: From tradition to digital», *Econ. Agro-Aliment. Food Econ.*, vol. 23, pp. 1–18, ago. 2021, doi: 10.3280/ecag2-2021oa12210.

[17] A. I. Obaisi, M. J. Adegbeye, M. M. M. Y. Elghandour, A. Barbabosa-Pliego, e A. Z. M. Salem, «Natural Resource Management and Sustainable Agriculture», in *Handbook of Climate Change Mitigation and Adaptation*, Springer, Cham, 2022, pp. 2577–2613. doi: 10.1007/978-3-030-72579-2_133.

[18] I. M. Hernández-Ochoa *et al.*, «Model-based design of crop diversification through new field arrangements in spatially heterogeneous landscapes. A review», *Agron. Sustain. Dev.*, vol. 42, fasc. 4, p. 74, lug. 2022, doi: 10.1007/s13593-022-00805-4.

[19] B. Basso, L. Sartori, e M. Bertocco, *Agricoltura di Precisione. Concetti teorici e applicazioni pratiche*. Edizioni l'informatore agrario, 2005.

[20] G. S. Khush, «Green revolution: preparing for the 21st century», *Genome*, vol. 42, fasc. 4, pp. 646–655, ago. 1999.

[21] M. Dhanaraju, P. Chenniappan, K. Ramalingam, S. Pazhanivelan, e R. Kaliaperumal, «Smart Farming: Internet of Things (IoT)-Based Sustainable Agriculture», *Agriculture*, vol. 12, fasc. 10, p. 1745, ott. 2022, doi: 10.3390/agriculture12101745.

[22] F. J. Ferrández-Pastor, J. M. García-Chamizo, M. Nieto-Hidalgo, J. Mora-Pascual, e J. Mora-Martínez, «Developing Ubiquitous Sensor Network Platform Using Internet of Things: Application in Precision Agriculture», *Sensors*, vol. 16, fasc. 7, p. 1141, lug. 2016, doi: 10.3390/s16071141.

[23] M. O'Grady e G. M. P. O'Hare, «Modelling the Smart Farm.», in *Information processing in agriculture*, vol. 4, 2017, pp. 179–187.

[24] V. K. Quy *et al.*, «IoT-Enabled Smart Agriculture: Architecture, Applications, and Challenges», *Appl. Sci.*, vol. 12, fasc. 7, p. 3396, gen. 2022, doi: 10.3390/app12073396.

[25] A. H. El Nahry e E. S. Mohamed, «Potentiality of land and water resources in African Sahara: a case study of south Egypt», *Environ. Earth Sci.*, vol. 63, fasc. 6, pp. 1263–1275, lug. 2011, doi: 10.1007/s12665-010-0799-5.

[26] Organisation des Nations Unies pour l'alimentation et l'agriculture, A c. di, *Climate-smart agriculture sourcebook*. Rome: FAO, 2014.

[27] G. Adamides *et al.*, «Smart Farming Techniques for Climate Change Adaptation in Cyprus», *Atmosphere*, vol. 11, fasc. 6, p. 557, giu. 2020, doi: 10.3390/atmos11060557.

[28] I. Zambon, M. Cecchini, G. Egidi, M. Saporito, e A. Colantoni, «Revolution 4.0: Industry vs. Agriculture in a Future Development for SMEs», *Processes*, vol. 7, p. 36, gen. 2019, doi: 10.3390/pr7010036.

[29] F. Bonomi, R. Milito, J. Zhu, e S. Addepalli, «Fog computing and its role in the internet of things», in *Proceedings of the first edition of the MCC workshop on Mobile cloud computing*, Helsinki Finland: ACM, ago. 2012, pp. 13–16. doi: 10.1145/2342509.2342513.

[30] «ESP32-DevKitC V4 Getting Started Guide - ESP32 - — ESP-IDF Programming Guide v5.1 documentation». Consultato: 15 settembre 2025. [Online]. Disponibile su: https://docs.espressif.com/projects/esp-idf/en/v5.1/esp32/hw-reference/esp32/get-started-devkitc.html

[31] M. Babiuch, P. Foltýnek, e P. Smutný, «Using the ESP32 Microcontroller for Data Processing», in *2019 20th International Carpathian Control Conference (ICCC)*, mag. 2019, pp. 1–6. doi: 10.1109/CarpathianCC.2019.8765944.

[32] R. R. Boralkar e S. S. Kulkarni, «IoT Based Smart Agriculture System Using ESP32», in *2024 4th Interdisciplinary Conference on Electrics and Computer (INTCEC)*, giu. 2024, pp. 1–7. doi: 10.1109/INTCEC61833.2024.10602915.

[33] L. S. Ley e S. A. Hamzah, «Real Time Monitoring System for Peat Soil», vol. 4, fasc. 2, 2023.

[34] N. H. Numbi, S. Mbuyu, e T. S. Hlahlele, «Development of an ESP32 Smart and Safe Outdoor Plant Watering System», in *2024 32nd Southern African Universities Power Engineering Conference (SAUPEC)*, gen. 2024, pp. 1–6. doi: 10.1109/SAUPEC60914.2024.10445039.

[35] G. P. Pereira, M. Z. Chaari, e F. Daroge, «IoT-Enabled Smart Drip Irrigation System Using ESP32», *IoT*, vol. 4, fasc. 3, Art. fasc. 3, set. 2023, doi: 10.3390/iot4030012.

[36] K. K. Y. Shin, T. P. Ping, M. G. B. Ling, C. Chee Jiun, e N. A. B. Bolhassan, «*SMART GROW* – Low-cost automated hydroponic system for urban farming», *HardwareX*, vol. 17, p. e00498, mar. 2024, doi: 10.1016/j.ohx.2023.e00498.

[37] A. Morchid *et al.*, «IoT-enabled smart agriculture for improving water management: A smart irrigation control using embedded systems and Server-Sent Events», *Sci. Afr.*, vol. 27, p. e02527, mar. 2025, doi: 10.1016/j.sciaf.2024.e02527.

[38] «esp32_datasheet_en.pdf». Consultato: 15 settembre 2025. [Online]. Disponibile su: https://www.espressif.com/sites/default/files/documentation/esp32_datasheet_en.pdf

[39] «ESP32 DevKitC 38 PIN Screw Terminal Board - Vendita Online su ZioTester», Ziotester. Consultato: 15 settembre 2025. [Online]. Disponibile su: https://www.ziotester.it/elettronica/boards/esp32-devkitc-38-pin-screw-terminal-board-scheda-di-sviluppo-con-morsettiera.html
[40] «SD2405AL datasheet».
[41] «SPI Lector Micro Memoria SD TF Tarjeta de Memoria Módulo Shield», AZ-Delivery. Consultato: 16 settembre 2025. [Online]. Disponibile su: https://www.az-delivery.de/es/products/copy-of-spi-reader-micro-speicherkartenmodul-fur-arduino
[42] S. Ansari, A. Ansari, A. Kumar, R. Kumar, e E. T. Nyamasvisva, «Environmental Temperature and Humidity Monitoring at Agricultural Farms using Internet of Things & DHT22-Sensor», *J. Indep. Stud. Res. Comput.*, vol. 21, fasc. 2, Art. fasc. 2, dic. 2023, doi: 10.31645/JISRC.23.21.2.5.
[43] F. N. Shuhaimi, N. Jamil, e R. Hamzah, «Evaluations of Internet of Things-based personal smart farming system for residential apartments», *Bull. Electr. Eng. Inform.*, vol. 9, fasc. 6, Art. fasc. 6, dic. 2020, doi: 10.11591/eei.v9i6.2496.
[44] A. M. Diniz, M. A. V. Boas, M. B. Remor, J. A. C. Siqueira, e L. K. Tokura, «Development of an Automated Real-Time System for Soil Temperature and Moisture Measurement», *J. Agric. Sci.*, vol. 11, fasc. 2, p. 192, gen. 2019, doi: 10.5539/jas.v11n2p192.
[45] C. Lee, M. Ramasamy, S. Deivasigamani, e A. Khan, «IoT Based Farming System», 2022. doi: 10.3233/ATDE221132.
[46] F. Irwanto *et al.*, «IoT and fuzzy logic integration for improved substrate environment management in mushroom cultivation», *Smart Agric. Technol.*, vol. 7, p. 100427, mar. 2024, doi: 10.1016/j.atech.2024.100427.
[47] A. Mishra, «Smart Agriculture Monitoring & Auto Irrigation System using IoT with ESP8266», *Int. J. Res. Appl. Sci. Eng. Technol.*, vol. 10, fasc. 6, pp. 2681–2685, giu. 2022, doi: 10.22214/ijraset.2022.44382.
[48] T. Liu, «Digital-output relative humidity & temperature sensor/module DHT22 (DHT22 also named as AM2302)».
[49] J. J. Estrada-López, J. Vázquez-Castillo, A. Castillo-Atoche, E. Osorio-de-la-Rosa, J. Heredia-Lozano, e A. Castillo-Atoche, «A Sustainable Forage-Grass-Power Fuel Cell Solution for Edge-Computing Wireless Sensing Processing in Agriculture 4.0 Applications», *Energies*, vol. 16, fasc. 7, Art. fasc. 7, gen. 2023, doi: 10.3390/en16072943.
[50] S. Nallani e V. B. Hency, «Low power cost effective automatic irrigation system», *Indian J. Sci. Technol.*, vol. 8, fasc. 23, 2015, doi: 10.17485/ijst/2015/v8i23/79973.
[51] W. Qin, «The Design of on Line Thermo-humidity Monitoring System Based on ZigBee Technology», presentato al 2016 International Conference on Education, Management and Computer Science, Atlantis Press, mag. 2016, pp. 520–524. doi: 10.2991/icemc-16.2016.107.
[52] J. James e M. Maheshwar P, «Plant growth monitoring system, with dynamic user-interface», in *2016 IEEE Region 10 Humanitarian Technology Conference (R10-HTC)*, dic. 2016, pp. 1–5. doi: 10.1109/R10-HTC.2016.7906781.
[53] X. Fengguo, C. Wei, H. Liang, Q. Bingyang, e G. Feng, «Research and design of monitoring and early warning system for agricultural meteorological element in greenhouse», in *2017 13th IEEE International Conference on Electronic Measurement & Instruments (ICEMI)*, Yangzhou, China: IEEE, ott. 2017, pp. 80–85. doi: 10.1109/ICEMI.2017.8265720.
[54] F. R. Saputri e B. Achmad, «Building Environment Monitoring System based on WiDo-Open Source IoT Node», in *2023 3rd International Conference on Smart Cities, Automation & Intelligent Computing Systems (ICON-SONICS)*, dic. 2023, pp. 85–90. doi: 10.1109/ICON-SONICS59898.2023.10434962.
[55] «Sensirion_Humidity_Sensors_SHT1x_Datasheet.pdf». Consultato: 6 marzo 2025. [Online]. Disponibile su:

https://sensirion.com/media/documents/BD45ECB5/61642783/Sensirion_Humidity_Sensors_SHT1x_Datasheet.pdf
[56] D. S. Corp, «Programmable Resolution 1-Wire Digital Thermometer».
[57] A. M. Okasha, H. G. Ibrahim, A. H. Elmetwalli, K. M. Khedher, Z. M. Yaseen, e S. Elsayed, «Designing Low-Cost Capacitive-Based Soil Moisture Sensor and Smart Monitoring Unit Operated by Solar Cells for Greenhouse Irrigation Management», *Sensors*, vol. 21, fasc. 16, p. 5387, ago. 2021, doi: 10.3390/s21165387.
[58] P. Singh e S. Saikia, «Arduino-based smart irrigation using water flow sensor, soil moisture sensor, temperature sensor and ESP8266 WiFi module», in *2016 IEEE Region 10 Humanitarian Technology Conference (R10-HTC)*, dic. 2016, pp. 1–4. doi: 10.1109/R10-HTC.2016.7906792.
[59] K. N. Bhanu, H. S. Mahadevaswamy, e H. J. Jasmine, «IoT based Smart System for Enhanced Irrigation in Agriculture», in *2020 International Conference on Electronics and Sustainable Communication Systems (ICESC)*, lug. 2020, pp. 760–765. doi: 10.1109/ICESC48915.2020.9156026.
[60] D. Schwamback, M. Persson, R. Berndtsson, L. E. Bertotto, A. N. A. Kobayashi, e E. C. Wendland, «Automated Low-Cost Soil Moisture Sensors: Trade-Off between Cost and Accuracy», *Sensors*, vol. 23, fasc. 5, Art. fasc. 5, gen. 2023, doi: 10.3390/s23052451.
[61] P. Placidi, L. Gasperini, A. Grassi, M. Cecconi, e A. Scorzoni, «Characterization of Low-Cost Capacitive Soil Moisture Sensors for IoT Networks», *Sensors*, vol. 20, fasc. 12, Art. fasc. 12, gen. 2020, doi: 10.3390/s20123585.
[62] E. A. A. D. Nagahage, I. S. P. Nagahage, e T. Fujino, «Calibration and Validation of a Low-Cost Capacitive Moisture Sensor to Integrate the Automated Soil Moisture Monitoring System», *Agriculture*, vol. 9, fasc. 7, p. 141, lug. 2019, doi: 10.3390/agriculture9070141.
[63] I. M. Kulmány *et al.*, «Calibration of an Arduino-based low-cost capacitive soil moisture sensor for smart agriculture», *J. Hydrol. Hydromech.*, vol. 70, fasc. 3, pp. 330–340, set. 2022, doi: 10.2478/johh-2022-0014.
[64] S. Kamon *et al.*, «Energy Consumption of a Wheel/Track Reconfigurable Mobile Robot on the Farm», in *2024 IEEE/SICE International Symposium on System Integration (SII)*, gen. 2024, pp. 798–803. doi: 10.1109/SII58957.2024.10417300.
[65] J. Dafonte, M. Á. González, E. Comesaña, M. T. Teijeiro, e J. J. Cancela, «Soil Water Status Monitoring System with Proximal Low-Cost Sensors and LoRa Technology for Smart Water Irrigation in Woody Crops», *Sensors*, vol. 24, fasc. 24, p. 8104, gen. 2024, doi: 10.3390/s24248104.
[66] «Waterproof_Capacitive_Soil_Moisture_Sensor_SKU_SEN0308_Datasheet». Consultato: 17 settembre 2025. [Online]. Disponibile su: https://wiki.dfrobot.com/Waterproof_Capacitive_Soil_Moisture_Sensor_SKU_SEN0308?gad_source=1&gad_campaignid=834127384&gbraid=0AAAADucPlCEAO4Y_WSsYvbmfXvwonB2q&gclid=Cj0KCQjwuKnGBhD5ARIsAD19RsY-lKflLLtIs-6hU-0AR3-4zkFMGPu4HRYkkBfn55MPtg7rkBDgYZQaAlmTEALw_wcB
[67] «Arduino IDE | Arduino Documentation». Consultato: 17 settembre 2025. [Online]. Disponibile su: https://docs.arduino.cc/software/ide/?_gl=1*17jijas*_up*MQ..*_ga*Njc3MTA0NzE5LjE3NTgxMzkwNDM.*_ga_NEXN8H46L5*czE3NTgxMzkwNDIkbzEkZzEkdDE3NTgxMzk1NzQkajYwJGwwJGgxOTIzMTgxOTY.
[68] «MongoDB: The World's Leading Modern Database», MongoDB. Consultato: 17 settembre 2025. [Online]. Disponibile su: https://www.mongodb.com/
[69] «FastAPI». Consultato: 18 settembre 2025. [Online]. Disponibile su: https://fastapi.tiangolo.com/
[70] J. Hrisko, «Capacitive Soil Moisture Sensor Theory, Calibration, and Testing», lug. 2020. doi: 10.13140/RG.2.2.36214.83522.

[71] A. Fares e V. Polyakov, «Advances in Crop Water Management Using Capacitive Water Sensors», in *Advances in Agronomy*, vol. 90, Academic Press, 2006, pp. 43–77. doi: 10.1016/S0065-2113(06)90002-9.
[72] N. Ida, *Engineering Electromagnetics*. Springer, 2015.
[73] G. C. Topp, J. L. Davis, e A. P. Annan, «Electromagnetic determination of soil water content: Measurements in coaxial transmission lines», *Water Resour. Res.*, vol. 16, fasc. 3, pp. 574–582, 1980, doi: 10.1029/WR016i003p00574.
[74] J. Singh *et al.*, «Soil Structure and Texture Effects on the Precision of Soil Water Content Measurements with a Capacitance- Based Electromagnetic Sensor», *Trans. ASABE*, vol. 63, fasc. 1, pp. 141–152, 2020, doi: 10.13031/trans.13496.
[75] J. O. Payero, X. Qiao, A. Khalilian, A. Mirzakhani-Nafchi, e R. Davis, «Evaluating the Effect of Soil Texture on the Response of Three Types of Sensors Used to Monitor Soil Water Status», *J. Water Resour. Prot.*, vol. 09, fasc. 06, pp. 566–577, 2017, doi: ada.
[76] G. Kargas, N. Ntoulas, e P. A. Nektarios, «Soil texture and salinity effects on calibration of TDR300 dielectric moisture sensor», *Soil Res.*, vol. 51, fasc. 4, p. 330, 2013, doi: 10.1071/SR13009.
[77] O. Adeyemi, T. Norton, I. Grove, e S. Peets, «Performance evaluation of three newly developed soil moisture sensors.», 2016.
[78] F. Puig, M. Garcia-Vila, M. A. Soriano, e J. A. Rodríguez-Díaz, «AquaCrop-IoT: A smart irrigation platform integrating real-time images and weather forecasting», *Comput. Electron. Agric.*, vol. 235, p. 110372, ago. 2025, doi: 10.1016/j.compag.2025.110372.
[79] S. Adla, N. K. Rai, S. H. Karumanchi, S. Tripathi, M. Disse, e S. Pande, «Laboratory Calibration and Performance Evaluation of Low-Cost Capacitive and Very Low-Cost Resistive Soil Moisture Sensors», *Sensors*, vol. 20, fasc. 2, p. 363, gen. 2020, doi: 10.3390/s20020363.
[80] M. Pramanik *et al.*, «Evaluation of capacitance-based soil moisture sensors in IoT based automatic basin irrigation system», 16 giugno 2023, *Research Square*. doi: 10.21203/rs.3.rs-3043138/v1.
[81] J. H. Zar, «Spearman Rank Correlation», in *Encyclopedia of Biostatistics*, John Wiley & Sons, Ltd, 2005. doi: 10.1002/0470011815.b2a15150.
[82] M. M. Mukaka, «A guide to appropriate use of Correlation coefficient in medical research», *Malawi Med. J.*, vol. 24, fasc. 3, pp. 69–71, 2012.
[83] Y. K. Kushwaha, R. K. Panigrahi, e A. Pandey, «Performance analysis of capacitive soil moisture, temperature sensors and their applications at farmer's field», *Environ. Monit. Assess.*, vol. 196, fasc. 9, p. 793, ago. 2024, doi: 10.1007/s10661-024-12946-y.
[84] D. N. Moriasi, J. G. Arnold, M. W. Van Liew, R. L. Bingner, R. D. Harmel, e T. L. Veith, «Model Evaluation Guidelines for Systematic Quantification of Accuracy in Watershed Simulations», Consultato: 29 settembre 2025. [Online]. Disponibile su: https://doi.org/10.13031/2013.23153
[85] I. H. Witten, E. Frank, e M. A. Hall, *Data Mining: Practical Machine Learning Tools and Techniques*, 3rd ed. Elsevier, 2011.